

STUDIES OF THE FORMATION, SEPARATION AND DEWATERING
OF AGGREGATED BIOLOGICAL MATERIALS

Alan Craig Bentham, M.A.

Submitted for the degree of Doctor of Philosophy
University of London, September 1989.

Department of Chemical and Biochemical Engineering
University College London

ProQuest Number: 10609820

All rights reserved

INFORMATION TO ALL USERS

The quality of this reproduction is dependent upon the quality of the copy submitted.

In the unlikely event that the author did not send a complete manuscript and there are missing pages, these will be noted. Also, if material had to be removed, a note will indicate the deletion.



ProQuest 10609820

Published by ProQuest LLC (2017). Copyright of the Dissertation is held by the Author.

All rights reserved.

This work is protected against unauthorized copying under Title 17, United States Code
Microform Edition © ProQuest LLC.

ProQuest LLC.
789 East Eisenhower Parkway
P.O. Box 1346
Ann Arbor, MI 48106 – 1346

ABSTRACT

The formation of aggregates of biological materials and their subsequent separation are key steps in the biological industry. Two systems involving the formation and dewatering of biological aggregates have been studied. In the first study soya protein was precipitated and then ultrafiltered in hollow-fibre membranes. It was shown that high protein concentrations could be obtained by appropriate choice of membrane geometry and pumping equipment. Rheological measurements of the suspension were used to explain the permeate flux rates at high protein concentration. The feasibility of using microfiltration for precipitate dewatering was assessed by studying the flux and protein transmission characteristics of flat-sheet microporous membranes.

The second study examined the suitability of a scroll decanter centrifuge for the removal of yeast cell debris from yeast homogenate. The cells were disrupted by high-pressure homogenisation and borax was used to aggregate the cell wall material by selectively cross linking carbohydrates having cis-1,2 diol groups. The effects of adjusting centrifuge parameters on the clarification of the homogenate, protein recovery and sediment dewatering were examined. The dewatering of homogenate solids was related to the shear modulus of the sediment.

Further clarification of the yeast homogenate suspension was achieved by centrifugation after flocculation of sub-micron cell debris using polyethylene imine (molecular weights 600-70,000). Maximum clarification of the suspension was found to occur at a polymer dose corresponding to zero electrophoretic mobility in the homogenate and it was seen that higher doses of polymers of higher molecular weight recharged and restabilised the homogenate suspension. It was found that the interaction of the polymer with the suspended solids and the soluble components (lipids, proteins and nucleic acids) of the homogenate was dependent on the pH and ionic concentration. Separation of the flocculated material was achieved on a pilot plant scale using a disc-stack centrifuge.

ACKNOWLEDGEMENTS

I would like to thank John Ireton, Geoff Taylor and Simon Gardiner for assistance in the microfiltration and ultrafiltration experiments, and the pilot plant team, Clive Orsborn and Chris Lees, for help with the large-scale work. I am also grateful for equipment modifications carried out by Don Montgomery and the workshop staff.

The efforts of Dr Mike Hoare and Professor Peter Dunnill in the supervision of my research work and their comments on the drafting of this thesis are very much appreciated.

The ultrafiltration equipment was kindly supplied by Romicon.

CONTENTS

	Page
ABSTRACT	2
ACKNOWLEDGEMENTS	3
LIST OF CONTENTS	4
LIST OF FIGURES	9
LIST OF TABLES	11
1. INTRODUCTION	
1.1 Problems in the Separation of Fine Biological Solids	12
1.1.1 Downstream Processing in Biochemical Engineering	
1.1.2 Problems in Purification	
1.1.3 Solid-liquid Separation	
1.1.4 Filtration	
1.1.5 Centrifugation	
1.1.6 Membrane Filtration	
1.1.7 Improvements in Solid-liquid Separation	
1.2 Precipitation	15
1.2.1 Precipitation in Biochemical Engineering	
1.2.2 Protein Solubility	
1.2.3 Precipitant	
1.2.4 Optimisation and Integration	
1.3 Aggregation of Particles	19
1.3.1 Promoting Solid-liquid Separation	
1.3.2 Stability of Colloidal Dispersions	
1.3.3 Coagulation using Inorganic Salts	
1.3.4 The Use of Polymeric Flocculants	
1.3.5 Cell Aggregation	

1.4	Particle Size Measurement	27
1.4.1	Size Distribution	
1.4.2	Direct Observation of Particles	
1.4.3	Sedimentation	
1.4.4	Electrical Sensing	
1.4.5	Light Scattering	
1.5	Rheology of Biological Materials	32
1.5.1	Particle Suspensions	
1.5.2	Non-Newtonian Flow	
1.5.3	Pipe Flow of Power Law Fluid	
1.5.4	Viscoelastic Behaviour	
1.6	Membrane Separation Processes	38
1.6.1	Introduction	
1.6.2	Ultrafiltration of Macromolecular Solutions	
1.6.3	Suspensions	
1.6.4	Microfiltration	
1.6.5	Fouling	
1.6.6	Geometry of Filtration System	
1.7	Centrifugation	49
1.7.1	Principles of Centrifugal Separation	
1.7.2	Types of Sedimentation Centrifuge	
1.7.3	Problems in Centrifuge Scale-up	
1.8	Systems for Study	54
1.8.1	Soya Protein Precipitate	
1.8.2	Yeast Cell Debris	
2. MATERIALS AND METHODS		
2.1	Membrane Filtration of Soya Protein	60
2.1.1	Preparation of Protein Solutions and Protein Precipitate Suspensions	
2.1.2	Microfiltration and Ultrafiltration	
2.1.3	Viscosity Measurements for Precipitate Suspensions	
2.1.4	Protein Adsorption on Microporous Membranes	
2.1.5	Protein Characterisation	

2.2	Clarification of Yeast Homogenate by Flocculation and Centrifugation	66
2.2.1	Preparation of Yeast Homogenate	
2.2.2	Flocculation of Cell Debris with Borax and Centrifugal Separation	
2.2.3	Measurement of Sediment Rheology	
2.2.4	Particle Size Measurement	
2.2.5	Particle Electrophoretic Mobility	
2.2.6	Titration of PEI with Hydrochloric Acid	
2.2.7	Treatment of Borax-clarified Homogenate with PEI	
2.2.8	Size Analysis during PEI Flocculation	
3.	SOYA PROTEIN PRECIPITATE RECOVERY USING MICROPOROUS MEMBRANES	
3.1	Introduction	73
3.2	Theory	73
3.3	Results	77
3.3.1	Unstirred Microfiltration	
3.3.2	Cross-flow Microfiltration	
3.3.3	Protein Adsorption	
3.4	Discussion	92
3.4.1	Protein Transmission	
3.4.2	Protein Adsorption	
3.5	Conclusion	95
4.	PILOT-SCALE ULTRAFILTRATION OF SOYA PROTEIN PRECIPITATE	
4.1	Results	97
4.1.1	Pure Water Flux Rates	
4.1.2	Concentration of Soya Protein Precipitate	
4.1.3	Hollow Fibre Geometry	
4.1.4	Suspension Rheology	

4.2	Discussion	112
	4.2.1 Flux Prediction in the Ultrafiltration of Soya Suspension	
	4.2.2 Polarisation of the Membrane	
	4.2.3 Hollow Fibre Geometry	
	4.2.4 Suspension Rheology	
4.3	Conclusion	116
5. SEPARATION OF BORAX-FLOCCULATED YEAST CELL DEBRIS		
5.1	Introduction	118
5.2	Results	119
	5.2.1 Variation of Shear Modulus with Dry Weight	
	5.2.2 Variation of Dry Weight with Relative Centrifugal Force	
	5.2.3 Clarification and Dewatering using a Scroll Decanter Centrifuge	
	5.2.4 Protein Recovery	
	5.2.5 Particle Size Analysis	
5.3	Discussion	130
5.4	Conclusion	131
6. POLYETHYLENE IMINE IN THE CLARIFICATION OF YEAST HOMOGENATE		
6.1	Mobility and Zeta Potential	133
6.2	Results	134
	6.2.1 Effect of Ionic Environment on Yeast Mobility	
	6.2.2 Effect of PEI on Mobility	
	6.2.3 Settling of PEI Floccs	
	6.2.4 Pilot-scale Clarification of Yeast Homogenate using PEI	

6.3	Discussion	155
6.3.1	Cell Surface	
6.3.2	Flocculation with PEI	
6.3.3	Flocculation Mechanism	
6.4	Conclusion	161
7.	CONCLUSION	164
8.	SUGGESTIONS FOR FURTHER WORK	
	LIST OF SYMBOLS	167
	LIST OF REFERENCES	171

FIGURES

- Figure 1.1 Electric Potential in the Double Layer.
- Figure 1.2 Variation of Shear Stress with Shear Rate for Non-Newtonian Fluids.
- Figure 2.1 Pilot Plant Ultrafiltration Equipment
- Figure 3.1 Unstirred Batch-cell Microporous Filtration of Protein Suspensions.
- Figure 3.2 Unstirred Batch-cell Microporous Filtration of Protein Suspension.
- Figure 3.3 Volume of Solution Permeated against $(\text{Time})^{1/2}$ for Unstirred Batch-cell Filtration.
- Figure 3.4 Cross-flow Microfiltration of Soya Protein Solution.
- Figure 3.5 Cross-flow Microfiltration of Soya Protein Solution.
- Figure 3.6 (a) Gel Electrophoresis (SDS PAGE) Scan of Retentate.
- Figure 3.6 (b) Gel Electrophoresis (SDS PAGE) Scan of Permeate.
- Figure 3.6 (c) Gel Electrophoresis (SDS PAGE) Scan of Permeate.
- Figure 3.7 Composition of Permeate Transmitted Through Microporous Membrane.
- Figure 3.8 Variation of Soluble Protein Transmission with Flux Rate for Cross-flow Microfiltration.
- Figure 3.9 Protein Adsorbed to Microporous Membrane after Immersion in Soya Protein Solution.
- Figure 4.1 The Concentration of Soya Protein Precipitate Suspension: Effect of Pressure Changes.
- Figure 4.2 The Concentration of Soya Protein Precipitate Suspension: Effect of Pump Type.
- Figure 4.3 The Concentration of Soya Protein Precipitate Suspension: Comparison of Membrane Types.
- Figure 4.4 The Concentration of Soya Protein Precipitate Suspension: Effect of Changing Fibre Length.
- Figure 4.5 The Concentration of Soya Protein Precipitate Suspension: Effect of Changing Fibre Diameter.
- Figure 4.6 Shear Stress versus Shear Rate for Soya Protein Precipitate Suspension.
- Figure 4.7 Variation of Apparent Viscosity with Shear Rate for Soya Protein Precipitate Suspension.
- Figure 4.8 Variation of Apparent Viscosity with Total Soya Protein Concentration.

- Figure 4.9 Log-log Plot of Shear Stress versus Shear Rate for Soya Protein Precipitate Suspension.
- Figure 5.1 Variation of Shear Modulus with Sediment Dry Weight.
- Figure 5.2 Variation of Shear Modulus with Oscillation Frequency.
- Figure 5.3 Variation of Sediment Dry Weight with Relative Centrifugal Force.
- Figure 5.4 Effect of Feed Flow Rate on Separation of Flocculated Yeast Homogenate.
- Figure 5.5 Effect of Differential Scroll Rate on Separation of Flocculated Yeast Homogenate.
- Figure 5.6 Effect of Pond Depth on Clarification and Dewatering of Flocculated Yeast Homogenate.
- Figure 5.7 Yeast Particle Size Distribution.
- Figure 6.1 Effect of pH on Yeast Mobility.
- Figure 6.2 Effect of Sodium Chloride Concentration on Mobility.
- Figure 6.3 Effect of Phosphate Concentration on Mobility.
- Figure 6.4 Variation of Mobility with PEI Concentration: Effect of Homogenate Dilution.
- Figure 6.5 Variation of Mobility with PEI Concentration.
- Figure 6.6 Titration of PEI against Hydrochloric Acid.
- Figure 6.7 Variation of Mobility with PEI Concentration: Effect of Polymer Molecular Weight.
- Figure 6.8 (a) Variation of Mobility in PEI 600: Effect of Sodium Chloride Concentration.
- Figure 6.8 (b) Variation of Mobility in PEI 600: Effect of pH.
- Figure 6.9 Variation of Mobility with PEI 600 Concentration: Effect of pH.
- Figure 6.10 Mean Floc Size during Mixing of Borax-clarified Homogenate and PEI.
- Figure 6.11 Effect of PEI on Turbidity and Protein Concentration in Borax-clarified Homogenate.
(a) PEI 600. (b) PEI 10,000.
(c) PEI 70,000. (d) PEI 50,000.
- Figure 6.12 Clarification of PEI-flocculated Yeast Homogenate using Disc-stack Centrifuges.

TABLES

- Table 3.1 Flux Characteristics of Microporous Membrane (0.2 μm).
- Table 4.1 Power Law Index and Consistency for Soya Protein Precipitate Suspension.
- Table 4.2 Power Law Index and Consistency at Transition Point in Soya Protein Ultrafiltration.
- Table 4.3 Flow Conditions at the Transition Point during Hollow-Fibre Ultrafiltration of Soya Protein Precipitate.
- Table 5.1 Comparison of Dry- and Flooded-beach Operation of the Scroll Decanter Centrifuge.

1. INTRODUCTION

1.1 Problems in the Separation of Fine Biological Solids

1.1.1 Downstream Processing in Biochemical Engineering

The advances made in genetic engineering techniques in the 1970's, such as those described by Hopwood (1981), have enabled the production of a wide variety of products from micro-organisms. These developments are now finding application in the biochemical industry for the improvement of traditional fermentation processes, the production of novel proteins and enzymes, and the provision of alternative routes to products made by the chemical industry. For the technological expectations of these developments to be fully realised in commercial exploitation, improvements in the efficiency of processing are required. In many cases the costs of purification can be critical. This is particularly true for the manufacture of proteins and enzymes where downstream processing costs are typically 60-70% of the selling price [Rosen (1983)].

1.1.2 Problems in Purification

The properties of biological solutions and suspensions provide a number of challenging problems for the process engineer. A typical suspension has a high viscosity and may exhibit non-Newtonian properties resulting in handling problems. The suspension must be processed under carefully controlled conditions since the products are likely to be sensitive to changes in temperature, pH and oxygen concentration and susceptible to contamination or denaturation. Biological separations are frequently complicated by the presence of intracellular components such as DNA, RNA, proteins and cell membranes. The complex mixture of compounds with very similar physical and chemical properties requires sophisticated separation techniques for successful purification. When the concentration of product is low, a common problem with fermentation broths, high costs can be incurred by the need to

handle large volumes of water. The treatment, disposal or recycling of waste material can also be a major cost consideration.

1.1.3 Solid-liquid Separation

The early stages of product isolation usually involve a solid-liquid separation step. High separation efficiencies are required since the presence of fine particles in the liquid stream can cause fouling problems further downstream, while losses of product in the early stages will result in low overall yields especially when many purification steps are involved [Fish and Lilly (1984)]. The physical properties of biological solids make removal difficult. They are usually finely dispersed with densities close to that of the suspending medium. They are also gelatinous materials, highly compressible and tend to adhere to surfaces. The economics of a number of separation techniques used in biotechnology are reviewed by Hacking (1986). High energy costs limit the application of methods such as drying or evaporation while other methods such as precipitation, ion exchange or solvent extraction may be useful only in specific applications or consume expensive reagents.

In general, mechanical methods are preferred for the removal of solids from a fermentation broth and the choice has been restricted to a few well-established unit operations, such as filtration and centrifugation, adapted from mainstream chemical engineering. These operations will be discussed briefly in this section, with particular reference to the difficulties of separating fine biological solids. More detailed discussion will be given in Sections 1.6 and 1.7.

1.1.4 Filtration

Belter (1985) has reviewed the applications of conventional filtration in the fermentation industry. Rotary vacuum filtration has been particularly effective for the separation of mycelial organisms (e.g. penicillin production, citric acid production) since the morphology of mycelial organisms leads to

the formation of permeable filter cake. For many other organisms the method is unsuitable due to blockage of the filter cloth with fine particles or the deposition of highly compressible filter cake of low permeability. Problems caused by the resistance of the filter cake to permeate flow are generally alleviated by the use of filter aids but the large amounts of filter aid required lead to high running costs, may be an unacceptable contaminant in the product and can cause loss of product by adsorption [Wagman et al. (1975)]. In many biological applications of filtration alternative methods are being sought, for example Gravatt and Molnar (1986) have examined ultrafiltration for the recovery of extracellular antibiotics.

1.1.5 Centrifugation

Centrifugation is a versatile technique for clarification of suspensions and dewatering of settled solids. Bell et al. (1983) have reviewed the use of centrifuges for the recovery of protein precipitates. Other common bioprocess applications, listed by Wiesmann and Binder (1982), include amino acid production, yeast separation and settling of single cell protein. Centrifugal separation is strongly dependent on the diameter and density of the solid fraction and is hindered when the fluid medium is of high viscosity. In the separation of bacteria (diameter 1-2 μm), clarification can be poor even when low throughputs are used. Heat generation in the centrifuge bowl will affect temperature sensitive products, containment of hazardous substances is a problem and cleaning can be difficult and labour intensive. Despite these problems centrifugal separators are currently used in many biochemical applications.

1.1.6 Membrane Filtration

Gabler (1985) has reviewed cross-flow membrane filtration as a dewatering technique that has potential applications in cell harvesting processes, removal of solids from protein streams and concentration of macromolecular solutions. This method has the advantages of high product recovery and good liquid clarity. In many cases the use of membrane techniques is restricted by the

tendency of biological materials to adsorb to the membrane or form gels at the membrane surface, thus reducing flux rates and giving poor separation. Hanisch (1986) suggested cross-flow filtration as a possible alternative to centrifugal separation for small bacterial cells such as *E. coli*. However, the economics of the process are heavily dependent on the membrane replacement costs which, since the membrane fouling is unpredictable for each application, must be considered for each individual product.

1.1.7 Improvements in Solid-liquid Separation

Removal of the solid can be facilitated by the conditioning of the particles to improve their separation characteristics using a variety of physical and chemical methods. The control of suspension properties, such as particle size and strength, using precipitating agents, flocculating agents and the manipulation of processing conditions will be discussed in Sections 1.2 and 1.3.

Alternatively the separation efficiency can be increased by improvements in the design and operation of the separation device. Developments in the use of membrane filtration and centrifugation in relation to the separation of fine biological solids will be discussed in Sections 1.6 and 1.7. In order to assess the effect of conditioning techniques and the efficiency of the separation equipment it is necessary to be able to characterise the suspension properties. Significant factors in the separation include the particle size of the solids and the rheological behaviour of the suspension and the sediment. These properties are discussed in Sections 1.4 and 1.5.

1.2 Precipitation

1.2.1 Precipitation in Biochemical Engineering

A number of biochemical processes currently use a precipitation step in the isolation of the product. Examples include the precipitation of penicillin as its potassium salt using potassium

acetate and the use of lime in citric acid precipitation. In the production of 6-aminopenicillanic acid via penicillin G the precipitant accounts for around 10% of the total operating cost [Hacking (1986)]. The nature of the precipitate will govern solid-liquid separation steps further downstream hence in the recovery of precipitates there is considerable incentive to improve precipitation methods. In an effort to understand the precipitation of biological materials extensive work has been applied to the study of protein solubility and this is described in the next section.

1.2.2 Protein Solubility

The development of theories for protein solubility has been discussed by Richardson (1988). Early approaches to the problem involved consideration of the solvated protein as a colloidal suspension and subsequent methods applied Debye-Huckel theory for activity coefficients of the soluble protein. Electrostatic interactions alone do not account for the behaviour of soluble protein and more recent theories involve the additional effect of hydrophobic interactions or preferential protein-solvent interactions. These theories have limited applications and detailed modelling of protein solutions with a quantitative thermodynamic description is not presently possible.

Qualitative description of the interaction of a protein with its environment can be useful in the analysis of precipitation of the protein. Protein molecules contain large numbers of hydrophilic and hydrophobic groups, may be ionised, and interact electrostatically with the solvent. Large amounts of water are usually loosely bound to protein molecules when in aqueous solution. The shape of the molecule, determined by the formation of intramolecular bonds, can be particularly important since it determines which parts of the molecule are exposed to the solvent and which can be shielded. Protein molecules containing hydrophobic amino acid residues can therefore remain stable in aqueous solution if the residues are held within the molecule while the surface of the molecule consists largely of hydrophilic groups. Proteins are sensitive to changes in their environment

and a number of reagents are capable of interacting with the solvated protein molecule and causing the precipitation of the protein. Acids, bases, metal ions, salts, organic solvents and polymers have proved effective in the precipitation of proteins [Bell et al. (1983)].

1.2.3 Precipitant

The choice of an effective precipitating agent for a particular protein is usually based on empirical testing. While there are many precipitating agents available, in practice there will be a number of factors restricting the method that can be used. The application of the product may preclude certain precipitants where the purity of the product is important. The requirements of clinical preparations are particularly demanding since it is necessary that the precipitating agent, which may be toxic even at low concentrations, should be easily removed without denaturing the product. For food products the effect of the precipitating agent on the flavour of the product may be significant. The use of organic solvents and metal ions is limited to situations where the processing conditions can be carefully controlled since damage to the protein molecule is a common problem with these reagents. There may also be difficulties in scaling up the process due to the precipitant being flammable (some organic solvents) or corrosive (acids, ammonium sulphate). Two common methods for protein precipitation, salting out or adjustment to isoelectric pH, are described below.

i) Isoelectric precipitation: It is usually found that at its isoelectric point, the pH at which the protein molecule has zero net charge, the protein is at its minimum solubility. The majority of proteins are negatively charged at neutral pH and it is possible to bring a protein to its isoelectric point and cause it to precipitate by adding acid to the solution. Salt et al. (1982), using soya protein, found that denaturation of protein was likely if the acid was not uniformly distributed throughout the solution and very poor mixing conditions need to be avoided. They noted that the nature of the anion of the acid was a

significant factor in determining protein damage during precipitation. Protein damage was observed to be inversely related to the position of the anion in the Hofmeister series which relates the effectiveness of neutral salts for the salting out of proteins in the order:

citrate > phosphate > sulphate > acetate - chloride > nitrate > thiocyanate

ii) Salting out: The Hofmeister series indicates that anions of greatest negative charge appear more effective in salting out soluble proteins. Salts at the higher end of this series (ammonium sulphate, sodium sulphate, potassium phosphate and sodium phosphate) have been widely used for protein precipitation but ammonium sulphate has proved the most useful due to its high solubility relative to the other salts at room temperature. Richardson (1988) has purified intracellular yeast proteins using ammonium sulphate precipitation and high resolution can be obtained by adjustment of the ammonium sulphate concentration at each 'cut'. Adjustment of pH alone would not generally be suitable for protein fractionation since the isoelectric points of the proteins are likely to be similar. If high resolution is not a primary consideration then acid precipitation may be preferred. For example, when the product is required for food use, sulphuric, phosphoric or hydrochloric acid would be acceptable and need not be removed. However, undesirable flavours would be produced by ammonium sulphate even at low concentrations. Other disadvantages of ammonium sulphate are the hazard of ammonia release under alkaline conditions and the corrosive nature of the solution at the concentrations employed for precipitation. Manipulation of the precipitation conditions may aid subsequent recovery of the protein as discussed in the following section.

1.2.4 Optimisation and Integration

When an acceptable precipitating agent has been found it is possible to then optimise the precipitation stage to give a high product yield. The requirements of the precipitation step will

be determined by the processing steps further downstream. A centrifugal separation would demand large, strong aggregates with high density compared to the suspension density. Ultrafiltration of the suspension would be independent of density difference and the concentration of soluble components which interact with the membrane would be of more importance [Devereux et al. (1984)].

The precipitation and recovery of isoelectric soya protein has been well characterised and is used as an example of a protein recovery process by Bell et al. (1983). It is possible to perform the precipitation at pH 4.8 using sulphuric acid under a wide range of processing conditions without significant damage to the protein. Bell et al. (1983) studied the adjustment of precipitation conditions for soya protein, particularly in relation to centrifugal recovery of the precipitate. They found that reactor configuration and conditioning of precipitate aggregates could be adjusted to improve the solid-liquid separation. These factors and their effect on recovery of soya protein are discussed in more detail in Section 1.8.

1.3 Aggregation of Particles

1.3.1 Promoting Solid-liquid Separation

The ability to control suspension properties is a significant factor in the choice of solid-liquid separation equipment. One approach to solving the problems encountered in the separation of solid material from biological suspensions, outlined in Section 1.1, is to ease the separation by aggregating the particles. The sedimentation properties of the solid are improved since the settling rate of the particles in a centrifugal field is dependent on the particle diameter; filtration characteristics are improved due to the formation of a more open cake structure of lower resistance to flow and the reduction of the number of fine particles which block the filter medium. The conditioning of microbial suspensions to produce aggregates can be understood in terms of colloid theory since it is the surface properties of the particles that dominate their behaviour. It is therefore

helpful to understand the factors that influence the stability of colloidal dispersions.

1.3.2 Stability of Colloidal Dispersions

A particle suspended in solution can acquire an electric charge through a number of mechanisms. For example, insoluble oxides such as silica and haematite are capable of gaining and losing protons to the solvent; silver halides exhibit different affinities for the adsorption of silver and halide ions from solution. The negative charge carried by biological materials at neutral pH is usually attributed to the dissociation of surface carboxyl groups [Gregory (1975)]. The charged particle will influence the surrounding solution to the extent that ions will be arranged around the particle. This arrangement is known as the 'double layer' since it consists of a charged surface together with a layer of ions of opposite charge (counterions). The layer of ions is usually broken down into two regions:

- i) Stern layer: close to particle surface containing tightly adsorbed counter-ions.
- ii) Gouy-Chapman layer: diffuse layer of counter- and co-ions, outside Stern layer.

The electric potential at the charged surface, Ψ_0 , falls to Ψ_d in the Stern layer as shown in Figure 1.1. It is possible to combine the Poisson equation:

$$\frac{d^2\Psi}{dx^2} = -\frac{\rho}{\epsilon} \quad \text{Equation 1.3.1}$$

with a Boltzmann distribution of ions:

$$\rho = zen_0 \left[\exp\left(-\frac{ze\Psi}{kT}\right) - \exp\left(\frac{ze\Psi}{kT}\right) \right] \quad \text{Equation 1.3.2}$$

to obtain an expression for the decay of potential in the diffuse part of the double layer.

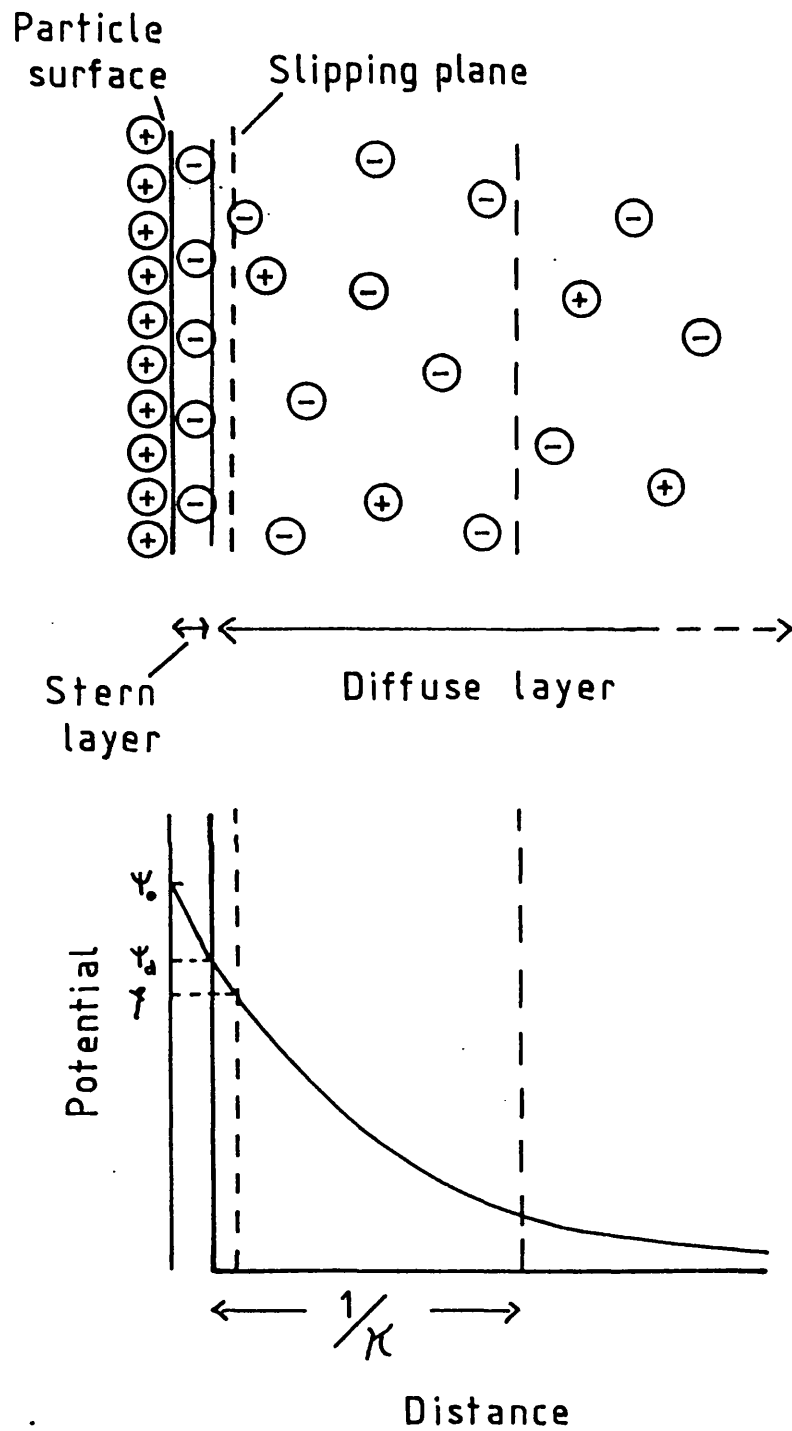


Figure 1.1 Electric Potential in the Double Layer.

ψ_0 , Surface Potential, ψ_d , Stern Potential, ψ , Zeta Potential.

Solution of the Poisson-Boltzmann equations leads to:

$$\psi = \frac{2kT}{ze} \ln \left[\frac{1 + \gamma \exp(-\kappa x)}{1 - \gamma \exp(-\kappa x)} \right] \quad \text{Equation 1.3.3}$$

$$\psi = 0, \left. \frac{d\psi}{dx} \right|_{x=\infty} = 0; \quad x = 0, \psi = \psi_d;$$

$$\kappa^2 = \frac{8\pi n e^2 z^2}{\epsilon kT}; \quad \gamma = \frac{\left[\exp\left(\frac{ze\psi_d}{2kT}\right) - 1 \right]}{\left[\exp\left(\frac{ze\psi_d}{2kT}\right) + 1 \right]}$$

When $\frac{ze\psi_d}{2kT} \ll 1$ (the Debye-Huckel approximation) it is possible to assume:

$$\exp\left(\frac{ze\psi_d}{2kT}\right) \approx 1 + \frac{ze\psi_d}{2kT} \quad \text{Equation 1.3.4}$$

and Equation 1.3.3 can be simplified to:

$$\psi = \psi_d \exp(-\kappa x) \quad \text{Equation 1.3.5}$$

where κ is the Debye-Huckel parameter and x is the distance from the Stern Plane. While the exact form of the potential distribution is dependent on the approximations that are made in obtaining the solution, it has been found that κ is an important parameter and can be used to calculate the effect of changes in the ionic environment on the particle. The reciprocal of κ is the distance (the 'Debye length') over which the potential decreases by a factor of $1/e$. The Debye length therefore represents the extent of the double layer and determines the range of electrical repulsion between particles.

The values of the surface potential, ψ_0 , and the Stern potential, ψ_d , cannot be measured experimentally but it is possible to obtain the zeta potential, ζ , the potential at the surface of shear between the charged surface and the solution, from electrophoresis measurements. The derivation of the zeta potential from measurement of particle mobility in an electric field will be discussed in Section 6.1. The exact location of the surface of shear is unknown but may be assumed to be slightly further out than the Stern layer and it is usually possible to take the value of the zeta potential as an estimate of the Stern potential.

The Gouy-Chapman treatment of the diffuse double layer contains many assumptions which have been criticised by a number of authors [see Hunter (1987)]. However, the theory has been found to be a good approximation provided that both the magnitude of the electric potential and the electrolyte concentration are not too large. The electrostatic repulsive forces between the particles and the effect of adding flocculating agents can then be assessed using measurements of the zeta potential.

Analysis of colloidal particles in suspension in terms of a balance of the attractive and repulsive forces acting on the particles can be used to determine the coagulation behaviour of the particles. This method was developed by Derjaguin and Landau (1941) and Verwey and Overbeek (1948) and is now known as the DLVO theory. The attractive forces, arising from London-van der Waals interactions between the atoms and molecules of each particle, act to destabilise the suspension by promoting coagulation of the solid. Coagulation is opposed by the electrostatic repulsion resulting from the charge interactions of the double layers. A suspension will therefore remain stable with respect to particle aggregation provided that the electrostatic forces are large enough to prevent particle coalescence.

It has long been established that electrolytes are capable of causing colloidal dispersions to aggregate. The valency of the coagulating agent was identified as a significant parameter by Schulze (1882) and Hardy (1900) and the strong dependence of the concentration required to achieve coagulation on the valency is recognized as the Schulze-Hardy rule. This rule supports the prediction from DLVO theory of a strong dependence of critical coagulation concentration on valency. More recent support for the theory is discussed by Hunter (1987).

Double layer theory suggests that the addition of salts to a colloidal dispersion can affect the stability of the particles in two ways. The ions may interact with the solid surface thus causing the surface potential to be altered. The ions are called 'potential determining ions' and may reduce the electrostatic repulsion force to a point where particle coalescence results.

Alternatively there may be no specific interaction with the particle surface but the electrolyte may cause the double layer to be 'compressed'. Since the Debye-Huckel parameter is dependent on the ionic strength of the suspension, increasing the ionic strength causes a reduction in the Debye length and consequently the range of the repulsive force is reduced.

1.3.3 Coagulation using Inorganic Salts

Inorganic salts generally compress the double layer and, if added in sufficient quantity, cause aggregation of colloids. The term 'coagulation' is used when the mechanism of aggregation occurs by double layer compression due to addition of electrolyte. A rather different aggregation mechanism ('flocculation') is described in section 1.3.4 in relation to polymeric reagents.

Electrolytes containing highly charged ions are the preferred coagulating agents since these bring about coagulation at low concentrations, in accordance with the Schulze-Hardy rule. Examples in the water treatment industry, given by Sontheimer (1978), employ salts of iron and aluminium to reduce turbidity of the water. The primary consideration in the choice of coagulant is the charge carried by the particulate material since it is the magnitude of the charge of the counterions in the double layer which determines the effectiveness of the reagent. Highly charged cations are therefore used for negatively charged colloids. The pH of the suspension, the solids concentration and the temperature may affect the coagulation and the choice may be limited by considerations of acceptability or cost of the reagent.

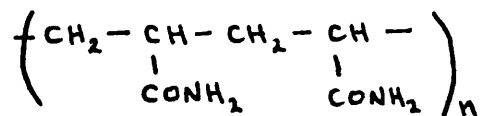
DLVO theory provides a useful basis for the description of the main features of particle interactions in the presence of electrolytes but in many practical situations, such as wastewater treatment, quantitative treatment of the behaviour of the charged species is not possible because of the complex composition of the suspension. Extensive testing of the suspension to determine the behaviour of the coagulated solids with respect to their removal by sedimentation or filtration is therefore required for the

selection of the most suitable coagulant. Where ions are specifically adsorbed to the particle the dose of the coagulant can be critical. Overdosing may lead to the adsorption of sufficient ions for charge reversal to take place and the colloid, if initially negatively charged, may then become restabilised as a positively charged particle. In these cases measurement of the mobility of the particles in an electric field is useful since charge reversal can thus be detected.

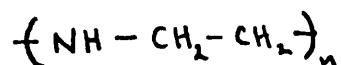
Although destabilisation of colloidal suspensions using inorganic salts has proved successful in many cases, an alternative approach using polymeric reagents has found more widespread applications. Aggregation is brought about by a linking up of the particles and does not require compression of the double layer although this may take place. Since the aggregation mechanism is fundamentally different from the coagulation mechanism occurring with the use of salts then 'flocculation' is often used to refer to the process. In some cases the term 'flocculation' is used indiscriminately since it is not always possible to determine the exact mechanism of aggregation.

1.3.4 The Use of Polymeric Flocculants

Early examples of the formation of loose flocs have been found to occur when natural polyelectrolytes such as isinglass, guar gum and sodium alginate are added to colloidal suspensions [Akers (1975)]. More recently a wide variety of synthetic polymers have been developed for use in the chemical industry, particularly the water treatment industry, as flocculating agents. The polymers are usually polyelectrolytes based on structures such as polyacrylamide



or polyethyleneimine



and can have molecular weights ranging from a few thousand to many millions. Acrylamide can be copolymerised with monomers having charged groups to give varying degrees of anionic or

cationic character. Polymers of opposite charge to that of the particle to be flocculated are often the most effective flocculants but neutral polymers, and even polymers of like charge, can bring about flocculation. Sections of the polymer are physically adsorbed to the particle in suspension (promoted by charge attraction, hydrophobic bonding and H-bonding) and, provided that the molecule can bridge the electrical double layers of the particles and adsorb to other particles, aggregation occurs. The polymer dosage is very important for this mechanism of aggregation since if the polymer concentration is too high a particle may become fully coated by segments of polymer and steric effects prevent the linking together of particles. The most effective aggregation is usually observed with high molecular weight molecules at concentrations of the order of a few parts per million. The chain length of a polymer will affect the ability of the polymer to link a number of particles and is controlled by the molecular weight of the polymer and the polymer charge density. Neutral polymers adopt various random coiled configurations, while charged polymers of the same molecular weight will tend to be more extended due to the mutual repulsion of charged groups. Increasing the ionic strength of the suspension may promote flocculation by reducing the double layer which the polymer has to bridge. However, other factors such as changes in polymer configuration or degree of polymer adsorption may result from increasing the ionic concentration and act against the flocculation. The overall effect of these factors is difficult to predict and empirical testing is usually required.

1.3.5 Cell Aggregation

Some microorganisms have the capacity to flocculate naturally during the final stages of a fermentation. This property has long been exploited in the brewing industry for the separation of yeasts and exocellular polymers have been extracted from microorganisms for use as flocculating agents [Forster et al. (1985)]. The mechanism of cell auto-flocculation is commonly thought to occur via the bridging of cells with extracellular polysaccharides which are produced by the cell, particularly in

the later stages of growth. Other important factors in the aggregation process include the cell wall structure and charge, the adsorption of macromolecules at the cell surface and the incorporation of multivalent ions into the surface. Extensive studies have been carried out on the factors affecting yeast flocculation because of the importance of the process in the brewing industry. With flocculent strains of yeast having the appropriate cell wall composition, aggregation appears to take place by the formation of calcium bridges between the cells [Esser et al. (1987)]. Bridging will be prevented if electrostatic repulsion is high or if steric repulsion due to adsorbed polymers occurs.

Where auto-flocculation does not occur it may be necessary to use a chemical flocculating agent to achieve solid separation. Electrolytes and polymer reagents are extensively used in the treatment of waste waters and the processing of minerals. While the experience gained in these industries may be usefully applied to the flocculation of biological materials there are number of factors which may limit the application of synthetic reagents in biological flocculations. For instance, in the selective removal of cell debris during the isolation of intracellular enzymes it is important to consider the effect of the flocculating agent on the activity of the enzyme. Also, where the microbial product is intended for medical or food use the toxicity of the flocculating agent or the ease of removal of the flocculating agent may be an overriding consideration.

1.4 Particle Size Measurement

1.4.1 Size Distribution

For the selection of solid-liquid separation equipment and the evaluation of the performance of such equipment, information on the particle size is required. The measurement of particle size for colloidal systems presents a number of difficulties. Direct observation of the particles is often not convenient and indirect methods of measuring the particle size must be employed. Since

practical systems will contain a range of particle sizes, the measurements have to take into account the distribution of particle sizes. A convenient method of gathering the data is to split the distribution into classes covering small ranges. The data can then be presented as a histogram of numbers of particles in each class or as a curve indicating the cumulative % of particles undersize or oversize. Mean sizes can then be calculated as a frequency averaged particle diameter,

$$d_m = \frac{\sum n d}{\sum n} \quad \text{Equation 1.4.1}$$

or a volume averaged diameter,

$$d_m = \left(\frac{\sum n d^3}{\sum n} \right)^{1/3} \quad \text{Equation 1.4.2}$$

Analytical functions such as the normal distribution can make the manipulation of particle size data more convenient; two parameters define the whole distribution and it is not necessary to list a table or make a plot of the whole distribution. Particle size distributions of real systems rarely fit the normal distribution exactly but it is usually possible to transform the data (commonly using the logarithmic form of the normal distribution) to approximate to a normal distribution. The problem becomes more complicated when multimodal distributions are examined since it is necessary to split up the distribution and fit analytical functions to each peak.

1.4.2 Direct Observation of Particles

Provided that the particles produce an image that contrasts with their environment, optical microscopy can reveal information on their size and shape. The resolving power of the the microscope is determined by the wavelength of light used, the geometry of the optical system and the refractive index of the immersion medium. In practice particles below 400 nm cannot be accurately viewed.

The image gives a sample of the particle cross sectional areas and there are a number of 'diameters' [Allen (1981)] that can be

measured if the particle shape is irregular. The most useful of these is the projected area diameter, derived from a circle of equivalent area to the particle. The counting procedure for a measurement involves the selection of a circle to match the area of each particle and recording the diameter. The method is laborious if statistically significant results are to be obtained and there is a dependence on the judgement of the operator in the selection of equivalent circles. Jelinek (1974) describes a number of automatic and semi-automatic devices available to speed up the process of analysis.

1.4.3 Sedimentation

i) Gravitational settling: Where a density difference exists between the solid particles and the suspending medium, it is possible to use the particle settling behaviour as an indication of particle size. After a short period of acceleration the settling velocity of colloidal particles in water is observed to reach a constant value, the terminal settling velocity, u_t . At this point there is no acceleration and the forces acting on the particle must balance. Hence the upward drag force of the surrounding medium can be set equal to the gravitational force, $(M_s - M_L)g$, acting on the particle. The drag force is proportional to the particle velocity, u_t , and for rigid spherical particles in the laminar flow region the force is given by Stokes' Law as $3\pi d\mu u_t$. The force balance then results in a terminal velocity given by:

$$u_t = \frac{(e_s - e_L)gd^2}{18\mu} \quad \text{Equation 1.4.3}$$

Measurement of the solid-liquid density difference and the liquid viscosity enables the calculation of the particle diameter from values of the terminal settling velocity.

In a typical suspension it is impractical to measure the velocities of large numbers of individual particles and it is more usual to follow the variation of particle concentration with time. Devices are available that employ techniques such as light adsorption, X-ray adsorption or direct sampling to monitor

concentration with time and such data can then be interpreted as a particle size distribution [Allen (1981)]. When the density difference is low and long settling times are required there is likely to be interference in the results due to convective currents unless the temperature throughout the sample is very carefully controlled. Shorter settling times and a reduction in such errors are achieved by using centrifugal sedimentation.

ii) Centrifugal sedimentation: The principles of centrifugal sedimentation are essentially the same as those of gravitational settling. It is assumed that the particle rapidly reaches its terminal velocity where the forces acting on the particle are balanced. In the centrifuge, however, the terminal velocity will depend on the position of the particle since the centrifugal force, given by, $(M_s - M_L)\omega^2 x$, increases with x . Assuming that the drag force is given by Stokes' Law and integrating from x_1 to x_2 over the time t_1 to t_2 it can be shown that the particle size can be calculated from:

$$\ln \left(\frac{x_2}{x_1} \right) = \frac{(\rho_s - \rho_L) \omega^2 d^2 (t_2 - t_1)}{18 \mu} \quad \text{Equation 1.4.4}$$

There is no simple procedure for producing a cumulative curve for the distribution of particle sizes in a polydisperse sample [Jelinek (1974)]. However, it is possible to overcome the difficulties by adopting suitable experimental procedures. The sedimentation can be followed over distances which are short compared to the distance of the particle from the axis of rotation. The analysis is then simplified to settling at a constant centrifugal force. An alternative method, used for the Joyce-Loebl centrifuge, involves a thin layer of the sample being applied to the dispersion medium. It can then be assumed that the particles all start from the same position and the particle size distribution can be derived from a measurement of the positions after a fixed time interval.

1.4.4 Electrical Sensing

Observation of the change in resistance across a small orifice as particles pass through can be used to count and size particles

electronically. The pulses generated are collected and used to produce a number distribution of particle size. This can then be converted to a mass distribution of spherical particles of constant density. The particles are suspended in an electrolyte solution (typically 10 kg/m³ sodium chloride); low particle concentrations are required to minimise 'coincidence effects', i.e. recording of the presence of more than one particle in the orifice at one time. The lower limit of the instrument is determined by the ability to manufacture small orifice sizes. Minimum orifice sizes of 16 μm are presently available and a lower limit of particle analysis of 0.3 μm is possible. In practice operation with small orifices may be hampered by the presence of large particles blocking the orifice.

1.4.5 Light Scattering

i) Intensity measurements: It has long been recognised that the intensity of light scattered from a particle, I , relative to the incident light, I_0 , is a strong function of the size of the particle, d . The equation for Rayleigh scattering is:

$$\frac{I}{I_0} = \frac{8\pi^4}{\lambda^4 r^2} \left(\frac{\alpha}{4\pi\epsilon_0} \right)^2 (1 + \cos^2 \theta) \quad \text{Equation 1.4.5}$$

where, for spheres, the polarisability, α , is given by:

$$\alpha = 4\pi\epsilon_0 d^3 \frac{(n^2 - 1)}{(n^2 + 2)}$$

n is the refractive index relative to the surrounding medium, n_0 . Obtained in the nineteenth century, Equation 1.4.5 relates the scattered light at an angle, θ , to the diameter, d , of a single particle. The Rayleigh equation applies only for $d \ll \lambda$ and is therefore suitable for macromolecular sizing. For typical colloidal particles d is of the same order of magnitude as the wavelength of light and the Mie theory of scattering is required. The intensity scattering patterns predicted by Mie theory are very complex even for simple particle shapes and the fitting of the patterns obtained for irregularly shaped particles presents formidable problems even with the current advances in computer analysis.

ii) Dynamic light scattering: The shift in frequency of re-radiated light from the frequency of the incident light, in accordance with the well-established Doppler principle, forms the basis of particle sizing in dynamic light scattering. The frequency shift, resulting from Brownian motion of the particle, enables the diffusion coefficient to be calculated and the particle size can then be derived using the Stokes-Einstein relation:

$$D = \frac{kT}{3\pi\mu d} \quad \text{Equation 1.4.6}$$

The development of instruments with laser light sources with beams of precisely defined frequency together with the use of photon detectors and computers for the detection and analysis of the scattered light have allowed the exploitation of this technique and a number of instruments are now commercially available.

1.5 Rheology of Biological Materials

1.5.1 Particle Suspensions

Newtonian behaviour is predicted from theoretical treatments of dilute suspensions of spherical particles. The increased viscosity of the suspension, μ , compared to the viscosity of the pure liquid, μ_0 , is related to the volume fraction of solid material, ϕ , by the Einstein equation:

$$\mu = \mu_0(1 + 2.5\phi) \quad \text{Equation 1.5.1}$$

Theoretical analysis of suspensions of non-spherical particles is complicated by the orientation of the particles in the shear field and non-Newtonian flow is found even for dilute suspensions. For spheroidal particles theoretical expressions can be derived for the high and low shear behaviour of the 'intrinsic viscosity', a parameter defined by the equation:

$$[\mu] = \lim_{\phi \rightarrow 0} \left(\frac{\mu/\mu_0 - 1}{\phi} \right) \quad \text{Equation 1.5.2}$$

Measurements of this parameter sometimes give valuable

information on the shape of particles in suspension but the viscosity dependence with increasing shear rate cannot be calculated for arbitrary particle shapes [Hunter (1987)].

Deviations from the Einstein equation are observed as the influence of particle-particle interactions becomes significant. This may occur as the particle concentration is increased beyond a few percent and it is then necessary to modify the equation. For example, yeast suspensions have been fitted to the Vand equation [Deindorfer and West (1960)]:

$$\mu = \mu_0 (1 + 2.5\phi + 7.25\phi^2) \quad \text{Equation 1.5.3}$$

provided that $\phi < 14\%$.

Analysis of suspension viscosity in terms of particle concentration, size and shape is possible in only very simple cases. Materials such as fermentation broths, cell debris suspensions and protein suspensions contain soluble macromolecules as well as particles of diverse shapes and sizes. The influence of particle characteristics can play a secondary role compared to the effect of the soluble macromolecular material. Such systems are usually too complex for theoretical analysis. For viscous dominated flow it is usually possible to make use of empirical relationships of the type discussed in the next section.

1.5.2 Non-Newtonian Flow

The flow behaviour of simple Newtonian liquids under steady shear can be characterised by the value of the viscosity, μ , where

$$\tau = \mu \dot{\gamma} \quad \text{Equation 1.5.4}$$

For many suspensions and solutions of biological interest it is not possible to assume a constant value of the viscosity and a curve of the variation of shear stress with shear rate is required to describe the viscous flow of the material. The apparent viscosity, μ_a , is then determined by the ratio, $\tau/\dot{\gamma}$.

There are a number of models available which provide convenient methods of representing the flow behaviour of Non-Newtonian fluids, such as:

i) The Power Law model, $\tau = k\dot{\gamma}^n$, can be applied, at least over part of the flow curve, to most materials. When $n = 1$ the power law reduces to $\tau = k\dot{\gamma}$ and the 'consistency', k , represents the Newtonian viscosity, μ . If the value of n is less than 1 the 'pseudoplastic' behaviour of decreasing apparent viscosity, illustrated by curve 1 (Fig. 1.2), is produced. If the value of n is greater than 1 then 'dilatant' behaviour (curve 2, Fig. 1.2) occurs.

ii) Bingham plastic materials. Newtonian flow occurs when the applied shear stress exceeds a yield value, τ_0 , and the flow is described by

$$\tau = \tau_0 + \mu\dot{\gamma} \quad \text{Equation 1.5.5}$$

This equation can be generalised to

$$\tau = \tau_0 + k\dot{\gamma}^n \quad \text{Equation 1.5.6}$$

when the flow at shear rates in excess of the yield value is non-Newtonian. Other equations have been developed for specific systems - the Casson equation, for example, has been successfully applied to the flow of blood - but wide application of such models is not generally possible.

1.5.3 Pipe Flow of Power Law Fluid

For power law fluids, the equations for laminar flow in a pipe can be adapted to give expressions for the shear rate at the wall, $\dot{\gamma}_w$, and the mean velocity, u .

$$\dot{\gamma}_w = \frac{8u}{d} \left(\frac{3n+1}{4n} \right) \quad \text{Equation 1.5.7}$$

$$u = \frac{n}{3n+1} \left(\frac{\Delta P}{2Lk} \right) \left(\frac{d}{2} \right)^{\frac{n+1}{n}} \quad \text{Equation 1.5.8}$$

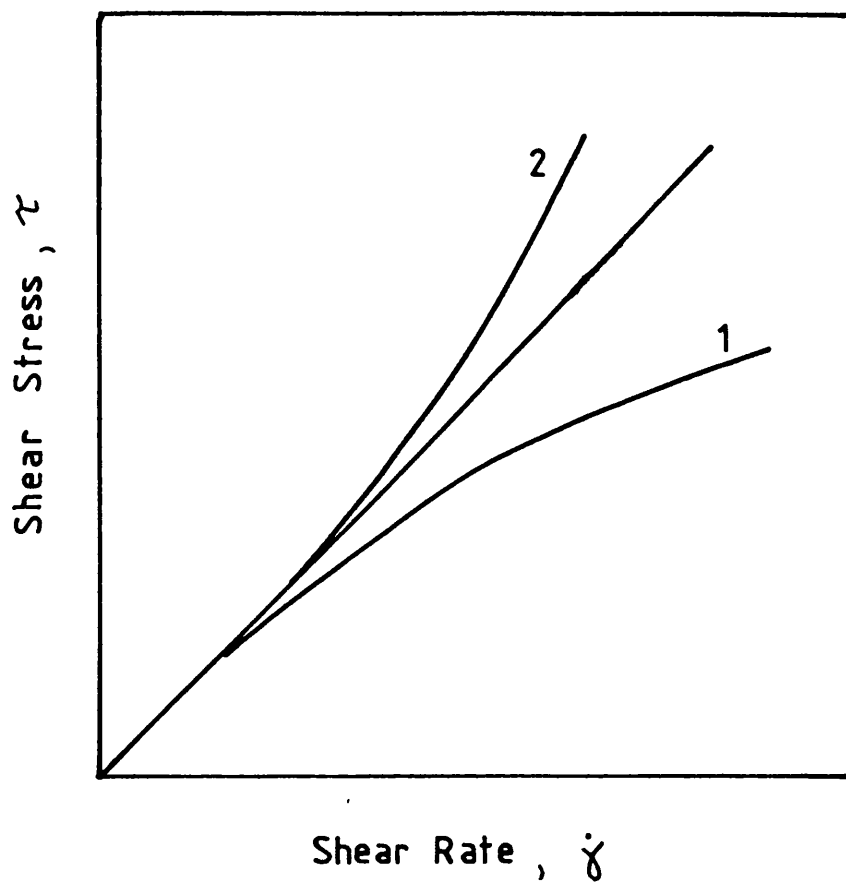


Figure 1.2 Variation of Shear Stress with Shear Rate for Non-Newtonian Fluids. 1. Pseudoplastic. 2. Dilatant.

The parameters n and k are derived from the power law equation, d is the pipe diameter and ΔP is the pressure drop along a pipe of length, L . A generalised Reynolds number, Re , is given by

$$Re = \frac{8\rho u^{2-n} d^n}{k(6 + 2/n)} \quad \text{Equation 1.5.9}$$

and the applied shear stress, τ , is given by

$$\tau = \frac{\Delta P d}{4L} \quad \text{Equation 1.5.10}$$

1.5.4 Viscoelastic Behaviour

Under high shear conditions the response of a suspension is dominated by the viscous characteristics and consideration of the shear stress - shear rate is appropriate. At lower shear rates solid-like properties may be displayed and it is necessary to consider the elastic response of the material. The strain produced by the imposition of a small shear stress on an ideal solid will be proportional to the shear stress and a shear modulus, G , can be defined by:

$$G = \frac{\tau}{\gamma} \quad \text{Equation 1.5.11}$$

On removal of the shear stress the original shape is completely recovered, since a perfect solid cannot flow. For 'viscoelastic' materials partial recovery of the original shape is observed and some flow occurs. The structure at any particular time is influenced by the entire deformation history up to that time. If it can be assumed that successive changes in strain are additive then the shear stress can be represented by:

$$\tau = \int_{-\infty}^t G(t-t') \dot{\gamma}(t') dt' \quad \text{Equation 1.5.12}$$

If a sudden strain is imposed on a material over a short period of time it is possible to show that:

$$\tau \approx G(t) \gamma \quad \text{Equation 1.5.13}$$

Where $G(t)$ is the time dependent analogue of G . Information about

the mechanical behaviour of the material can be obtained by following the decay of the shear stress with time at a fixed strain.

Alternatively it is possible to define the strain in terms of the rate of change of shear stress, $\dot{\tau}$, and the 'creep compliance', J , by:

$$\gamma = \int_{-\infty}^t J(t-t') \dot{\tau}(t') dt' \quad \text{Equation 1.5.14}$$

Under the imposition of a sudden shear stress it can be shown that:

$$\gamma = J(t) \tau \quad \text{Equation 1.5.15}$$

Following the variation of strain with time after subjecting the material to a sudden fixed shear stress therefore gives information on the creep compliance. In general the creep compliance is not related to the shear modulus; only for a perfectly elastic material does $J = 1/G$.

A number of experimental arrangements for following the variation of shear rate with strain are possible but it is generally more convenient to characterise a material by examining its response to an oscillating shear field. Under a periodic strain of maximum amplitude, γ_0 , and frequency, ω , given by:

$$\gamma = \gamma_0 \sin \omega t \quad \text{Equation 1.5.16}$$

the shear rate will vary according to:

$$\dot{\gamma} = \omega \gamma_0 \cos \omega t \quad \text{Equation 1.5.17}$$

Using the equation relating the shear stress to the shear strain given above it can be shown that:

$$\tau = \gamma_0 (G' \sin \omega t + G'' \cos \omega t) \quad \text{Equation 1.5.18}$$

where the component of the shear modulus that is in phase with the strain, G' , is known as the storage modulus and the component that is out of phase with the strain, G'' , is the loss modulus. For a purely elastic solid the stress and strain are always in

phase, $G'' = 0$, and G' is equal to the shear modulus. For a purely viscous liquid $G' = 0$ and the shear stress is always in phase with the strain rate. Hence the viscosity is given by:

$$\mu = \frac{\tau}{\dot{\gamma}} = \frac{\tau}{\omega \gamma_0 \cos \omega t} = \frac{G''}{\omega} \quad \text{Equation 1.5.19}$$

For a viscoelastic fluid a viscosity can therefore be defined in terms of the components that are in phase and out of phase with the strain rate:

$$\mu = \mu' \sin \omega t + \mu'' \cos \omega t \quad \text{Equation 1.5.20}$$

The shear stress equation is commonly expressed in terms of a phase lag, δ , so that:

$$\tau = \tau_0 (\sin \omega t + \delta) \quad \text{Equation 1.5.21}$$

and it can be shown that:

$$G' = \frac{\tau_0}{\gamma_0} \cos \delta \quad ; \quad G'' = \frac{\tau_0}{\gamma_0} \sin \delta \quad \text{Equation 1.5.22}$$

1.6 Membrane Separation Processes

1.6.1 Introduction

Ultrafiltration and microfiltration are useful methods for the processing of biological fluids. Both processes use semi-permeable membranes which allow the removal of solvent and small molecules when moderate pressures, 50-500 kPa, are applied across the membrane. The distinction between ultrafiltration and microfiltration is somewhat arbitrary but the conventional classification defines a microfiltration membrane as one which allows the passage of soluble species while rejecting particles exceeding the nominal pore size of the membrane (usual range 0.1-10 μm). An ultrafiltration membrane, in addition to rejecting small particles, is capable of rejecting soluble species such as protein macromolecules and is usually characterised by a molecular weight cut-off rather than a typical pore size.

Membrane processes are particularly attractive for the concentration of fragile biological species since mild conditions can be used. Denaturation of products sensitive to changes in temperature, pH and ionic strength can therefore be avoided by maintaining a constant microenvironment on both sides of the membrane. In biochemical engineering the potential applications of membrane separations include cell harvesting and product separation from fermentation broths, the purification of macromolecular solutions and the dewatering of protein precipitate and colloidal suspensions. It is also possible to incorporate a membrane separation into a bioreactor to enable product removal while retaining the active species (cells or enzymes) in the reactor.

Widespread application of ultrafiltration and microfiltration has been limited by the poor and unpredictable flux rates that are obtained in many cases. Although membranes have been developed to give high flux rates with pure water, the flux rates with process streams are much lower. The result of using a semi-permeable membrane is that the rejected species builds up on the surface of the membrane, producing a concentration gradient (known as concentration polarisation) and hindering subsequent solvent flow. Flux reduction due to polarisation cannot be avoided but it can be alleviated by providing a mechanism of removing the polarised species from the membrane surface and back into the bulk of the solution. This is commonly achieved by stirring the fluid or flowing the fluid across the surface of the membrane. The use of mass transfer models to describe the polarisation of the membrane is discussed in Sections 1.6.2 and 1.6.3. Although the precise mechanism of flux reduction is uncertain it is nevertheless established that polarisation can be controlled by the flow of fluid across the membrane surface and a variety of cross-flow modules have been developed. The use of cross flow geometry to optimise the process is discussed in Section 1.6.6.

In addition to concentration polarisation it has been observed that flux rates decline with time due to fouling of the membrane surface and blockage of the pores. Many membranes are

particularly susceptible to fouling by adsorption of proteins and severe flux reductions have been observed. The fouling problem is more acute with microfiltration membranes where flux rates can be reduced below the levels obtained with the less porous ultrafiltration membranes. The effects of fouling and methods of reducing the problem will be discussed in section 1.6.5.

1.6.2 Ultrafiltration of Macromolecular Solutions

If the flow through a membrane is considered to result from the flow through cylindrical channels of radius r then the flux rate, J , will be given by the Hagan-Poiseuille law for streamline flow:

$$J = \frac{\epsilon r^2 \Delta P}{8 \mu x} \quad \text{Equation 1.6.1}$$

With real membranes it may be difficult to measure precisely the values of the pore size, r , the porosity, ϵ , and the membrane thickness, x , because the channels will not be uniform in size or shape. However for a particular membrane it is expected that a constant value of $\epsilon r^2/x$ will be found and therefore the flux rate should be proportional to the applied transmembrane pressure, ΔP , and inversely proportional to the viscosity, μ , of the permeating solution.

Porter (1972), Blatt et al. (1970) and other workers have indeed found a linear increase of flux rate with pressure for the ultrafiltration of many solutions but only under a limited range of operating conditions. They also found a region in which the flux rate became independent of pressure and depended on the concentration of the rejected species in the fluid and the flow conditions at the membrane surface. In this region modelling of the mass transfer at the membrane surface has been applied to explain the flux rate behaviour.

As solvent molecules are removed from the solution there will be an accumulation of rejected macromolecules at the membrane surface and a concentration profile is set up with bulk concentration, C_b , in the main body of the fluid and a concentration, C_w , at the membrane surface. At sufficiently high

pressure it is supposed that the concentration at the membrane reaches a limiting value, C_g , where the solution gels and forms a layer on the membrane. At this point the flux rate is controlled by the hydrodynamic resistance of the gel layer and further increases in transmembrane pressure result only in the formation of a thicker gel layer without increasing the flux rate.

Michaels (1968) has shown that, when the membrane is gel-polarised, it is possible to derive an equation for the limiting flux, J :

$$J = k \ln(C_g/C_b) \quad \text{Equation 1.6.2}$$

The mass transfer coefficient, k , is determined by the flow conditions at the membrane surface and can be obtained from correlations of the Sherwood number, Sh , with the Reynolds number, Re , and the Schmidt number, Sc :

$$Sh = A_0(Re)^a(Sc)^b \quad \text{Equation 1.6.3}$$

The values of A_0 , a and b depend on the development of the concentration and velocity profiles, as discussed by Cheryan (1986). The usual expression used for laminar flow is:

$$Sh = 1.86 [(Re)(Sc)(d_h/L)]^{0.33} \quad \text{Equation 1.6.4}$$

The physical basis of the formation of a gel on the membrane surface at a fixed concentration is questionable. Nakao et al. (1979) have found that gel concentrations for polyvinyl alcohol and ovalbumin are dependent on the feed concentration and the flow conditions. Ingham et al. (1980) reported that C_g values for albumin were below the solubility limits at which gelling of the protein solution was expected.

It is assumed in the gel polarisation model that the osmotic pressure of the rejected species is negligible compared to the applied pressure across the membrane. At typical ultrafiltration feed concentrations, osmotic pressures (calculated from the van't Hoff equation) are much less than the usual applied pressures of ca. 200 kPa [Cheryan (1986)]. However polarisation of the

membrane can produce concentrations at the membrane surface outside the range of application of the van't Hoff equation which gives a good approximation only for dilute solutions. Vilker et al. (1984) measured osmotic pressures of 100-400 kPa at concentrations of 300-500 g/L for BSA but other macromolecular solutions (bovine fibinogen, human low density lipoprotein and polyethylene oxide) exhibited much smaller osmotic pressures. Vilker et al. (1984) concluded that osmotic pressure could describe the flux rate for the ultrafiltration of medium molecular weight solutes using an equation of the form:

$$J = \frac{P - \pi_0}{\mu(R_m + R_p)} \quad \text{Equation 1.6.5}$$

Where π_0 is the osmotic pressure, P is the applied pressure, R_m is the membrane resistance, and R_p is the resistance of the polarisation layer. A similar conclusion was reached by Wijmans et al. (1984) who introduced a quantity, $\pi_0 n / R_{mk}$, to determine the relative importance of the osmotic pressure. For high values of this ratio (>19) they reported osmotic pressure limitation more likely than gel layer limitation.

The doubts concerning the formation of a true gel at a fixed concentration [Nakao et al. (1979)] and the large overprediction of flux rates in some systems (notably colloidal suspensions, discussed in section 1.7.3) are fundamental shortcomings in the gel polarisation theory. Despite these problems the gel model has been used by many workers to produce plots of flux against log feed concentration and is convenient for estimating the effect of operating conditions on the flux rate using mass transfer correlations.

1.6.3 Suspensions

For colloidal suspensions, variations in flux rates with cross-flow velocity which do not conform to mass transfer correlations and experimental flux rates one or two orders of magnitude higher than predicted by the gel polarisation model have been reported by Porter (1972). With dilute suspensions flowing through thin channels, Segre and Silderberg (1961) observed the migration of

particles away from the walls of the channel. This 'tubular pinch effect', according to Porter, augments the back diffusion of particles from the membrane during cross flow ultrafiltration and results in higher permeate flux rates and a greater dependence of flux rates on cross flow velocity.

Consideration of the result of a lift force away from the membrane and the permeation drag force taking the particle towards the membrane led Belfort et al. (1982) to conclude that, for a given system, the flux rate, J , can be obtained from an equation of the form:

$$J = A_1u^{0.33} + A_2u^2 \quad \text{Equation 1.6.6}$$

which implies a greater sensitivity of flux rate to crossflow velocity, u , than predicted by the gel polarisation model. Belfort and Altena (1983) claim that this extension of the gel polarisation model to include a lateral migration term is supported by the many examples in the literature of dependence of flux on crossflow velocity raised to a power in the range 0.33-2. Further development of this analysis by Altena and Belfort (1984) demonstrated that the lift force would dominate migration away from the membrane for particle diameters exceeding $1 \mu\text{m}$. The method of Belfort can be used to give improved accuracy of flux prediction for colloidal suspensions [Green and Belfort (1980)] when combined with standard filtration theory but requires iterative calculation.

Fane (1984) compared the ultrafiltration behaviour of colloid suspensions with particle sizes ranging from 25 nm to $20 \mu\text{m}$ under stirred and unstirred conditions. Without stirring the finer colloid gave the lower flux rate as predicted when the process is considered as cake filtration and the resistance of the cake related to the particle properties. However when the suspension was stirred the finer colloid gave the higher flux. Evidently the permeate flux is determined by the result of two effects:-

i) the permeability of the cake or polarized layer, which increases with increasing particle size.

ii) the thickness of the cake layer which, in the presence of forces to provide back transport, increases with increasing particle size.

When mixtures of both suspended solids and dissolved macromolecules are ultrafiltered, the interaction of the solids with the soluble components causes further complications. The presence of particles may enhance the flux rate by 'scouring' the macromolecular polarised boundary layer and reducing its resistance as described by Fane et al. (1982). On the other hand, particles may hinder the back diffusion of the macromolecules from the polarised layer and thus increase the resistance. It is difficult to predict which of these effects will dominate in a given system. Fane (1986) has taken a number of examples from the literature of protein and polysaccharide ultrafiltration and tabulated characteristics of systems where the effect of suspended solids is to reduce flux and compared these parameters with systems where flux is enhanced by suspended solids. From this comparison Fane (1986) concluded that fine colloids ($< 0.1 \mu\text{m}$) are likely to cause flux reduction while for large, rigid particles ($> 1 \mu\text{m}$) flux enhancement is probable. These guidelines must be applied with care since many exceptions have been noted. For relatively large solids such as bacterial cells a reduced flux is observed and is attributed to the compressible nature of the solids. Also, when the soluble macromolecular concentration is low and the flux is high, flux reduction may occur with large, rigid solids.

1.6.4 Microfiltration

The higher porosities of microfiltration membranes, compared to ultrafiltration membranes, and the resulting high water flux rates make the use of microfiltration potentially more efficient for the concentration of suspensions. A number of important separations in biotechnology could be achieved using microfiltration, since the pores of microfiltration membranes are large enough to allow the passage of proteins while retaining particles such as cells, cell debris and precipitates.

In the prediction of flux rates for microfiltration no single model has found universal acceptance. It has been argued that because the particle sizes involved in microfiltration are several orders of magnitude larger than those in ultrafiltration [Fischer and Raasch (1985)] then the role of the diffusion coefficient in the process is negligible and the principles applied to ultrafiltration are unsuitable for the modelling of microfiltration flux rates. Zydney and Colton (1986) have found agreement with experimental values by predicting flux rates from a concentration polarisation model incorporating a shear enhanced diffusivity. Others, such as Bertera et al. (1984), have found that their studies do not fit any specific model and indicate that prediction of performance is difficult without extensive trials with individual products.

While microfiltration membranes have been applied to some separation processes, their performance often falls short of their full potential. The primary cause of poor performance is the fouling of the membrane, frequently more severe than for ultrafiltration membranes due to the adsorption of the foulant within the pores of the microfiltration membrane. Entrapment of material in the pores limits the effectiveness of cleaning operations and precludes the use of surface coatings to control fouling. In the early stages of many microfiltration trials rapid flux decline has been observed [Kroner et al. (1984), Le et al. (1984a), Datar (1985)] and the resultant flux rates may be no better than those obtained with ultrafiltration as shown by Patel et al. (1987) for the filtration of yeast cells. Low transmission of the required product in the permeating stream leads to unacceptably low efficiencies when compared to alternative separation methods [Kroner et al. (1984)] although some analyses, for example Tutunjian (1985), have demonstrated cost savings when cross flow microfiltration is used instead of centrifugation for the recovery of *E. coli* bacteria.

In some circumstances the containment of hazardous organisms may favour the use of microfiltration over other operations, even when the operating efficiency is low. However, the widespread application of the process will not be achieved unless reliable

high flux rates can be obtained and the efficiency of the separation improved.

1.6.5 Fouling

The ultrafiltration theories outlined in section 1.6.2 require that the membrane acts simply as an inert barrier to species exceeding a certain size. Deviations from this ideal situation are encountered in practice because of the tendency for the membrane to interact with the solution and cause time dependent changes in the flux rate. The initial flux decline observed with ultrafiltration membranes can be attributed to the polarisation of the rejected species. This polarisation is reversible and rapidly reaches equilibrium with typical polarisation times of ca. 60 s [Fane (1986)]. It is often found that the decline in flux rate continues beyond this initial period and the original membrane performance is not easily recovered. The membrane is then 'fouled' and a number of factors may be responsible. These include the contamination of the membrane by bacteria, ion binding, solvent interaction, changes in pore structure, adsorption of solute and plugging of pores.

In the ultrafiltration of proteins the adsorption of the macromolecule plays a key role and has been linked to flux decline in studies by Chudacek and Fane (1984) and Reihanian et al. (1983). Bovine serum albumin adsorption of the order of 0.02-0.05 g/m² has been deduced from the carbon-14 labelling technique used by Matthiasson (1983). Indirect measurements of BSA adsorption by Fane et al. (1983) indicate values of 0.5-2 g/m². The nature of the membrane, presence of an air-liquid interface, salt concentration, pH and system hydrodynamics can affect the deposition and complicate the prediction of flux rates. It is possible to accommodate the fouling process within the theoretical analysis of ultrafiltration by incorporating a time dependent fouling resistance which is added to the membrane and polarisation resistances of equation 1.6.5 to give an equation of the form:

$$J = \frac{P - \Pi_0}{\mu(R_m + R_p + R_f)} \quad \text{Equation 1.6.7}$$

It may be convenient to represent data using semi-empirical models which allow for fouling effects and the deposition of BSA has been modelled in this way by Suki et al. (1984).

Adsorption of solutes will also affect the rejection by the membrane. The molecular weight cut-off of a particular membrane will depend on the solute used to determine the cut-off, the solute environment and the extent to which the solute adsorbs to the membrane [Zeeman (1983)]. Particular difficulties are encountered when the fractionation of a mixture of proteins is attempted since the adsorption of one protein will affect the rejection of the others [Ingham et al. (1980)]

It has been suggested by Reihanian et al. (1983) that surface treatment to minimise adsorption would be a promising method of sustaining high ultrafiltration rates. Bauser et al. (1986) demonstrated that permanent improvements in ultrafiltration flux rates resulted from the use of a carbon coating on ultrafiltration membranes. An alternative method of reducing fouling, proposed by Howell and Velicangil (1980) is to immobilize a proteolytic enzyme on the membrane surface where it can break down foulant as it is deposited.

The work of Breslau et al. (1980) on the recovery of electrocoat paint illustrated that the choice of membrane can be critical with some process streams. They found that a negatively charged membrane which had been successfully employed for the concentration of anodic paint became severely fouled within a short time when used for the processing of cathodic paint. However by switching to a positively charged membrane for the cathodic paint they were able to reduce the fouling problem.

While the tailoring of the membrane to suit the feed solution is possible in some cases, there may be technical or economic limitations to the widespread employment of such an approach. Control of fouling by the adjustment of the system hydrodynamics is likely to find more general application. For the ultrafiltration of complex suspensions high cross flow velocities will limit fouling by a combination of diffusible mass transfer,

radial migration and scour [Fane et al. (1982)].

In practice it is not possible to eliminate fouling completely and flux decline often has to be reversed by including a cleaning cycle in the process. Cleaning may be effected by reversing the flow of permeate through the membrane to remove the fouling layer or by the use of chemicals such as enzymes or detergents.

1.6.6 Geometry of Filtration System

For the concentration and purification of small volumes of material a batch cell, with pressure applied across a flat sheet of membrane, may be suitable provided that the polarisation and fouling of the membrane are not severe. For efficient membrane filtration alternative designs are required in which the polarisation and fouling of the membrane can be reduced. A number of designs for commercial filtration modules have arisen from the use of cross-flow to enhance permeate flux. The commonly applied systems include:

i) Plate and frame. Flat sheets of membrane are stacked together and separated by mesh spacers through which fluid can be pumped across the membrane surface. This is the simplest cross-flow design, has low capital costs and is useful if membrane sheets frequently need replacing since individual membrane sheets can easily be removed.

ii) Spiral wound. One continuous flat sheet is wound into a spiral together with a sheet of spacer material to separate the membrane surface and allow cross-flow of fluid. The winding of flat sheets into spiral modules has the advantage of lowering the space required per unit membrane area compared to the plate and frame arrangement.

iii) Hollow fibre. Where the membrane material can be cast in the form of hollow fibres the use of mesh spacers can be avoided. Hollow fibre modules have typically 200-300 fibres of ca. 1mm diameter sealed in an outer shell in which the permeate can collect. The modules are expensive to replace and if one fibre

fails in a unit it is often necessary to replace the whole module.

iv) Tubular. The thin channel systems (i-iii) are susceptible to blockage by particles lodging in the channels. Hence for the filtration of slurries containing relatively large particles tubular membranes with flow channels of 10-25 mm are often used.

Mass transfer theory indicates that it is desirable to operate cross-flow systems with high wall shear rates. Thin channel systems are particularly effective because they can produce high shear rates at the membrane surface while operated in laminar flow. Flat sheet systems are likely to be more expensive to operate than hollow fibres because the presence of mesh spacers to separate the membrane causes drag on the fluid and consequently increases pumping costs. Tubular systems are usually the most expensive to run since they are operated in the turbulent flow regime and the power requirements in terms of pumping costs are therefore higher than for laminar flow systems.

1.7 Centrifugation

1.7.1 Principles of Centrifugal Separation

Equations for the unhindered settling of a single particle in an infinite fluid medium can be used to develop a theory of sedimentation in a centrifugal field. When a particle reaches equilibrium in the laminar flow region a balance of the centrifugal force and the viscous drag acting on the particle leads to the Stokes' law equation for the terminal velocity of the particle:

$$u_t = \frac{\Delta \rho g d^2}{18 \mu} \quad \text{Equation 1.7.1}$$

This equation applies when the diffusion due to Brownian motion is negligible and the Reynolds number is small ($Re < 0.2$). For larger particles and higher velocities ($Re > 0.2$) the analysis of Stokes' law is invalid. Expressions for the terminal settling

velocity outside the Stokes' region are developed using drag coefficients appropriate to non-laminar flow conditions [Hsu (1981)] but these equations are not normally implemented in connection with centrifuge performance. It is usually assumed that the larger particles will be separated with 100% efficiency and it is the behaviour of the fine particles, in the Stokes' region, which needs to be considered in evaluating the overall efficiency of the centrifuge.

The performance of a centrifugal separator can be assessed in terms of a total efficiency defined as the ratio of the mass of all particles separated to the mass of all solids in the feed. Since this measurement will depend on the particle size distribution of the feed it is unsatisfactory as a general assessment of efficiency without particle size information being supplied. Svarovsky (1977) describes how for a given set of operating conditions it is possible to obtain a grade efficiency curve indicating the mass efficiency of separation for each particle size. This enables a limit of separation - the particle size above which all particles are separated with 100% efficiency - to be defined. It is also possible to define an equiprobable size on the grade efficiency curve at the point of 50% separation efficiency and this point is often used as the 'cut' size in the measurement of centrifuge performance.

The point of equiprobable separation was used by Ambler (1959) to develop the 'Sigma Theory' as a basis for centrifuge scale up. For a simple tubular centrifuge where the liquid layer thickness, s , is small compared to the radius of the cylinder, r , it was shown that with the critical particle diameter, d , at 50% separation efficiency:

$$Q = \frac{\Delta \rho d^2 V \omega^2 r}{9 \mu s} \quad \text{Equation 1.7.2}$$

where Q is the rate of liquid flow through the bowl, V is the volume of liquid in the bowl, $\Delta \rho$ is the density difference between solid and liquid, ω is the speed of rotation of the bowl and μ is the liquid viscosity.

An index of centrifuge size, Σ , is defined by rewriting equation 1.7.2 as:

$$Q = 2 u \Sigma \quad \text{Equation 1.7.3}$$

where u is given by Stokes' law, Equ. 1.7.1, and Σ is given by

$$\Sigma = \frac{\omega^2 r' V}{g s'} \quad \text{Equation 1.7.4}$$

with r' and s' the effective radius and settling distance for any centrifuge of this type.

1.7.2 Types of Sedimentation Centrifuge

A number of designs of industrial centrifuge have resulted from the variety of methods that can be used for the collection of the solid and liquid streams and the choice of geometries for the centrifuge. The centrifuge commonly falls into one of three basic categories:

i) Solid Bowl: The suspension is fed along the axis of a cylindrical bowl while the bowl rotates about that axis. Solids are collected on the wall of the bowl and the clarified liquid exits when the liquid level reaches the overflow height. When the length-to-diameter ratio is large, typically 4-8, the centrifuge is known as a 'tubular' centrifuge; when the ratio is smaller, around 0.5, the centrifuge may be referred to as a cylindrical bowl centrifuge or an imperforate basket centrifuge. A multi chamber centrifuge, consisting of a number of concentric chambers, is often used when increased clarification area is required.

The solid bowl centrifuge is the simplest in design and is capable of generating high accelerations (17,000g in a tubular bowl) for the separation of very fine particles provided that the solids concentration is low. This type of centrifuge is unlikely to be suitable for solids concentrations greater than 1% since frequent emptying of the bowl by hand is then required.

ii) Disc-stack: The disc-stack centrifuge consists of a rotating bowl in which closely spaced conical discs - typically 1 mm apart - separate the feed suspension into thin layers. In each layer the denser phase settles on the underside of the upper disc and then slides towards the edge of the disc while the clarified liquid flows inwards and then out through the top of the centrifuge. Operation may be batch-wise with the solids discharged by opening the bowl by hand, semi-continuous with solids ejected from the bowl intermittently but without interrupting the process, or fully continuous with solids discharge controlled by valves or nozzles on the bowl periphery. Solids-ejecting centrifuges can handle feed concentrations as high as 20% with throughputs up to 100 m³/h while nozzle centrifuges will cope with 10% solids at up to 200 m³/h. The flow properties of the concentrated sediment may be a limitation in the use of disc-stack machines.

iii) Scroll Decanter: Scroll decanter centrifuges can have a conical or cylindrical bowl although current designs usually have both cylindrical and conical sections. The feed may be introduced at any point in the bowl via a tube and the solids which settle on the wall are continuously removed by the action of a scroll which rotates at a slightly different speed to that of the bowl. The depth of the 'pond' formed by the liquid in the bowl is governed by adjustable discharge ports and can determine the area of 'beach' formed at the conical end of the bowl where the solids are conveyed out of the liquid before being discharged.

For the centrifugal processing of suspensions over a wide range of solids content (up to 80% by volume) scroll centrifuges are probably the most versatile design. The continuous discharge of solid material makes this centrifuge attractive for the settling of biological solids which have difficult rheological properties at high solids concentrations. The development of a high yield stress in, for example, soya protein precipitate sludges [Devereux et al. (1984)] and yeast debris sediments [Mosqueira et al. (1981)] may cause the discharge ports of intermittent-discharge centrifuges to become blocked. The sticky nature of

such materials causes problems for tubular bowl centrifuges which have to be frequently cleaned.

The scroll centrifuge is not capable of generating the high centrifugal forces possible in tubular bowl and disc-stack centrifuges and is consequently unsuitable when removal of very fine solids (ca. $1\ \mu\text{m}$), with density close to the suspension, is required. However, when the solids are fine it may still be convenient to use the scroll centrifuge if the solids can be aggregated as described in section 1.3.

1.7.3 Problems in Centrifuge Scale-up

While Stokes' law and the Sigma theory provide a useful starting point for the design of centrifugal separators and the prediction of separation performance, in practice such theoretical treatments should be applied with caution. The sigma theory considers only throughput and effective settling area of the centrifuge and does not include a number of factors which will influence the clarification of a suspension or the extent of dewatering achieved by a centrifuge. Faust and Gosele (1986), using a scroll decanter centrifuge with a transparent perspex bowl, observed resuspension of settled material due to the impact of the incoming feed stream. In disc-stack centrifuges irregularities in the flow of suspension between the discs will affect particle settling rates and capture by the disc. The effects of non-ideal flow patterns and the levels of turbulence in the centrifuge on the separation are difficult to scale from one type of centrifuge to another. It is therefore difficult to use laboratory data obtained in bottle centrifuges for prediction of the performance of large-scale industrial machines such as the scroll centrifuge although there have been attempts to introduce efficiency factors [Morris (1966)] to account for the differences between centrifuge geometries.

The scale-up of centrifuges from pilot-scale to full-scale industrial operations is more reliable when identical types of centrifuge are used [Svarovsky (1977)] but even then there can be problems. Gosele (1980), examining the scale-up of scroll

centrifuges, has shown that turbulent backmixing may affect the observed clarification and recommended scale up on the basis of turbulent power per unit volume. However, for particles which break up in the turbulent inlet zone but reaggregate as they are carried through the centrifuge bowl, Gosele (1980) found that the residence time in the centrifuge may be more important than the turbulence.

In the design of industrial-scale centrifuges the collection of extensive amounts of data using pilot machines is required. This data is particularly important for the scroll decanter centrifuge where the solids transport in the screw conveyer and the turbulence created by the rotation of the screw relative to the bowl leads to complex flow patterns in the centrifuge. Variation in performance can be expected from adjustment of the machine operating parameters such as liquid discharge height and scroll speed relative to bowl speed. Records (1974) has described these factors from a practical point of view for scroll operation.

1.8 Systems for Study

1.8.1 Soya Protein Precipitate

Soya protein solutions and precipitates provide a convenient system for study since a soya protein mixture can be easily and cheaply prepared from soya flour. The properties of the particles formed by precipitation of the protein solution will determine the requirements of the separation process. For soya protein, the formation of the precipitate by adjustment of the pH to the isoelectric point has been used in a number of studies. Salt et al. (1982) found that a wide range of mixing conditions could be used without causing extensive loss of protein when sulphuric acid was used as the precipitating agent.

The properties of the precipitate particles such as size, shape and density have been studied by Virkar et al. (1982), Bell and Dunnill (1982), Bell et al. (1982), and Hoare et al. (1982). Methods of improving these properties to enhance the efficiency

of centrifugal recovery of the precipitate have been demonstrated by Bell and Dunnill (1982a). They found that the strength of the precipitate aggregates could be improved by ageing the suspension in a stirred tank and thus reducing break-up during pumping to the centrifuge and in the high shear feed zone of the centrifuge. Changing the reactor configuration from a stirred tank to a tubular reactor for the preparation of the precipitate produced weaker aggregates which were found to be more difficult to recover in a scroll centrifuge [Bell and Dunnill (1982)].

The separation efficiency of soya aggregates in a disc-stack centrifuge was not affected by the strength of the aggregates when examined by Bell and Dunnill (1982). While precipitate break-up still occurs in the centrifuge feed zone, the disc-stack centrifuge was able to recover the fine particles produced by shear break-up and thus differences between the strength of batch- and tubular-prepared precipitates did not affect the separation. During disc-stack operation, extensive dewatering of the protein sediment leads to a product which is difficult to discharge from the bowl. For the recovery of soya protein precipitate, which is readily sedimented, the use of the disc-stack centrifuge of relatively high centrifugal force (rcf 9215) is not required and the scroll centrifuge (rcf 2130) is more appropriate.

Particle size and resistance to shear break-up have been found to affect membrane recovery of soya protein precipitate. Devereux and Hoare (1986) observed lower resistance to permeation with higher particle diameters during the ultrafiltration of soya protein precipitate with protein concentrations in the range 33-106 kg/m³. Since membrane systems are operated under conditions of high shear to minimise concentration polarisation, it is important that the protein aggregates prepared are resistant to shear break-up. The ageing experiments which Bell and Dunnill (1982a) applied to centrifugation can be usefully adapted to the preparation of soya suspensions for ultrafiltration.

Devereux et al. (1984) have compared disc-stack centrifuges and scroll centrifuges with ultrafiltration equipment for the

separation of soya protein precipitate. The capacity of a membrane or centrifugal separator will be dependent on particle properties. Centrifuge throughput will be limited by the settling characteristics of the particles and membrane flux rates will be limited by the interaction of the suspension with the membrane.

In all three types of separation equipment the performance of the process is limited by the rheological properties of the concentrated suspension or sediment. It is important that the flow properties of the concentrate are considered in the design of the separation process. In a disc-stack centrifuge the viscoelastic flow properties of the sediment affect the discharge from the centrifuge bowl and the production of a non-homogeneous sediment may be detrimental to the further processing of the product. In the scroll centrifuge the viscous flow properties of the sediment will affect the transport of solids along the screw conveyor and out of the centrifuge bowl. The compression of the sediment in the centrifugal field and the response of the sediment to the shearing of the scroll centrifuge will determine the extent of dewatering obtained in the centrifuge. The viscous flow of the concentrated suspension also limits the extent of dewatering in the cross flow ultrafiltration of soya [Devereux et al. (1986)] where polarisation of the membrane and permeate flux rates can be controlled by the flow of the suspension across the membrane surface.

Devereux et al. (1984) observed a rapid rise in the shear modulus of soya precipitate sediment as the concentration of the sediment increased from 250-300 kg/m³ and concluded that in this range the suspension was becoming structured and developing solid-like properties. At these concentrations it is expected that problems will be encountered in maintaining the flow of the suspension. This was indeed found by Devereux et al. (1986) during the concentration of soya protein precipitate using hollow fibre ultrafiltration membranes. They found it was possible to maintain constant permeate flux rates through the membrane up to concentrations of 240 kg/m³ and 290 kg/m³ using fibre lengths of 1.09 m and 0.31 m respectively. At these concentrations they

observed a rapid decline in flux rate to values close to zero. This decline was too rapid to be attributed to concentration polarisation effects and was instead explained by the increasing viscosity of the retentate and the difficulties in maintaining cross-flow in the fibres.

In the scroll centrifuge, soya protein concentrations as high as 350 kg/m^3 have been obtained [Devereux et al. (1984)]. It is one purpose of the studies in this thesis to examine whether using cross-flow ultrafiltration, with appropriate choice of pumping equipment and hollow fibre geometry, it is possible to reach protein concentrations comparable to centrifugal separation. The rheological measurements of Devereux et al. (1984) will be extended to concentrations beyond 200 kg/m^3 and these measurements will be used to explain the flux behaviour of hollow fibre ultrafiltration systems at high concentrations.

Devereux et al. (1986) found permeate flux rates at high concentrations became limited by the soluble components of the protein mixture which were retained by the membrane. They proposed that improved permeate flux rates would be obtained if the membrane allowed the passage of this soluble fraction. Attempts to concentrate soya suspensions using microporous membranes which could pass the soluble proteins while retaining the precipitate particles in an unstirred batch cell [Devereux et al. (1986)] and in cross-flow hollow fibres [Devereux and Hoare (1986)] resulted in severe flux decline due to pore blockage and final flux rates below those obtained with the less porous ultrafiltration membranes. In this study the interaction of soya protein solutions and suspensions with microporous membranes will be investigated further.

1.8.2 Yeast Cell Debris

The use of high pressure homogenisation for the disruption of Bakers' yeast has been described by Hetherington et al. (1971) for the release of intracellular protein and Follows et al. (1971) for the release of intracellular enzymes. Consistent supplies of yeast homogenate can therefore be prepared in order

to study the separation of protein solutions and cell debris material.

The commercial production and purification of intracellular proteins from yeast cells following high pressure homogenisation requires efficient methods for the removal of cell debris particles. The separation of cell debris from suspension is troublesome when the traditional methods of solid/liquid separation, such as filtration and centrifugation, are applied. Filtration is limited by the compressible nature of the solids, giving filter cake of low permeability, and penetration of fine particles into the filter medium, producing blockages. Filter aids alleviate these problems, as demonstrated by Gray et al. (1973), but filter aids are costly and are not always suitable because of the possible contamination of the product. The relatively new developments of membrane microfiltration may be useful for the removal of low level solids but the methods are not currently applicable for high solids concentrations. Fouling of the membranes reduces the flux rates and may cause rejection of the soluble proteins required in the product stream.

The typical characteristics of cell debris - small, highly hydrated particles, with a low density difference between debris and suspension - make centrifugal settling difficult. Mosqueira et al. (1981), using a disc-stack centrifuge for the separation of mechanically disrupted yeast cells, found removal of sediment was hampered by the blockage of discharge ports with viscous solids and the low flowrates required led to a temperature rise which may damage biological materials.

Centrifugal separation is strongly dependent on particle size (Stokes' Law) and is therefore more readily accomplished as the size of the particles to be separated is increased. The treatment of yeast homogenate with borax solutions to produce large flocs has yielded promising results in the laboratory experiments of Bonnerjea et al. (1988). Borax solutions flocculated the yeast cell debris and the flocs separated in a short time at low centrifugal forces in a laboratory centrifuge. Yeast enzymes, e.g. fumarase and alcohol dehydrogenase, remained

in solution without loss of activity. A mechanism of selective cross-linking of the debris through borate-carbohydrate bridges was proposed.

In this thesis the separation of flocculated yeast cell debris on a pilot plant scale is examined. The efficiency of a scroll decanter centrifuge for the clarification of the flocculated suspension and for the dewatering of the cell debris sediment is investigated. Particular reference is made to the rheological properties of the sediment in relation to the dewatering in the centrifuge.

After centrifugation of the borax-flocculated yeast homogenate there is still some residual turbidity in the supernatant [Bonnerjea et al. (1988)] and the remaining solids are characterised in terms of particle size and electrophoretic mobility. The effect of a polymer flocculating agent, polyethylene imine, on the mobility, aggregation and settling of the solids is described.

2. MATERIALS AND METHODS

2.1 Membrane Filtration of Soya Protein

2.1.1 Preparation of Protein Solutions and Protein Precipitate Suspension

For unstirred, laboratory, batch-cell studies, defatted soya flour (Interfood Ltd, Hemel Hempstead, Herts, England), 0.007 or 0.04 kg, was slurried with distilled water, 0.4 L, 295 K, using a magnetic stirrer. The suspension was adjusted to pH 9.0 +/- 0.1 with 2.5 M sodium hydroxide, and mixed for 0.25 h. The insoluble material, mainly carbohydrate, was removed by centrifugation at 1.2×10^4g and 298 K for 1.0 h (Hi-spin 21, MSE, Crawley, Sussex, England). Total water extract (TWE), 0.25 L, was decanted off and paper filtered once (Whatman No. 1 filter, W & R Balston Ltd., Maidstone, Kent, England). Soya precipitate suspension was obtained by adjusting the TWE to pH 4.6 with 3.5 M sulphuric acid and stirring for 0.25 h. The removal of protein precipitate by centrifugation at 1.2×10^4g and 298 K for 1.0 h (Hi-spin 21) produced supernatant protein solution, pH 4.6, which was paper filtered (Whatman No. 1 filter). Solutions were assayed for protein concentration using the Biuret method of Gornall et al. (1949). The amount of flour was selected to give a final soluble concentration of 6-7 kg/m³.

The laboratory cross-flow experiments required 3 L of TWE containing 9.0 +/- 0.5 kg/m³ protein. The starting material for this extract was 0.4 L of a dispersion of defatted soya flour at 200 kg/m³ in deionised water. Sodium azide, 0.2 kg/m³, was added to prevent microbial growth during long term experiments at room temperature and 0.125 kg/m³ mercaptoethanol was added to prevent oxidation of thiol groups and subsequent protein aggregation. The dispersion was adjusted to pH 9.0 +/- 0.1 using 10 M sodium hydroxide and after 0.5 h mixing at 313 K the insoluble carbohydrate was removed by centrifugation as described above. The TWE was filtered through two glass fibre filters (Whatman GF/D, W & R Balston Ltd.) and the resulting solution diluted 1:7

with deionised water to give the final required protein concentration.

For pilot plant cross-flow filtration experiments, soya flour (Interfood Ltd.), 11 kg, was mixed with deionised water, 100 L, at 293 K using a 3-bladed paddle of diameter 0.19 m driven at 48 rad/s in a baffled tank of volume 0.25 m³. The suspension was adjusted to pH 9.0 +/-0.1 using sodium hydroxide, 2.5 M, and mixing was continued for a further 0.5 h. The insoluble carbohydrate was removed using a disc-stack centrifuge (SAMR 3036, Westfalia Separators Ltd, Wolverton, Bucks., England) at a throughput of 0.18 m³/h with partial discharging of the bowl at intervals of 0.2 h. A back pressure of 3600 kPa was used to prevent excessive aeration of the supernatant. The clarified stream was collected and returned to the tank on completion of the centrifugation. After the addition of another 11 kg of soya flour (Interfood Ltd.) to the supernatant solution and further centrifugation (SAMR 3036) at pH 9 (as above) a protein solution of concentration 125 +/-15 kg/m³ was obtained and stored overnight at 276 +/-2 K.

The protein solution was heated to the required precipitation temperature and sulphuric acid, 3.5 M, was added to precipitate the protein from solution at its isoelectric point, pH 4.6 +/-0.1. The precipitate suspension was aged for 0.5 h before transferring a known volume of precipitate suspension to the ultrafiltration holding tank.

2.1.2 Microfiltration and Ultrafiltration

Laboratory microfiltration without cross-flow was carried out at 293 K in a batch cell (TCF 10, Amicon Ltd, Woking, Surrey, England) fitted with a microporous filter of effective area 4 x 10⁻³ m² (Asypor, Domnick-Hunter, Birtley, Co. Durham, England), using a new filter for each experiment. The filters, having asymmetric pores of nominal diameter 0.2 μm, were fixed with either the open or tight side adjacent to the feed; these are described as 'open side up' (OSU) and 'tight side up' (TSU), respectively. When charged with soya TWE (pH 8.8), soya

precipitate suspension (pH 4.6), or soya precipitate supernatant (pH 4.6 or 8.8), the cell was pressurised to 69 kPa gauge and the permeate volume was measured over fixed time periods.

Laboratory studies of the cross-flow microfiltration of TWE solutions were carried out with microporous filters (TSU) of nominal pore diameters 0.2, 0.45, 0.65, 0.8 and 1.2 μm in a stainless steel cell (in-house construction). A Perspex disc, incorporating a channel of cross-sectional area 10^{-5} m^2 (perpendicular to flow), supported the filter. The channel directed fluid over the membrane surface at a mean velocity of 1.28 m/s for a volumetric flow rate 12.8 mL/s. The equipment was operated with total recycle of permeate and retentate streams therefore, with negligible sample volumes, maintaining constant feed conditions. Inlet and outlet pressures were recorded and samples of permeate and retentate were taken for protein characterisation. The permeate protein concentration and permeate flow rates were monitored. Flux rates were calculated on the basis of a total exposed membrane area of $1.58 \times 10^{-3} \text{ m}^2$ and soluble protein transmission was defined as the ratio of soluble protein concentrations in the permeate and the feed, C_P/C_S .

The equipment used for the pilot-scale ultrafiltration of soya protein, illustrated in Figure 2.1, consisted of a holding tank, a pump and sections of pipework which could be adjusted to accommodate hollow fibre ultrafiltration cartridges of variable lengths. The rig has been described previously by Devereux et al. (1986) for the concentration of soya protein but the equipment was modified for the experiments described here to facilitate the processing of high concentration suspensions. The small cooling coil used in previous experiments was replaced by a larger coil running along the sides of the holding tank from the top of the tank to the outlet. Baffles were fitted in the holding tank and the retentate was mixed with an air-driven stirrer (GR-11, Gast, MFG, Benton-Harbor, Michigan, U.S.A.).

The majority of the experiments were run using a positive displacement pump (Mono Merlin, model SAC 12 HIR5/H1, Monopumps,

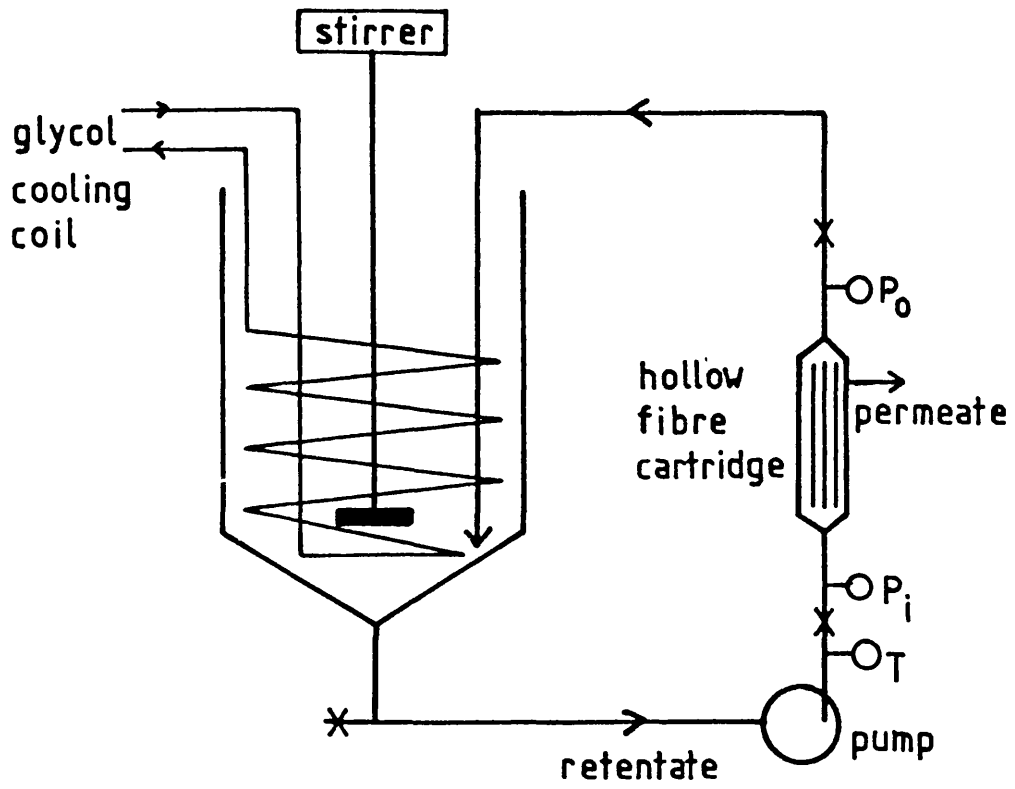


Figure 2.1 Pilot Plant Ultrafiltration Equipment

Manchester, England) to recirculate the retentate at flow rates of 0.3 - 2.0 m³/h through the hollow fibres although some experiments were carried out using a centrifugal pump (Puma shrouded centrifugal pump, APV Ltd., Crawley, Sussex, England). Cartridges (Romicon Inc., Woburn, Mass., U.S.A.) of type XM 50 and PM 50 were used. Each type was conditioned in accordance with the manufacturer's instructions and cleaned at the end of each experiment with sodium hydroxide, 0.5 M, recirculated through the fibres for 0.5 h.

Prior to each run the soft water flux was measured at fixed temperature and transmembrane pressure. Before concentration the suspension was recirculated through the fibres with the permeate outlet valves closed for 0.25-0.5 h to achieve uniform particle size and temperature. The outlet valve was then opened and the permeate flow rate and permeate volume were monitored with time as the retentate was concentrated. Constant values of the inlet and outlet pressures of the hollow-fibre cartridge were maintained by adjusting the flow rate delivered by the pump as the viscosity of the retentate increased. Permeate samples were assayed for protein concentration using the Biuret method of Gornall et al. (1949) and the retentate concentration was calculated by a mass balance of the total protein in the system. Retentate samples were taken for viscosity measurements and were also centrifuged (Centaur 2, MSE, Crawley, Sussex, England) at $\text{rcf} = 4000$ for 0.25 h to produce a supernatant which was assayed for soluble protein concentration (Biuret).

2.1.3 Viscosity Measurements for Precipitate Suspensions

Retentate samples taken from the holding tank during the ultrafiltration of protein precipitate suspension, pH 4.6, were sheared in cone and plate apparatus (No.1 cone, Rheomat 30, Contraves AG, Zurich, Switzerland) and the shear stress noted for a series of fixed shear rates in the range 100 - 3950 s⁻¹. A water bath maintained a constant temperature of 300 K or 313 K, corresponding to the temperatures used during the ultrafiltration process.

2.1.4 Protein Adsorption on Microporous Membranes

Total Water Extract, pH 8.8, and supernatant, pH 4.6, were prepared as for the laboratory filtration studies without cross-flow to a final protein concentration of ca. 10 kg/m³. Solutions of lower concentration were prepared by dilution with deionised water. Unused membranes, diameter 47 mm, pore size 0.2 μm, were immersed for 1.0 h in protein solution, 0.05 L, 301 K. Each membrane was then carefully removed from the solution, washed with distilled water and soaked for 1.0 h in 0.05 L sodium dodecyl sulphate solution, 50 kg/m³, 301 K. The resultant protein solution was assayed using a procedure based on the Folin-Lowry method, modified for use in the presence of SDS, described by Markwell et al. (1978).

2.1.5 Protein Characterisation

Bovine serum albumin (BSA) solution, 1 mL, with concentration in the range 1-10 kg/m³, was mixed in a test tube with 4 mL of Biuret reagent [copper (II) sulphate, 1.5 kg/m³, sodium potassium tartrate, 6.0 kg/m³, sodium hydroxide, 30 kg/m³] and allowed to stand for 0.5 h at room temperature. The optical density of each sample was read at 550 nm on a dual beam spectrophotometer (Pye Unicam Ltd., Cambridge, England) against a blank of 4 mL of Biuret reagent and 1 mL of deionised water. The standard curve thus obtained with BSA was used to determine the soya protein concentration in samples taken from the microfiltration and ultrafiltration experiments.

Folin reagent was prepared by mixing Folin A (sodium carbonate, 20 kg/m³, sodium hydroxide 4 kg/m³, sodium tartrate, 1.6 kg/m³, SDS 10 kg/m³) with Folin B (copper (II) sulphate, 40 kg/m³) in the ratio 100:1. BSA solution (in the range 0.01-0.1 kg/m³), 1 mL, was added to 3 mL of Folin reagent and held at 301 K for 0.5 h using a water bath. Folin-Ciocalteu, 0.3 mL, diluted in advance with deionised water to a 50% solution, was added to the protein/Folin mixture while vigorously mixing the solutions. The resulting mixture was kept in the water bath at 301 K for a further 1.0 h before reading the absorbance at 660 nm against a

blank of Folin reagents mixed with deionised water. The BSA/Folin standard curve was used to determine the concentration of protein in the SDS solutions for the measurement of protein adsorption on microporous membranes.

For the laboratory cross-flow microfiltration experiments, the soluble protein components making up the retentate or permeate were identified by zonal electrophoresis using polyacrylamide gels under dissociating conditions in the presence of sodium dodecyl sulphate (SDS). Samples were dissociated and denatured by heating to 373 K in the presence of a thiol reagent and excess SDS. A modified Laemmli discontinuous buffer system [Hames (1981)] was used to give high resolution of the protein samples in 10% polyacrylamide gels (Pharmacia gel electrophoresis, GE-2/4 LS, Pharmacia Ltd., Milton Keynes, England). A full description of the gel preparation and staining techniques has been given by Herbert (1985). Photographs of the stained gels were scanned quantitatively using a laser densitometer (Ultrascan XL, LKB Instruments Ltd., South Croydon, Surrey England).

2.2 Clarification of Yeast Homogenate by Flocculation and Centrifugation

2.2.1 Preparation of Yeast Homogenate

For the laboratory-scale experiments with yeast homogenate, a block of yeast (Distillers Co. Ltd., Sutton, Surrey, England), 1 kg, was crumbled into 430 mL of phosphate buffer (dipotassium hydrogen phosphate, 0.1 M, sodium chloride, 0.15 M). The cells were disrupted in a model 15M 8BA Manton Gaulin high-pressure homogeniser (APV Ltd., Crawley, Sussex, England) with 4 passes at 5×10^7 Pa, 277 K and the suspension adjusted to pH 7 using sodium hydroxide, 2.5 M. In the preparation of yeast particles for the mobility measurements 430 mL of deionised water was used as the suspending medium instead of phosphate buffer.

For the pilot plant experiments, 47 kg of yeast (DCL) were suspended in 20 L of phosphate buffer. The cells were disrupted

in a model KR3 high-pressure homogeniser (APV Ltd.) with 4 passes at 5×10^7 Pa, 277 K. The yeast homogenate was adjusted to pH 7 using sodium hydroxide, 2.5 M.

2.2.2 Flocculation of Cell Debris with Borax and Centrifugation

In the laboratory separation of cell debris from yeast homogenate, borax solution, 100 mL, 0.1 M, pH 8.5, was mixed with an equal volume of homogenate, pH 7, for 60 s. The flocculated suspension was centrifuged using a range of gravitational fields (0-200g, model 161 frozen image centrifuge, Triton Electronics Ltd., Dunmow, Essex, England; 2000g-10000g, Europa centrifuge, MSE; 10000g-30000g, Pegasus centrifuge, MSE) for 0.5 h. The dry weight of the sediment obtained was determined by drying the sample in an oven at 378 K for 24 h.

The same range of gravitational fields was applied to the separation of non-flocculated yeast homogenate. The homogenate was mixed 1:1 with phosphate buffer and, after centrifugation for 0.5 h, the dry weight of the sediment was determined.

In the preparation of material for further clarification with PEI or mobility measurements with PEI a standard centrifugation procedure ($rcf = 3,000g$, 277 K, 5 mins) was used to remove the borax-flocculated material.

For the pilot-scale separation of cell debris, yeast homogenate was flocculated using borax solution, 0.1 M, pH 8.5, 50 L, added to the homogenate, 50 L, in a tank of volume 0.12 m^3 stirred at 26.7 rad/s with a 3-bladed paddle of diameter 0.18 m. Stirring was continued for 0.25 h before pumping the suspension to the centrifuge.

In the continuous flocculation of the homogenate the yeast and borax streams were fed into a scroll decanter centrifuge (Sharples P600, Pennwalt Ltd, Camberley, Surrey, England) using two gear pumps (SSP Pumps Ltd., Eastbourne, Sussex, U.K.). Identical flow rates, measured using magnetic flow meters (Turbo-Werk GmbH, Cologne, West Germany) and controlled by a

microprocessor (System 6366, Turnbull Control Systems Ltd, Worthing, West Sussex, England), were used for both streams to give a borax concentration in the mixed stream of 0.05 M.

Wet solids concentrations in the feed and overflow streams were measured by weighing the pellet produced after high-speed centrifugation of samples, ca. 12 mL, of these streams in the laboratory (110,000g, Pegasus centrifuge, MSE Scientific Instruments, Crawley, Sussex, U.K.). The supernatants obtained from high-speed centrifugation were assayed for protein using a dye-binding assay reagent (Pierce Ltd, Cambridge, U.K.) and the dry weights of the soluble components (protein, buffer, etc.) in the feed and overflow streams were determined by drying samples of the supernatants. Mass flow rates and percentage dry weights of the centrifuge exit streams were recorded and the effects of pond depth, differential scroll rate and feed flow rate on the performance of the centrifuge were investigated.

The separation efficiency, E , was calculated by dividing the mass flow of dry solids recovered in the underflow stream (obtained from a mass balance of dry solids in the feed and overflow streams) by the mass flow of dry solids fed into the centrifuge. While E defines the total solids recovery, a better guide to the separation performance of the centrifuge is required when there is a significant underflow [Svarovsky (1977)]. The separation is therefore assessed using an alternative definition of efficiency [Van Ebbenhorst and Rietema (1961)], the 'Reduced' efficiency, E' , where:

$$E' = (E-R)/(1-R) \qquad \text{Equation 2.1}$$

R is the ratio of the underflow to the feed flowrate. In these calculations 'dry solids' are calculated by subtracting the contribution of soluble material from the total dry weight. The dry weight of the supernatant obtained after the removal of all solids, with the high-speed centrifugation described above, was used to calculate the percentage dry weight of soluble material in the feed and overflow streams.

2.2.3 Measurement of Sediment Rheology

Yeast homogenate (diluted 1:1 with phosphate buffer) and flocculated yeast homogenate (final borax concentration, 0.05 M) were settled in a laboratory centrifuge (Europa, MSE) at forces ranging from 2000g to 10000g for 300 s and the supernatant decanted from the sediment. The shear modulus of the sediment was determined using oscillatory measurements (0.01-10 Hz, 293 K) on a parallel plate rheometer (system PP 30, Bohlin Rheometer VOR, Bohlin Rheologi AB, Lund, Sweden) and the dry weight of the sample was then measured.

2.2.4 Particle Size Measurement

Yeast homogenate was diluted in filtered (0.2 μm depth filter, Sartobran capsule, Sartorius GmbH, Gottingen, West Germany) sodium chloride, 100 kg/m^3 and sized using an electronic particle counter (model 80XY Elzone, Particle Data Inc., Elmhurst, Illinois, USA) fitted with 30 μm orifice and calibrated with latex particles (Particle Data Laboratories Ltd., Elmhurst, Illinois, USA). Supernatant was suspended at a sample concentration 5x greater than that used for the homogenate (to give comparable particle concentrations) in filtered sodium chloride, 100 kg/m^3 , and sized using the same orifice.

2.2.5 Particle Electrophoretic Mobility

Stock solutions of polyethylenimine (PEI, M.Wt. 600, 10,000, 50,000 and 70,000), 10 kg/m^3 , sodium chloride, 100 kg/m^3 , and dipotassium hydrogen phosphate, 100 kg/m^3 were prepared in filtered, deionised water (Milli-Q water purification system, Millipore Corp., Bedford, Mass., U.S.A.) with final water filtration through a microporous filter, pore size 0.2 μm (Asypor, Domnick-Hunter). These solutions were further diluted in filtered water and a fixed volume, 30 mL, was then passed through a 0.2 μm filter (Acrodisc, Gelman Sciences Ltd., Brackmills, Northampton, U.K.) into a beaker that had been thoroughly cleaned with filtered water. Samples of yeast particles (whole yeast suspension before homogenisation, yeast

homogenate, and homogenate clarified by treatment with borax) were diluted into the filtered solution to give particle concentrations appropriate to the 'ideal' range for mobility measurement in the Zetasizer (model 2c, Malvern Instruments Ltd., Malvern, Worcs, U.K.).

The samples were injected into the Zetasizer fitted with the PC4 cell. The cell was positioned so that measurements were made at the stationary layer of the capillary. Temperature, 298 K, was controlled to ± 0.1 K and a constant potential difference, typically 100 V, was applied across the cell. In some cases, at higher electrolyte concentrations (>4 kg/m³ sodium chloride solution), a high current was obtained (>5 mA) and heating of the sample during the measurement became apparent. In these cases the Zetasizer was operated in current-stabilised mode with a fixed current and a potential difference which fell as the temperature increased during the measurement. In this mode the falling potential, lowering the velocity at which the particles move in the cell, compensates for the increased velocity resulting from the rising temperature and errors due to heating within the cell are minimised.

Whole yeast suspension, yeast homogenate and borax-clarified homogenate were suspended in filtered sodium chloride solution, 1 kg/m³, the pH was adjusted with hydrochloric acid, 0.025 M, or sodium hydroxide, 0.025 M, and particle mobilities were measured over the range pH2-pH9. The particle mobilities for the borax-clarified homogenate were also measured at fixed pH with a range of concentrations of sodium chloride (1-5 kg/m³), dipotassium hydrogen phosphate (1-5 kg/m³), and PEI (0.01-2.0 kg/m³; M.Wt. 600, 10,000 and 50,000 and 70,000). All PEI solutions were adjusted to pH 7 with concentrated hydrochloric acid before the addition of the yeast particles. The effect of changing the pH after the addition of borax-clarified yeast to PEI was investigated for PEI of M.Wt. 50,000.

2.2.6 Titration of PEI with Hydrochloric Acid

The charge densities of the polyethylene imine samples of

different molecular weights were compared by titrating the polymer solutions with hydrochloric acid. An Autoburette (ABU 80, Radiometer, Copenhagen, Denmark) was used to monitor the change in pH of 25 mL of PEI solution, 5 kg/m³, 293 K, as Hydrochloric acid, 1.00 M ('Volucon'), was added at a rate of 8.33×10^{-3} mL/s. The added volume of acid was recorded as the pH fell from pH 10 to pH 4 for the PEI samples of M.Wt. 600, 10,000, and 70,000 (all supplied by Polyscience) and 50,000 (Sigma).

2.2.7 Treatment of Borax-clarified Homogenate with Polyethylene Imine

PEI solutions (M.Wt. 600, 10,000, 50,000 and 70,000), 50 kg/m³, were adjusted to pH 7.0 using concentrated hydrochloric acid, then diluted into the range 0.5-50 kg/m³ and mixed 1:1 with borax-clarified yeast, pH 6.8, in centrifuge tubes. The mixtures were allowed to stand at room temperature, 293 K, for 0.5 h and then remixed by inverting the tubes before centrifugation (Centaur 2, MSE) of the samples at 2000g for 300 s. The relative turbidities of the supernatants obtained after centrifugation with PEI were determined by measuring the absorbance of the supernatant against deionised water on a spectrophotometer (Pye Unicam) at 650 nm. Protein concentrations in the supernatants were assayed using a dye-binding reagent (Pierce UK Ltd.) standardized with BSA solution.

In pilot-scale experiments, borax-clarified yeast homogenate, 0.05 m³, prepared by scroll centrifugation, was mixed in a tank, volume 0.12 m³, using a 3-bladed paddle, diameter 0.18 m, driven at 26.7 rad/s, as 0.05 m³ of polyethylenimine (M.Wt. 50,000), 1.5 kg/m³, was added. Stirring was continued for 1.0 h and samples were taken for size analysis (Malvern 3600 Sizer) as described in Section 2.2.8. The suspension was fed to a disc-stack centrifuge (SAOOH 205, Wesfalia Separator AG, Oelde, Westfalia, W.Germany) at flow rates ranging from 0.007 - 0.042 m³/h. The efficiency of the separation was measured in terms of the solids content of the feed and overflow streams.

In a separate experiment the PEI-flocculated suspension was fed to a larger disc-stack centrifuge (BSP7-47, Wesfalia Separator AG) at flowrates of 0.1 m³/h and 0.2 m³/h and the solids content of the feed and overflow streams measured. Borax-clarified homogenate was diluted 1:1 with phosphate buffer and the operation of the disc stack centrifuge with non-flocculated material at a flow rate of 0.1 m³/h was compared to the separation of PEI-flocculated suspension.

2.2.8 Size Analysis during PEI Flocculation

PEI solutions (M.Wt. 600, 10,000, 50,000 and 70,000) were mixed 1:1 with borax-clarified homogenate in beakers, 100 mL, to a final PEI concentration of 1 kg/m³. Mixing was continued with a magnetic stirrer for times up to 1.5 h as samples, ca. 0.2 mL, were taken from the beaker at fixed intervals and diluted (ca.1/50) into filtered, deionised water (Millipore filtration system, Asypor 0.2 μ m pore size final filtration) to prevent aggregation before size analysis. Samples were then further diluted (typically 1/50) in filtered, deionised water to give a suitable particle concentration for size analysis by laser light diffraction (model 3600 Sizer, Malvern Instruments Ltd.) in a stirred cell (batch cell, Malvern Instruments Ltd.).

The same sampling and dilution techniques were used to follow the pilot-scale flocculation of borax-clarified homogenate with PEI (M.Wt. 50,000) as the suspension was stirred in a tank of volume 0.12 m³ as described in Section 2.2.7. The size distribution of the particles present in the borax-clarified homogenate, before flocculation with PEI, was determined using the pc4 cell of the Zetasizer (model 2c, Malvern Instruments Ltd.) in size analysis mode. The yeast suspension was diluted in filtered, deionised water to a concentration on the low side of the 'ideal' range for the Zetasizer to minimise errors due to multiple scattering of laser light which may occur at higher particle concentrations.

3. PROTEIN PRECIPITATE RECOVERY USING MICROPOROUS MEMBRANES

3.1 Introduction

This chapter examines the flux and soluble protein transmission achieved with microporous membranes when processing three types of material: soya protein precipitated under isoelectric conditions, supernatant from soya protein precipitate and alkaline soya protein solution. Experiments were initially performed using flat sheet membranes in an unstirred batch cell to allow the study of the membrane characteristics and interaction of the process suspension with the membrane in the absence of cross flow. Subsequently, experiments were performed using flat sheet membranes in a cross-flow cell.

3.2 Theory

When processing soluble or precipitated proteins using microfiltration membranes it is necessary to consider several mechanisms which might determine the flux rate through the membrane. First, for macromolecular solutions, where there is no selective retention of the macromolecules and no fouling of the pore surfaces, the flux rate will be determined by the viscosity of the solution. Hence the flux rate will be reduced with increasing solution viscosity with the base flux rate determined by the membrane resistance.

Secondly, if the macromolecules are retained in the form of a concentrated protein gel layer over the membrane surface it has been shown by Trettin and Doshi (1980) that:

$$\Delta V = B_m t^{1/2} \quad \text{Equation 3.1}$$

Where ΔV is the volume permeated in time t . The parameter B_m , which describes the properties of the protein solution in relation to the membrane surface, is given by:

$$B_m = 2A \left(\frac{D}{\pi} \right)^{1/2} \ln \left(\frac{C_w - C_p}{C_b - C_p} \right) \quad \text{Equation 3.2}$$

Where A is the membrane surface area; D is the protein molecule diffusion coefficient; C_w is the protein concentration at the membrane surface; C_p is the permeate protein concentration; and C_b is the protein concentration in the bulk solution. Equation 3.2 is based on a linear concentration profile in a gel layer adjacent to the membrane surface. Trettin and Doshi (1980) found that, for unstirred batch-cell studies of the ultrafiltration of bovine serum albumin, the flux behaviour is more accurately predicted using a concentration profile of the form:

$$C = C_b + (C_w - C_b) \left(1 - \frac{y}{\delta}\right)^n \quad \text{Equation 3.3}$$

where C is the protein concentration at a distance y from the membrane surface; δ is the boundary layer thickness; and n is a function of C_w , C_b and C_p . This gives a description of the change in flux with time:

$$\Delta V = B'_m t^{1/2} \quad \text{Equation 3.4}$$

where:

$$B'_m = 2A \left(\frac{C_w - C_b}{C_w - C_p} \right) \left(\frac{C_w - C_p}{C_b - C_p} \right)^{1/2} \left(\frac{nD}{2(n+1)} \right) \quad \text{Equation 3.5}$$

It is assumed that osmotic pressure gradients are negligible compared to the applied transmembrane pressure.

A third mechanism of flux rate limitation is possible when only particles are present. If the particles adjacent to the membrane surface determine the flux rate, Doshi and Trettin (1981) have shown that:

$$\Delta V = B_p t^{1/2} \quad \text{Equation 3.6}$$

where:

$$B_p = A d_p \left(\frac{2\Delta P}{\mu} \right)^{1/2} \left(\frac{\epsilon^2 [P_s - (\frac{1}{1-\epsilon}) C_s]}{150 (1-\epsilon) C_s} \right) \quad \text{Equation 3.7}$$

where d_p is the particle diameter, ϵ is the cake porosity, P_s is

the density of the particle, ΔP is the applied transmembrane pressure drop, and μ is the solvent viscosity.

If there is significant plugging of the pores by the particles then it may be the resulting higher membrane resistance, rather than the cake resistance, which determines the flux rate. According to Dimitrieva and Pakshver (1951) plugging is likely when π exceeds 1000 where, assuming Stokes' law of sedimentation holds:

$$\pi = \frac{18 \Delta P}{d_p^2 R_m (\rho_s - \rho_l) g} \quad \text{Equation 3.8}$$

where ρ_l is the liquid density and R_m is the membrane resistance as determined by the water flux rate.

The relative values of B_m , B_m' and B_p may be useful in determining the controlling resistance to flux, especially when processing mixtures of precipitated and soluble protein. Devereux et al. (1986) examined the ultrafiltration and microfiltration of soya protein precipitate suspensions with a range of soluble protein content, C_s , and mean particle size, d_p . For anisotropic polysulphone ultrafiltration membranes, with nominal molecular weight cut-off of 50000, experimental values of the slope B were of the same order of magnitude as the predicted values of B_m or B_m' (Eqs. 3.2 and 3.5). The values of B were considerably smaller than the predicted values of B_p (Eq. 3.7) indicating that it was a film of soluble protein rather than a packed precipitate cake which determined the flux rate. When using microporous membranes with protein precipitate suspensions similar relationships were obtained between B and predicted values of B_m , B_m' and B_p . These results indicated that there may be sufficient retention of macromolecules by the microfiltration membrane for gel formation to occur at the membrane surface. It was not possible to ascertain whether flux behaviour was better described using B_m or B_m' values.

Table 3.1 Flux characteristics of microporous membrane (0.2 μm), unstirred batch studies.

	pH	C_t	C_b	kg/m ³	Flux rate			B											
					initial	45 s	90 s	2700s	Protein Transmission %	B_i	B_f	B_p	B_m	B'_m					
					L/m ² h														
Precipitate ^a Suspension	4.6	43	7.0	54	21	12	1.0	87-96 ^c	0.28	0.12	18.1	0.22	1.0						
Precipitate ^b suspension	4.6	42	6.8	75	33	13.5	0.65	76-114	0.48	0.07	18.3	0.22	1.0						
Supernatant ^a	4.6	5.9	5.9	120	45	24	5.2	88-103	0.60	-	-	0.23	1.1						
Supernatant ^a	8.8	5.7	5.7	2200	1300	1000	-	84-96	21	-	-	0.23	1.1						
TWE ^a	8.8	6.6	6.6	3200	2400	-	-	97-102	28	-	-	0.22	1.0						

^a membrane 'open side up'

^b membrane 'tight side up'

ⁱ initial

^f final

^c initial transmission 49%

3.3 Results

3.3.1 Unstirred Microfiltration

Table 3.1 presents typical flux rates and protein transmissions for the solutions and suspensions studied in the unstirred batch cell with a 0.2 μm pore size membrane. The transmission is based on the soluble protein concentration on the retentate side, C_s , and all the examples have a similar C_s value (i.e. within the range 5.7-7.0 kg/m^3). Each trial exhibited a decline in flux rate with time. Total water extract (TWE), $C_s = 6.6 \text{ kg}/\text{m}^3$, had the highest initial flux rate and filtration of the 0.25 L batch was complete within 90 s. For isoelectrically precipitated soya, total protein concentration 43 kg/m^3 , $C_s = 7.0 \text{ kg}/\text{m}^3$, the flux was much reduced. Supernatant, pH 4.6, $C_s = 5.9 \text{ kg}/\text{m}^3$, obtained by the removal of the protein precipitate, yielded higher flux rates than those obtained with the precipitate suspension, but still considerably less than those obtained with TWE at a similar protein concentration. When supernatant was adjusted to pH 8.8, behaviour similar to that of TWE was obtained (i.e. high initial flux rate and filtration of a 0.25 L batch in ca. 120 s). The comparison of flux rates and soluble protein transmissions for the precipitate suspension and the supernatant, pH 4.6, is examined in more detail in Figure 3.1.

The flux rates obtained for precipitated protein suspension with the membrane configurations 'open side up' and 'tight side up' are compared in Figures 3.1, 3.2 and Table 3.1. Although the flux rates are initially higher for the 'tight side up' example (Table 3.1), after 150 s of filtration the flux rates are at all times lower than those observed for the 'open side up' filtration [compare Figs. 3.1 (OSU) and 3.2 (TSU)].

Soluble protein transmissions of at least 80% were recorded in all experiments (Fig. 3.1 and Table 3.1) except for the early part of the trial with the precipitate suspension (Figs. 3.1 and 3.2). In the case of the membrane in open side up configuration (Fig. 3.1), the low initial flux enabled the transmission data to be recorded for the first 1 mL of permeate. There was a low

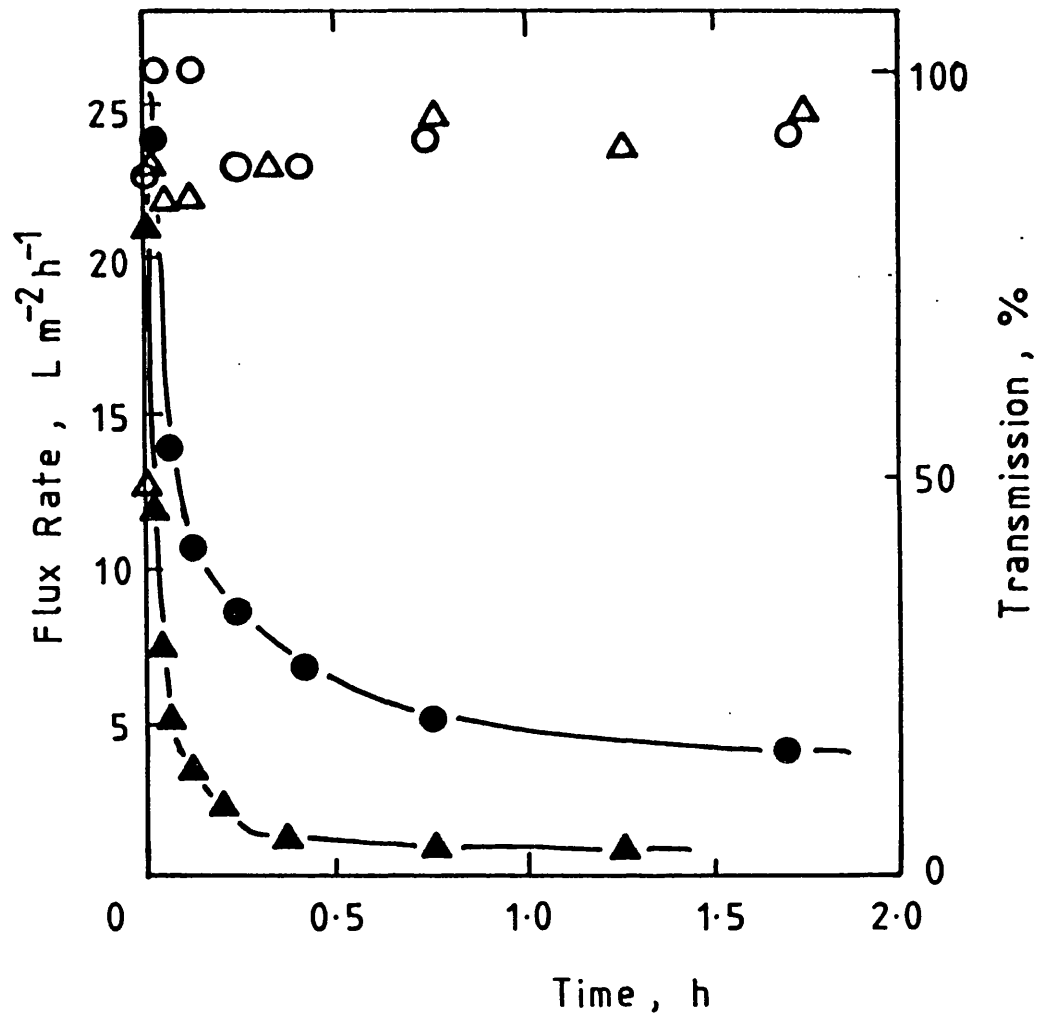


Figure 3.1 Unstirred Batch-cell Microporous Filtration of Protein Suspensions. Membrane nominal pore size, $0.2 \mu m$, open side up; temperature, 293 K; ΔP , $0.69 \times 10^5 N/m^2$; ●,▲, flux rate; ○,△, % transmission of soluble protein. ●, ○, soya protein supernatant, pH 4.6; C_s , $5.9 kg/m^3$. ▲, △, soya precipitate suspension, pH 4.6; C_t , $43 kg/m^3$; C_s , $7 kg/m^3$.

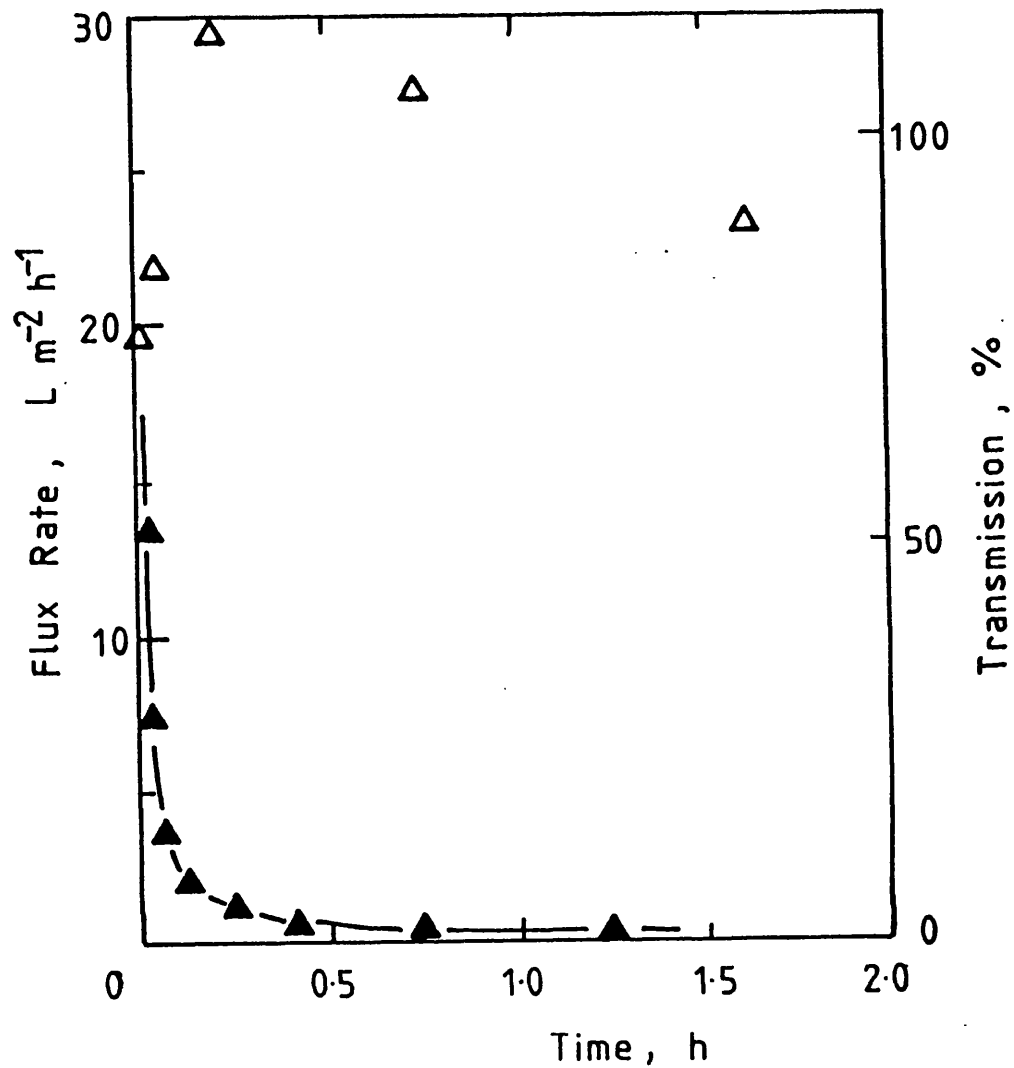


Figure 3.2 Unstirred Batch-cell Microporous Filtration of Protein Suspension. Membrane nominal pore size, $0.2 \mu m$, tight side up; temperature, 293 K; ΔP , $0.69 \times 10^5 N/m^2$; \blacktriangle , flux rate; \triangle , % transmission of soluble protein. \blacktriangle , \triangle , soya precipitate suspension, pH 4.6; C_t , $42 kg/m^3$; C_s , $6.8 kg/m^3$.

initial transmission of 49%, which may be attributed to the adsorption of protein to the new membrane at the start of the experiment. Similar observations of low initial transmission have been made with ultrafiltration membranes by Howell and Velicangil (1982). After this low initial value, protein transmission rose quickly to 80% and remained above this value for the rest of the experiment.

Predictions of the values of B_p , B_m and B_m' (Table 3.1) are made in accordance with the theory outlined in Section 3.2. Relevant values of the properties of the soya precipitate suspension are given by Devereux et al. (1986) as a soluble protein diffusivity, D , of $6.0 \times 10^{-11} \text{ m}^2 \text{ s}^{-1}$, a solution viscosity, μ , of $1.07 \times 10^{-3} \text{ N s m}^{-2}$, a retentate cake voidage, ϵ , of 0.17, and a precipitate particle density, ρ_s , of 1132 kg/m^3 . A concentration of soluble protein at the membrane surface, C_w , of 400 kg/m^3 is assumed in accordance with the results of soya protein ultrafiltration obtained by Narendranathan (1981).

Plots of the volume permeated, ΔV , versus the square root of the time (Fig. 3.3) show that while a linear relationship might apply for the solution of supernatant protein, the value of the slope, B , decreases with time for the precipitated protein. Measured values of B are given in Table 3.1 for the early, B_1 , and later, B_f , stages of the filtration where a constant slope was not obtained. For supernatant, pH 8.8, and TWE, pH 8.8, the values of B are two orders of magnitude greater than the corresponding calculated values of B_m and B_m' and evidently a theory based on the formation of a protein film on the membrane surface does not apply to the early stages of the microfiltration of these solutions. In the microfiltration of precipitate and supernatant, pH 4.6, the B values are of the same order of magnitude as one of the predictions for macromolecular solutions, B_m , while they are approximately two orders of magnitude less than the predicted value of B_p based on the soya precipitate particles.

A comparison of the results for supernatant protein, pH 4.6, in the presence and absence of precipitated protein provides an indication of the effect of particles on the flux. Only in the

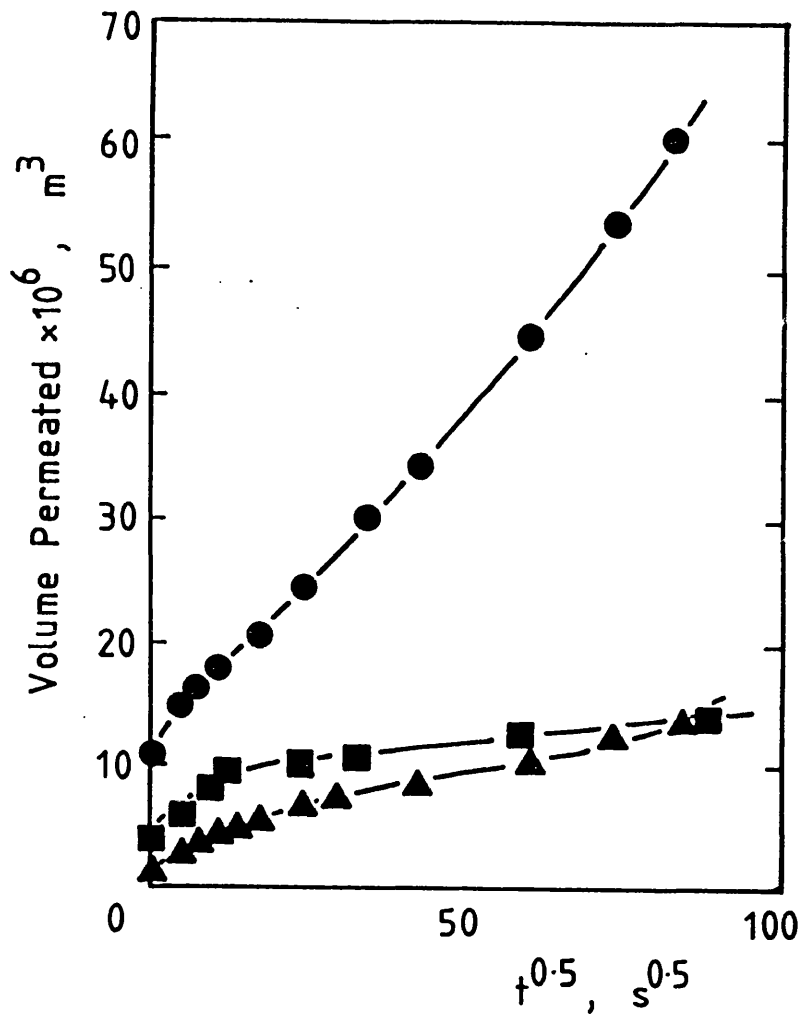


Figure 3.3 Volume of Solution Permeated against $(\text{Time})^{1/2}$ for Unstirred Batch-cell Filtration. Membrane pore size, $0.2 \mu\text{m}$ (data from Figs 3.1, 3.2); temperature, 293 K; Δ P, $0.69 \times 10^5 \text{ N/m}^2$. \blacktriangle , Soya precipitate suspension, pH 4.6; C_t , 43 kg/m^3 ; C_s , 7.0 kg/m^3 ; membrane open side up. \bullet , Soya supernatant, pH 4.6; C_s , 5.9 kg/m^3 ; membrane open side up. \blacksquare , Soya precipitate suspension, pH 4.6; C_t , 42 kg/m^3 ; C_s , 6.8 kg/m^3 ; membrane tight side up.

early stages of microfiltration of a precipitate suspension are the values of B comparable with those obtained for supernatant protein (Table 3.1). The flux declines rapidly in the presence of precipitate to give a value of B several fold lower than observed for supernatant protein. Further, the membrane in 'tight side up' configuration gives an overall lower value of B compared with the membrane used 'open side up' for protein precipitate suspension (Fig. 3.3).

3.3.2 Cross-flow Microfiltration

The cross-flow results (Fig. 3.4) were obtained using a 1.2 μm nominal pore size membrane. While there was a rapid decline in flux rate the soluble protein transmission values remained high with a slight but steady decrease over the period of the experiment. However for the 0.2 μm pore size membrane the rapid flux decline was accompanied by a rapid decline in soluble protein transmission (Fig. 3.5). An increase in transmembrane pressure led to a restoration of the flux rate and protein transmission values of an earlier stage of the filtration but the recovery was only temporary and further decline in flux rate and transmission was observed.

Gel electrophoresis of retentate and permeate samples from cross-flow filtration with a 0.2 μm pore size membrane revealed that the protein composition of the permeate was similar to that of the retentate (Fig. 3.6 a,b,c). The electrophoresis patterns of Figure 3.6 are of soya protein treated with sodium dodecyl sulphate which dissociates the proteins into their subunits. The transmissions of the two major proteins in soya, glycinin and β -conglycinin, have been examined in detail. Glycinin constitutes ca. 52% of soya protein, has a molecular weight in the range $3.2\text{--}3.63 \times 10^5$ and has no associated carbohydrate component. β -conglycinin constitutes ca. 28% of the protein, has a molecular weight in the range $1.41\text{--}1.70 \times 10^5$ and has a significant carbohydrate content of 4.0-5.2% by weight. The properties of soya proteins have been reviewed by Kinsella (1979). For the flux/protein transmission trials using the 0.2 μm membrane (Fig. 3.5), the transmissions of glycinin and β -conglycinin have been

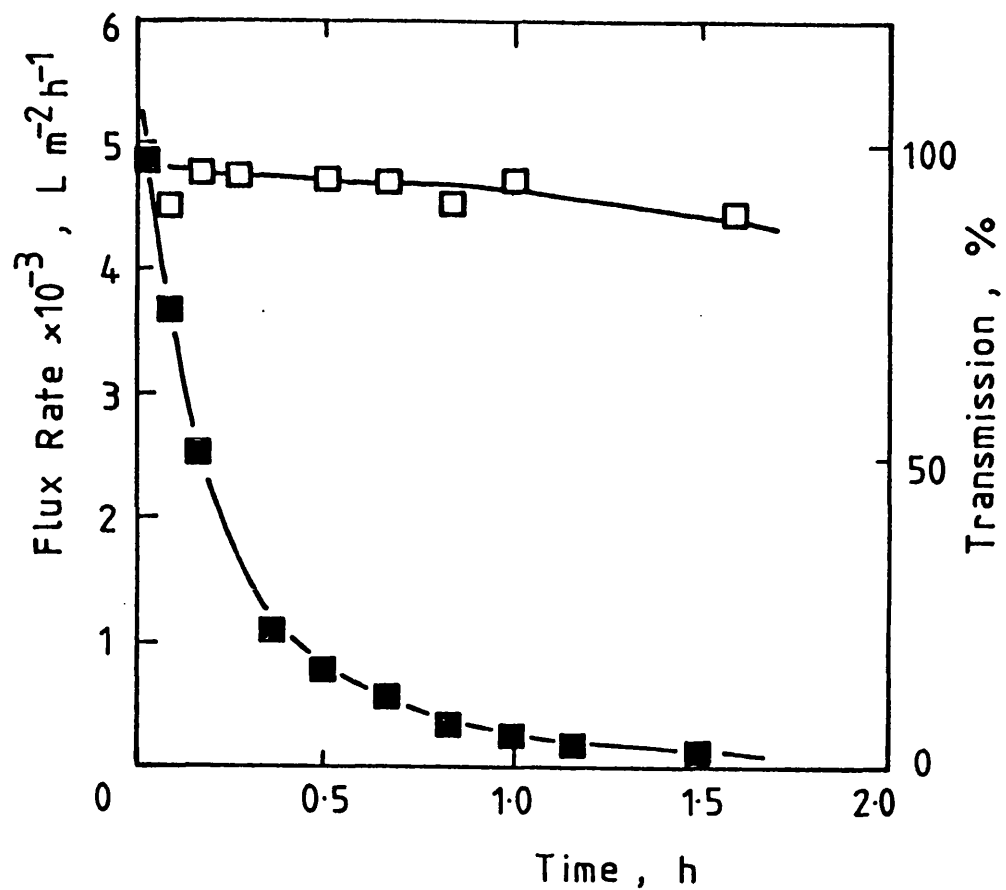


Figure 3.4 Cross-flow Microfiltration of Soya Protein Solution. C_s , 9.4 kg/m^3 ; pH 8.8; inlet gauge pressure, 0.41×10^5 ; outlet gauge pressure, zero; nominal pore size, $1.2 \mu\text{m}$; membrane tight side up; temperature, 293 K. ■, flux rate; □, % transmission of soluble protein.

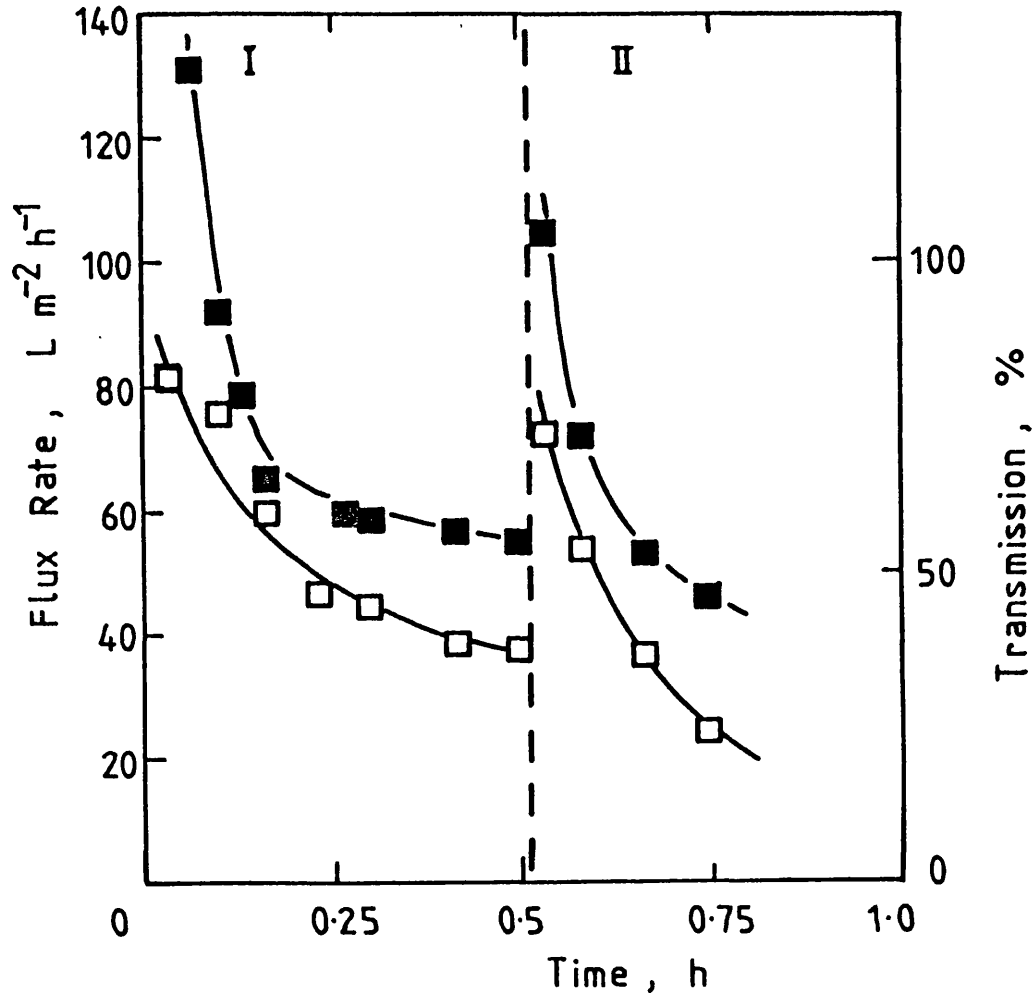


Figure 3.5 Cross-flow Microfiltration of Soya Protein Solution. Cs, 9.6 kg/m^3 ; pH 8.8; nominal pore size, $0.2 \mu\text{m}$, tight side up; temperature, 293 K. I, inlet gauge pressure, 0.41×10^5 ; outlet gauge pressure, zero; II, inlet gauge pressure, 0.97×10^5 ; outlet gauge pressure, 0.69×10^5 ; ■, flux rate; □, % soluble protein transmission.

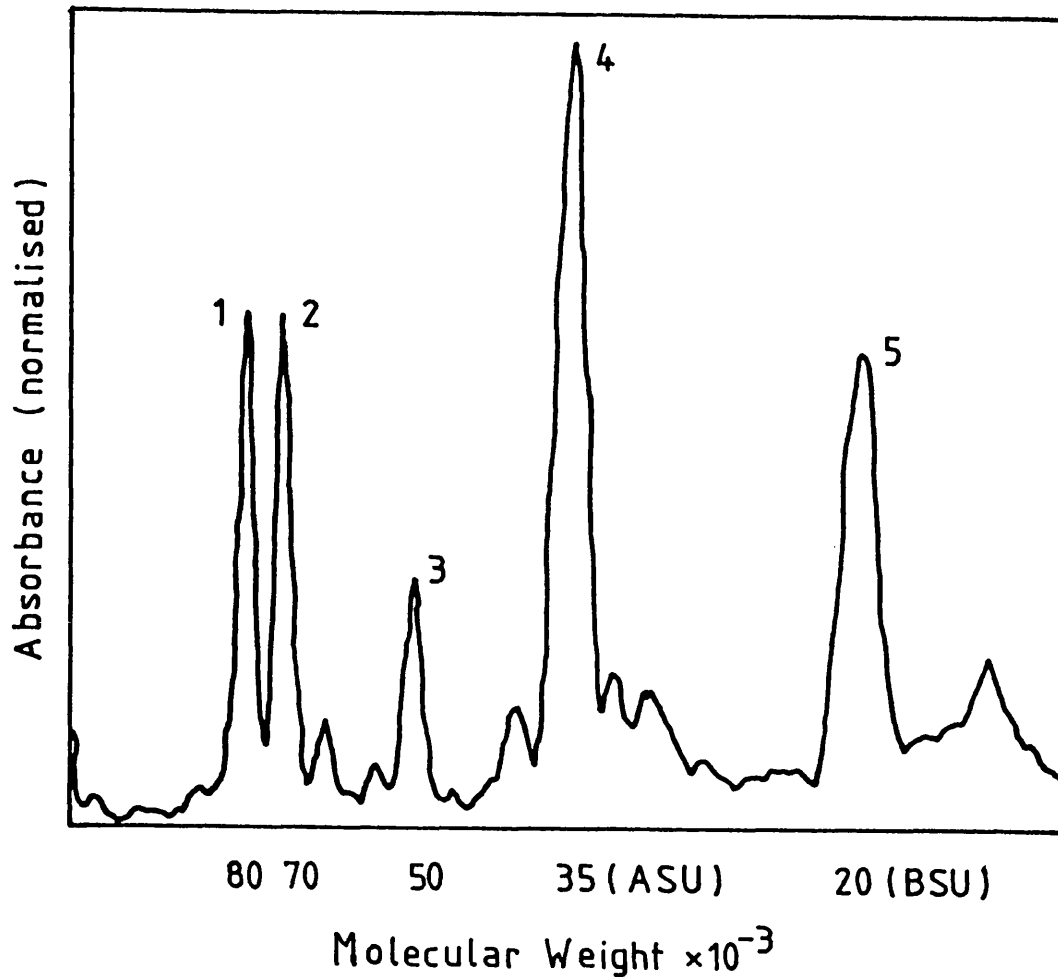


Figure 3.6 (a) Gel Electrophoresis (SDS PAGE) Scan of Retentate. See Fig. 3.5 for experimental conditions and corresponding flux/time and protein transmission characteristics. Pore size, $0.2 \mu\text{m}$; 600 s operation. Peaks 1, 2, and 3 are respectively the 8×10^4 , 7×10^4 and 5×10^4 subunits of β -conglycinin. Peaks 4 and 5 are the acidic (ASU) and basic (BSU) subunits of glycinin and are of molecular weights 3.5×10^4 and 2×10^4 , respectively.

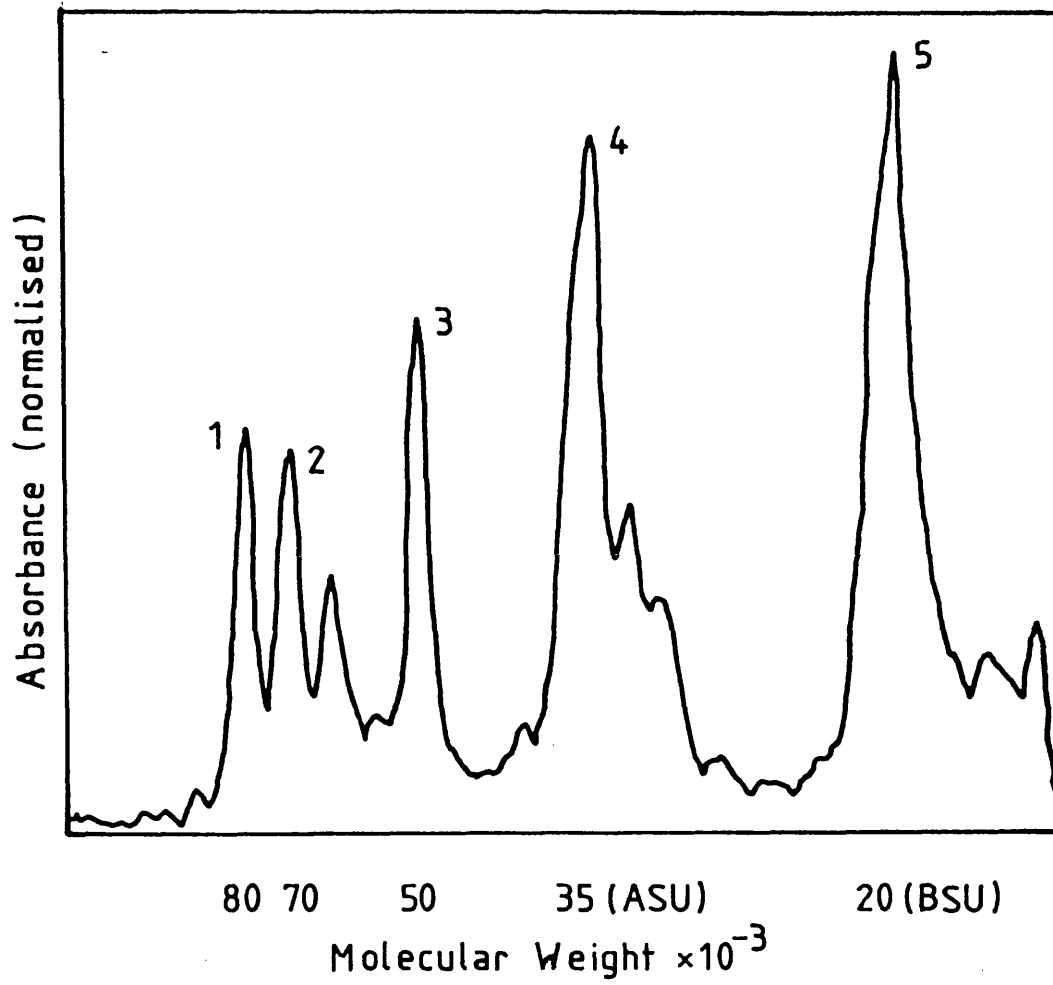


Figure 3.6 (b) Gel Electrophoresis (SDS PAGE) Scan of Permeate. 0.2 μ m membrane after 600 s operation; experimental details as for Fig. 3.6 (a).

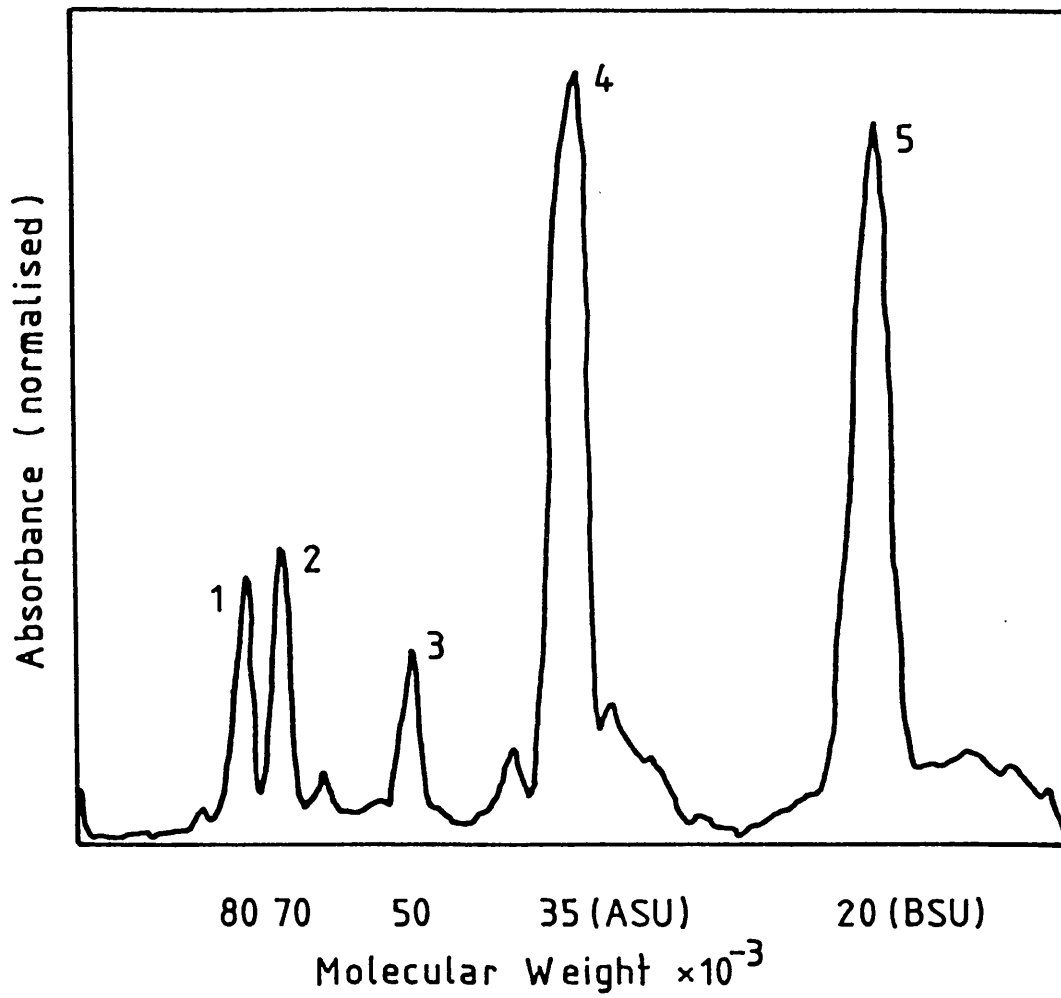


Figure 3.6 (c) Gel Electrophoresis (SDS PAGE) Scan of Permeate. Pore size, 0.2 μm ; 0.75 h operation; experimental details as for Fig. 3.6 (a).

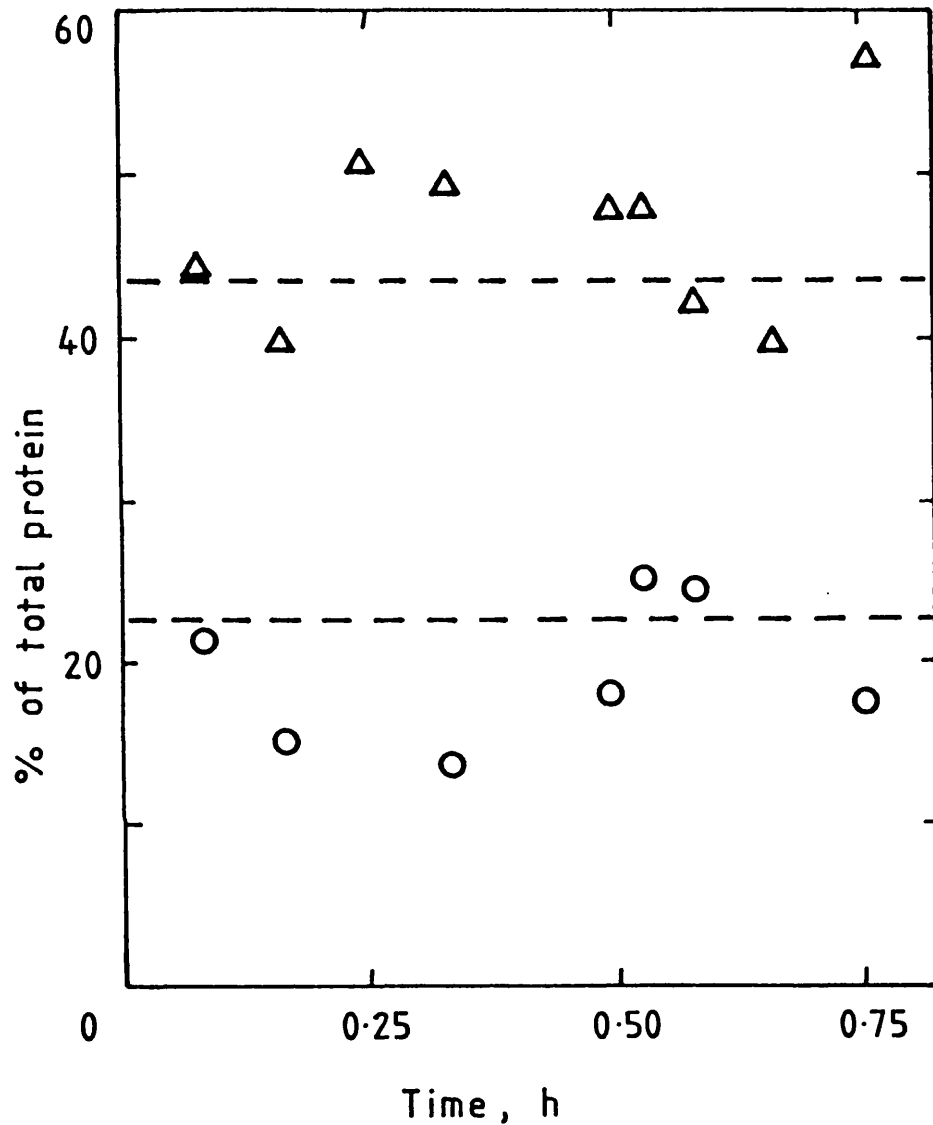


Figure 3.7 Composition of Permeate Transmitted Through Microporous Membrane. See Fig. 3.5 for experimental conditions and corresponding flux/time and protein transmission characteristics. Pore size, $0.2\mu\text{m}$. Soya protein components in the permeate as a % of total protein components. Δ , glycinin; \circ , β -conglycinin; (- - -) retentate composition for glycinin (11S) and β -conglycinin (7S).

derived from their SDS-dissociated components and are compared to the relative amounts of these proteins in the retentate (Fig. 3.7). There is some experimental scatter in the results and there may be variation in the staining intensity of the subunits but there is no significant trend in the β -conglycinin or glycinin content of the permeate which has a similar composition to that of the retentate even after 0.75 h [Fig. 3.6(c)], when the total soluble protein transmission has dropped to 30% (Fig. 3.5). Similarly there is no significant trend in the ratio of glycinin to β -conglycinin throughout the experiment indicating that the membrane is not selectively retaining one of these proteins.

Flux/time and transmission/time characteristics similar to those presented for the 0.2 μm membrane (Fig. 3.5) were also obtained in cross-flow experiments with membranes of nominal pore sizes of 0.45, 0.65 and 0.8 μm . It was observed that the larger the pore size the higher the initial flux and the longer the time of processing required before there was a substantial decline in the soluble protein transmission to a value of, for example, 90%. The results for a range of membrane pore sizes, 0.2, 0.45, 0.65, 0.8 and 1.2 μm , are presented as a plot of transmission against flux rate in Figure 3.8. The results for the different pore sizes might not be expected to be directly comparable due to the differences in membrane pore densities and support structures, especially if the membrane determines the relationship of flux rate to protein transmission. However, for the different pore sizes, Fig. 3.8, there is a general decline in transmission with declining flux. A soluble protein transmission of 90-100% is obtained at flux rates greater than 130 $\text{L m}^{-2} \text{h}^{-1}$ while below these flux rates a decline in transmission is observed.

3.3.3 Protein Adsorption

The variation of membrane-adsorbed protein with concentration is illustrated in Figure 3.9 for unused 0.2 μm membranes exposed to supernatant, pH 4.6, or TWE, pH 8.8. It is evident that, at soya protein concentrations of 6 kg/m^3 , the protein adsorbed to the membrane is 50% higher for the solution at pH 4.6 than for the

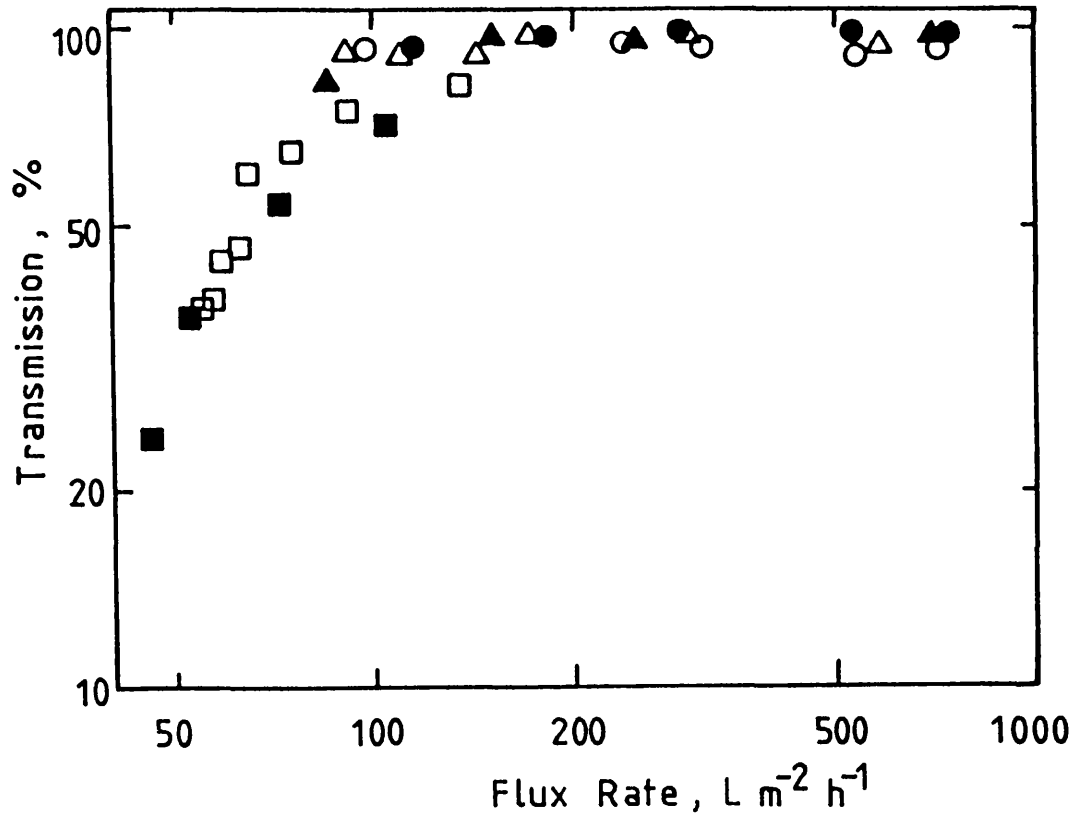


Figure 3.8 Variation of Soluble Protein Transmission with Flux Rate for Cross-flow Microfiltration. Soya protein solution, pH 8.8, membrane tight side up. Membrane pore size and soluble protein concentration, C_s , respectively: ○, 1.2 μm, 9.4 kg/m³; ●, 0.8 μm, 9.0 kg/m³; △, 0.65 μm, 9.0 kg/m³; ▲, 0.45 μm, 9.7 kg/m³; ■, □, 0.2 μm, 9.6 kg/m³. Inlet gauge pressure: ○, ●, △, ▲, □, 0.41 x 10⁵ N/m²; ■, 0.97 x 10⁵ N/m². Outlet gauge pressure: ○, ●, △, ▲, □, 0 N/m²; ■, 0.69 N/m².

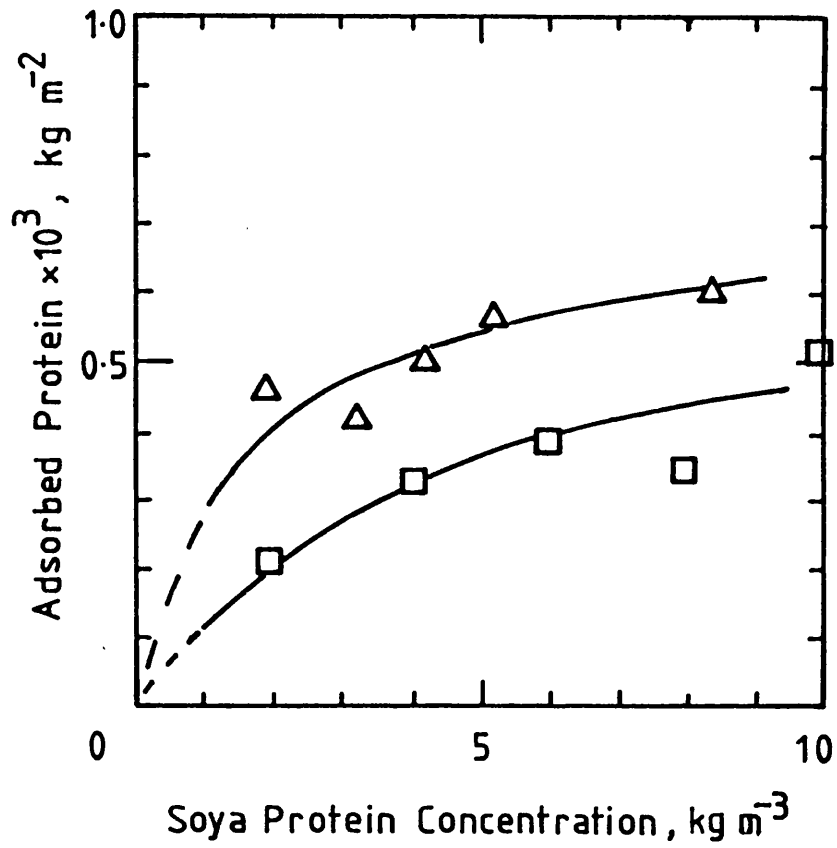


Figure 3.9 Protein Adsorbed to Microporous Membrane after Immersion in Soya Protein Solution. Temperature, 301 K; pore size, $0.2 \mu\text{m}$. Δ , soya protein supernatant, pH 4.6; \square , soya protein solution, pH 8.8.

solution at pH 8.8. Based on Figure 3.9 a membrane of exposed area $4 \times 10^{-3} \text{ m}^2$ would remove 2.4 mg from the first millilitre of permeate originally containing 7 kg/m^3 protein at pH 4.6. This would result in a soluble protein transmission of 66% compared with the observed initial transmission of 49% (Fig. 3.1).

3.4 Discussion

3.4.1 Protein Transmission

The evidence of the trials suggests that while high transmission of soluble protein may be maintained for some time, the decline in flux rate is eventually accompanied by a fall in transmission. Of the wide range of proteins making up the soya protein solution, the transmissions of the two major components, glycinin and β -conglycinin, have been examined quantitatively. From Figure 3.7 it is evident that during cross-flow filtration the membrane is not selectively retaining one of these proteins with respect to the other or with respect to the overall protein content of the soya extract. This observation applies for the membrane operating with high (ca. 80%) and low (ca. 30%) soluble protein transmissions (Fig. 3.5). Results reported by Datar (1985) for the microfiltration of cell homogenates indicate that there may be some membrane selectivity for protein in the early stages of microfiltration but that such selectivity is quickly diminished with increased exposure of the membrane to protein.

The membranes of nominal pore sizes ranging from 0.2 to $1.2 \mu\text{m}$ behaved in a similar manner when used for cross-flow filtration of TWE although a greater process time elapsed for larger pore membranes before the flux rate fell below a particular value and transmission began to decline. The flux/transmission relationship for the range of membrane pore sizes (Fig. 3.8) shows an apparent link between permeate flux rate and soluble protein transmission. As the flux rate falls below ca. $130 \text{ L m}^{-2} \text{ h}^{-1}$, the soluble protein transmission also falls. The higher flux rates and transmissions obtained during the unstirred filtration (Table 3.1) result from the considerably lower

quantity of protein which comes into contact with the membrane than in the case of the cross-flow studies where larger volumes of material were processed.

3.4.2 Protein Adsorption

Protein adsorption on surfaces has been linked with decline of flux rate through ultrafiltration membranes in the work of Howell and Velicangil (1982), Reihanian et al.(1983) and Ingham et al. (1980). According to Fane et al. (1983), partially permeable membranes are more markedly affected by adsorption than retentive membranes and it is expected that protein adsorption plays a significant role in the behaviour of microporous membranes. Bauser et al. (1986) attributed the decline in the performance of microporous membranes to protein adsorption at the surface of the pore walls. Hence, during the microfiltration of TWE, protein adsorption within the pores would cause reduction in the effective pore size and the rapid decline of flux rate observed in Figures 3.4 and 3.5.

Transmission is reduced when the pore size is small enough to reject protein macromolecules while allowing the passage of water. For transmissions down to values as low as 30% the gel electrophoresis results indicate that when retention of soluble protein occurs the protein macromolecules are partially retained over the range of molecular weights present in the solution. A 'secondary membrane' may account for the rejection behaviour encountered here. The formation of secondary membranes has been proposed to explain the rejection behaviour of microfiltration membranes in the separation of proteins from cells by Kroner et al. (1984) and Le et al. (1984). Protein molecules, hindered by pore fouling, may accumulate at the membrane surface and form a secondary layer which can partially reject other macromolecules as they are brought to the surface.

Figure 3.9 indicates that protein adsorption on the membrane at pH 4.6 will be greater than at pH 8.8 and this difference will contribute to the lower flux rates obtained at the lower pH (Table 3.1). However, the rapid flux decline for pH 4.6

precipitate suspension is not accompanied by the related fall in soluble protein transmission (Figs. 3.1, 3.2) which is observed with TWE in the cross flow experiments (Fig. 3.5). In the presence of precipitate particles an additional factor in flux rate decline is provided by the settling of precipitate cake on the membrane surface and the blocking of pores by fine particles. Such a mechanism is consistent with the maintenance of soluble protein transmission even at low flux rates since unblocked pores will allow passage of protein molecules. The effect of fine particles ($2 \mu\text{m}$) is supported by the calculated value of Π (Eq. 3.8), the parameter used in the filtration theory of Dimitrieva and Pakshver (1951). For a $0.2 \mu\text{m}$ membrane of resistance, R , as determined by the water flux rate ($4.5 \times 10^{10} \text{ m}^{-1}$), a particle size, d_p , $2 \mu\text{m}$, particle density, ρ_s , 1189 kg m^{-3} , fluid density, ρ_f , 1000 kg m^{-3} , and transmembrane pressure, ΔP , $0.69 \times 10^5 \text{ N m}^{-2}$, a value of $\Pi > 3500$ is obtained. This meets the authors' criterion of $\Pi > 1000$ for plugging of the filter medium.

The improved performance during the filtration of precipitate suspension with the membrane in the 'open side up' configuration as compared to 'tight side up' agrees with the observations of Le et al. (1984) for the filtration of microbial homogenates. However, Mackay et al. (1989) report that although the 'open side up' configuration gives better retention of particles it is also more susceptible to pore blockage by particles and consequently produces lower flux rates than the 'tight side up' configuration.

Unstirred filtration of the supernatant obtained from the pH 4.6 suspension gives similar low flux rates and high transmission of soluble protein as obtained for the precipitate suspension. Devereux et al. (1986) noted that the supernatant is unstable and fine particles tend to form after the removal of precipitate by centrifugation. Therefore, the low flux rates may be attributed to colloidal particles blocking the pores. The adjustment of supernatant to pH 8.8 will redissolve any remaining precipitated protein and reduce the tendency for protein to form precipitate, thus reducing membrane fouling due to pore plugging and protein adsorption (Fig. 3.9). Higher flux is indeed observed for pH 8.8 supernatant and soluble protein transmission is high.

3.5 Conclusion

For microporous membranes it has been shown that it is possible to achieve high levels of protein transmission. However, adsorption to the membrane eventually leads to a decline in flux rate accompanied by a reduction in soluble protein transmission. Such behaviour occurred for all pore diameters used though the time taken for flux and transmission to fall below certain values did vary. Adjustment of the protein to its isoelectric point leads to greater protein adsorption on the membrane and more rapid flux decline. Microfiltration studies, in the absence of cross-flow, indicated further flux reduction in the presence of the protein precipitate particles. This increased decline was attributed to plugging of the membrane pores by precipitate particles.

The same problems of declining flux rates and poor transmission of proteins have been found for other suspensions of interest in biochemical engineering. Pearson and Quirk (1989) observed flux decline and falling product transmission with membranes of pore diameter 0.2 and 0.45 μm in the separation of human serum albumin from a yeast fermentation. Mackay et al. (1989) found that flux rate was reduced during the dewatering of *E. coli* cells with a 1.2 μm membrane in the presence of BSA. In the recovery of products from yeast homogenate, Huddleston et al. (1989) found that transmission of protein through a 0.22 μm membrane was less than 20%.

For the membrane separation of soluble products from protein precipitates and cell suspensions, permeate flux rates in excess of ca 150 $\text{L m}^{-2} \text{h}^{-1}$ are generally required [Mackay et al (1989)] although the economic viability of the process will vary for individual cases. Where the product is valuable and alternative separations are costly, the problems of low fluxes and poor selectivity of the membrane may be overcome by having large membrane areas and using diafiltration to maintain low protein concentrations. The separation of a protein monomer from a tetramer through an ultrafiltration membrane has been achieved by Wagner (1989) using diafiltration and it is supposed that the

formation of a secondary layer on the membrane is minimised by maintaining low protein concentrations.

Higher productivity in membrane filtration may arise from the development of low fouling membrane materials such as Nylon 66 [Orchard (1989)] where the membrane charge can be adjusted to minimise interaction with process fluid. Another approach, used by Rushton and Zhang (1989) and Kroner et al. (1989), is to operate at low transmembrane pressures while maintaining high shear rates with rotating cylindrical membranes. The production of Taylor vortices in these devices can improve separation performance [Kroner et al. (1987)] and operation at low transmembrane pressures may reduce the effects of fouling and secondary layer formation [Pearsson and Quirk (1987)]. However, it seems unlikely that membrane fouling can be completely eliminated in microfiltration and, in the dewatering of soya protein precipitates to high concentrations, ultrafiltration membranes may produce higher flux rates than microfiltration membranes [Devereux and Hoare (1986)] while also retaining the soluble protein fraction. The concentration of soya protein precipitate suspension using pilot-scale hollow-fibre membranes is examined in the next section.

4. PILOT-SCALE ULTRAFILTRATION OF SOYA PROTEIN PRECIPITATE

4.1 Results

4.1.1 Pure Water Flux Rates

Measurements of the soft water flux rates indicated a higher resistance to permeation for the PM type membrane compared to the XM type. A water flux of $340 \text{ L m}^{-2} \text{ h}^{-1}$ was obtained at inlet pressure 138 kPa, outlet pressure 103 kPa with the XM fibres (length 0.31 m, diameter $1.52 \times 10^{-3} \text{ m}$) while a flux rate of $116 \text{ L m}^{-2} \text{ h}^{-1}$ was obtained with the PM fibres under the same conditions. The membrane resistance, controlled by the membrane material and the method of manufacture, was found to vary even for fibres of the same membrane type. A higher flux rate ($582 \text{ L m}^{-2} \text{ h}^{-1}$) was observed for the narrower XM fibres (length 0.31 m, diameter $1.14 \times 10^{-3} \text{ m}$) and a lower flux rate for the longer XM fibres (length 0.64 m, diameter $1.52 \times 10^{-3} \text{ m}$). All the membranes used had a nominal molecular weight cut-off of 50,000 but differences in water flux rates may arise due to different pore structure and membrane thickness.

4.1.2 Concentration of Soya Protein Precipitate

The change in permeate flux rate for a PM 50 membrane during the concentration of soya protein suspension is shown in Figure 4.1. After an initial period of flux decline due to membrane fouling the flux/concentration curve, at fixed pressures, consists of two regions. The first region, up to approximately 240 kg/m^3 , is identified by a gradual reduction in flux rate with increase in concentration. In the second region a more rapid decline in flux rate was observed. A temporary increase in transmembrane pressure, whilst maintaining constant pressure drop along the cartridge, increased the flux rate when the process was in region 1, but produced a slight decrease in flux rate when operating in region 2. An increase in the flux rate in region 2 was obtained when the transmembrane pressure was held constant and the pressure drop along the cartridge was increased (Fig. 4.1).

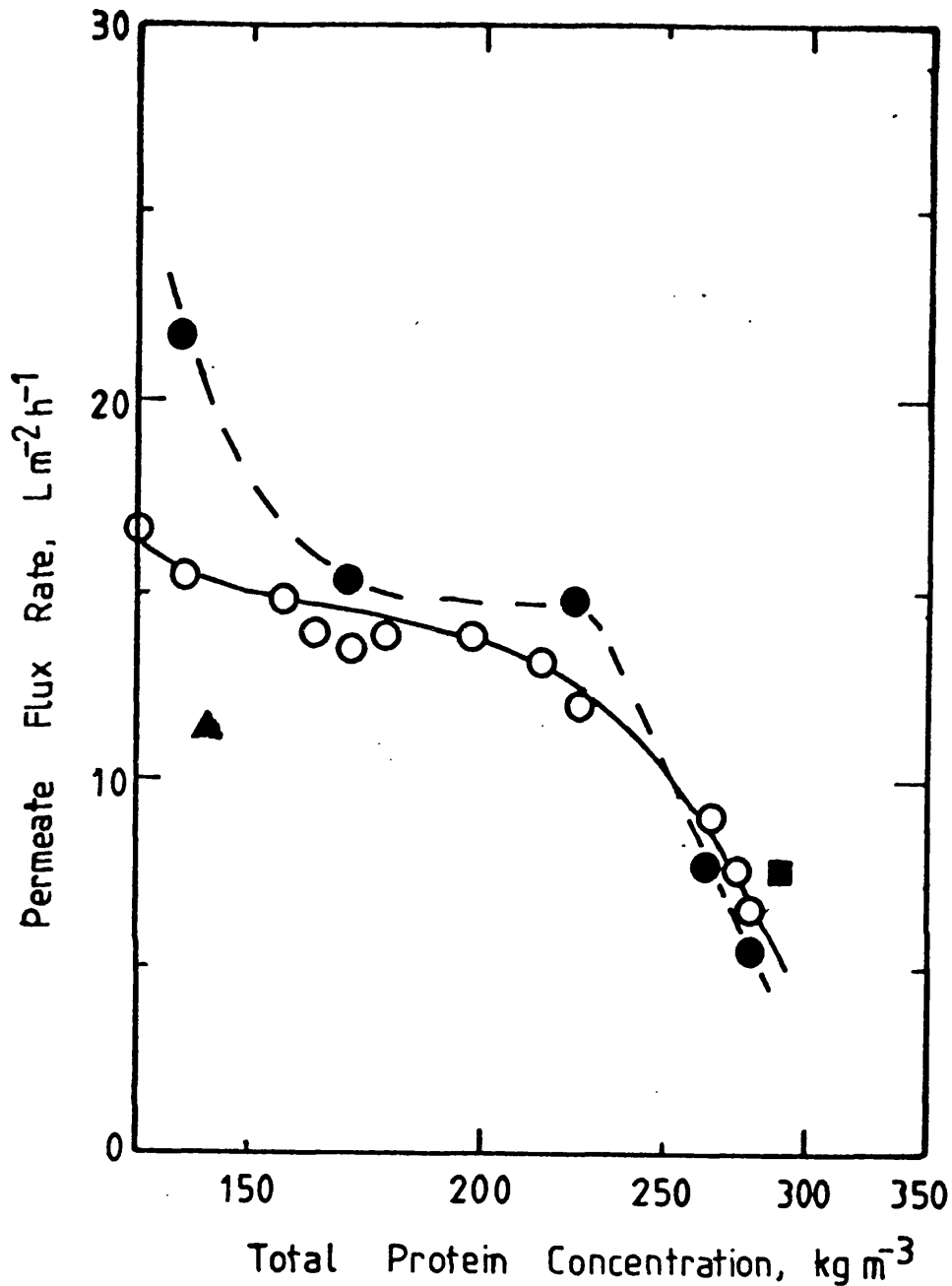


Figure 4.1 The Concentration of Soya Protein Precipitate Suspension: Effect of Pressure Changes. PM 50 membrane; fibre length, 0.31 m; membrane area, 0.65 m²; fibre diameter, 1.52 mm; temperature, 300 K. Inlet and outlet gauge pressures respectively: ○, 172 kPa, 69 kPa; ●, 207 kPa, 103 kPa; ▲, 138 kPa, 41 kPa; ■, 193 kPa, 55 kPa. Initial fraction of protein soluble, 0.24; Mono pump used.

In Figure 4.2 the permeate flux rate obtained using a positive displacement pump to circulate the retentate through XM 50 membrane hollow fibres is compared to that obtained for the same membrane using a centrifugal pump. In both cases similar flux rates were obtained and a gradual decline in flux rate observed as the concentration increased from 150 kg/m^3 to 240 kg/m^3 . At this point, with the centrifugal pump, the pressure dropped below the value set at the start of the process. The original pressure setting could not be regained and flux behaviour characteristic of region 2 was not observed. Instead a sudden decline in flux rate occurred over a small increase in retentate concentration.

When the positive displacement pump was used a transition from region 1 to region 2 was observed at 250 kg/m^3 and concentration of the retentate was continued at constant pressure until the flux rate had declined to ca. $8 \text{ L m}^{-2} \text{ h}^{-1}$. At this point the outlet pressure was lowered from 103 kPa to 69 kPa while the inlet pressure was maintained at 172 kPa . As observed in Figure 4.1, improved flux rates were produced by the increase in transcartridge pressure (in this case accompanied by a decrease in transmembrane pressure). The concentration was continued to a final protein concentration of 325 kg/m^3 when, with increasing viscosity of the retentate, the inlet pressure started to rise.

A comparison of the permeate flux rates for different membrane types, PM and XM, is made in Figure 4.3. Both membranes exhibited the two regions of flux rate behaviour with changing retentate concentration. The transition point from region 1 to region 2 appeared at 236 kg/m^3 for the PM 50 membrane and at 260 kg/m^3 for the XM 50 membrane. Beyond 280 kg/m^3 , the flux rate profiles of the membranes (XM and PM) converge.

4.1.3 Hollow Fibre Geometry

Cartridges of the same membrane type and fibre diameter but different fibre length, 0.31 m and 0.64 m , are compared in Figure 4.4 at the same transmembrane and transcartridge pressure drops. Increasing the cartridge length resulted in lower flux rates under these conditions. When the cartridges were operated in

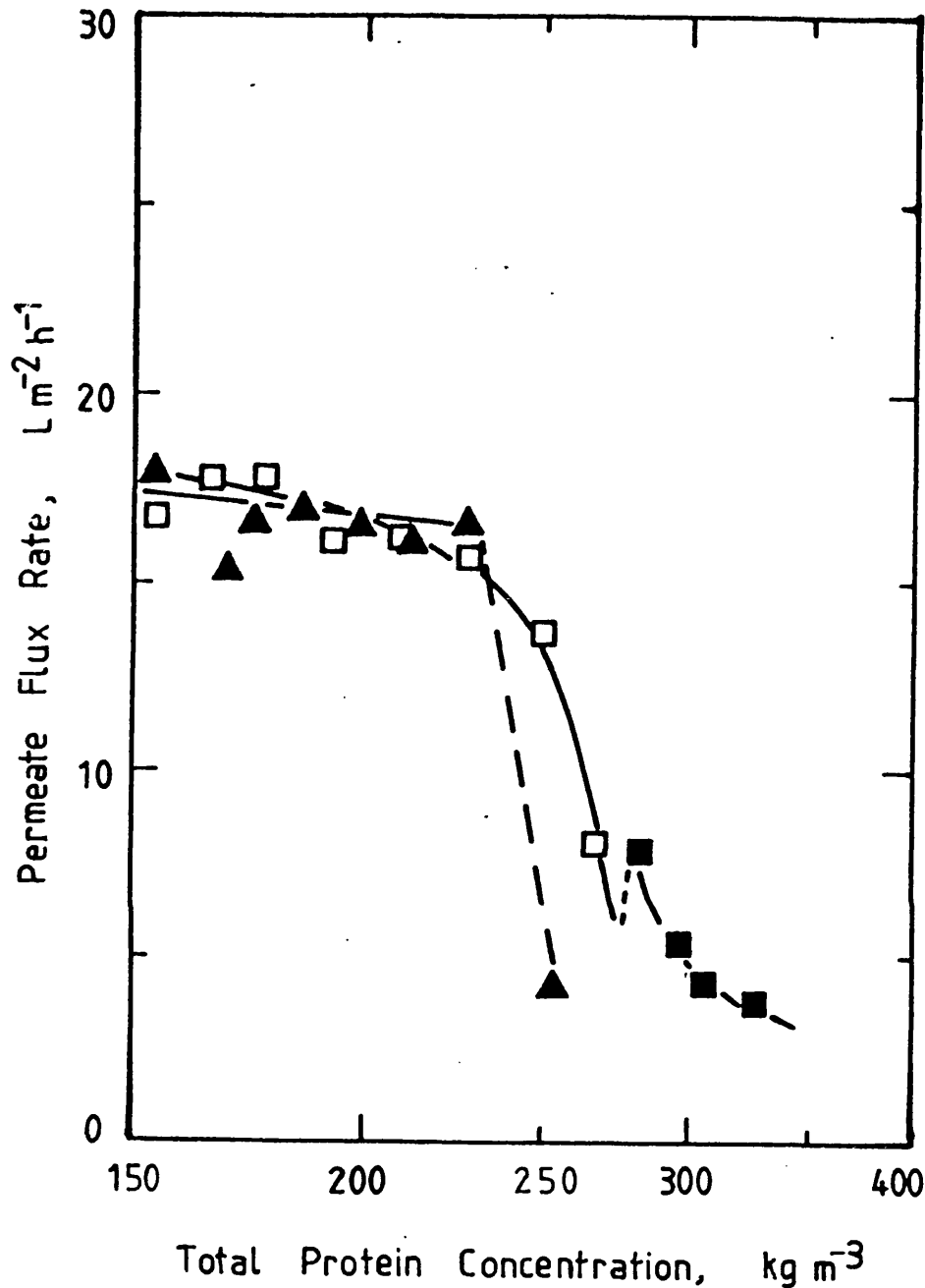


Figure 4.2 The Concentration of Soya Protein Precipitate Suspension: Effect of Pump Type. XM 50 membrane; fibre length, 0.31 m; membrane area, 0.70 m²; fibre diameter, 1.53 mm. Experimental conditions: ▲, centrifugal pump; temperature, 315 K; inlet and outlet gauge pressures respectively, 172 kPa, 103 kPa; initial fraction of protein soluble, 0.19. □, ■, positive displacement pump; temperature, 300 K; inlet and outlet gauge pressures respectively: □, 172 kPa, 103 kPa; ■, 172 kPa, 69 kPa; initial fraction of protein soluble, 0.23.

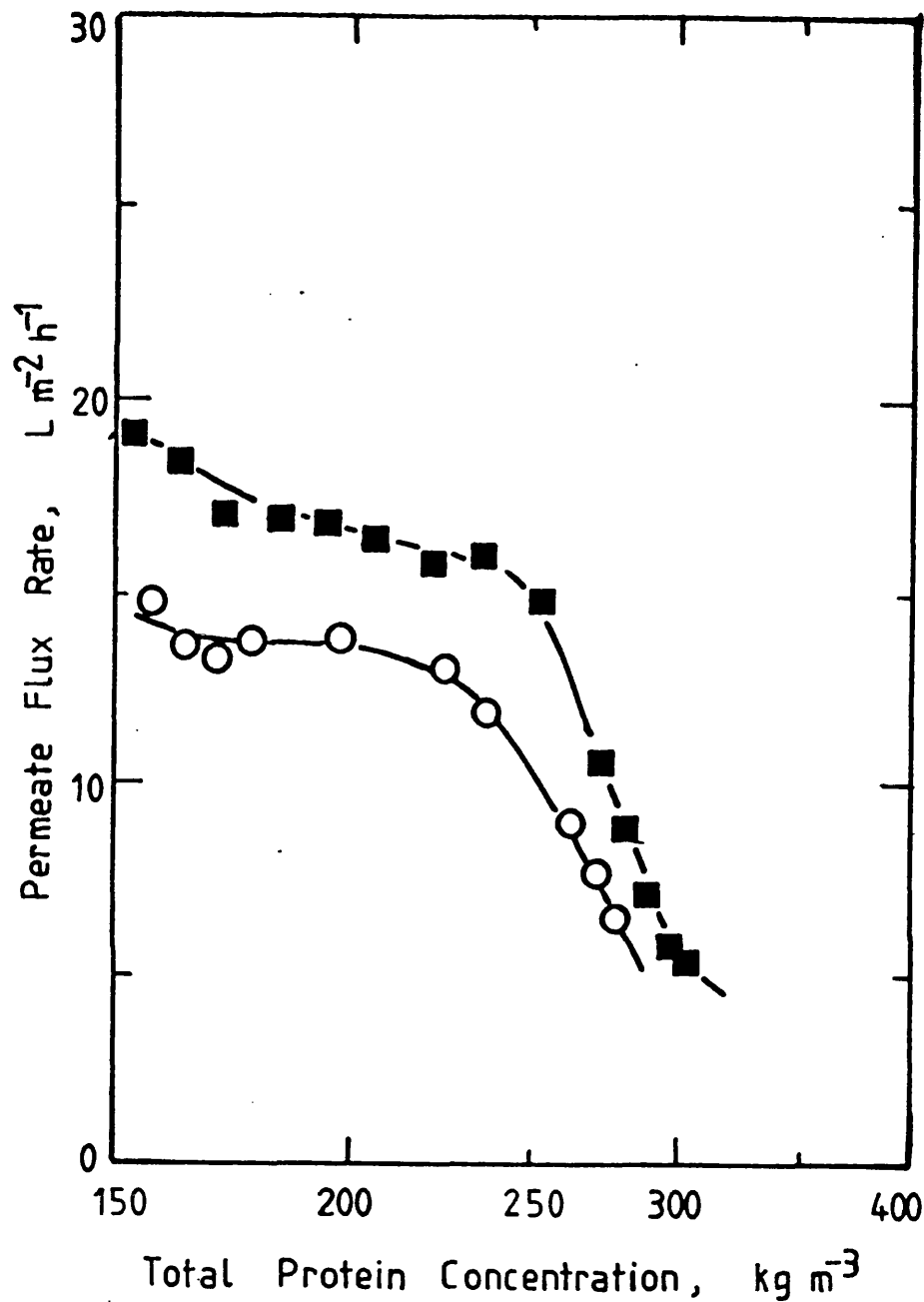


Figure 4.3 The Concentration of Soya Protein Precipitate Suspension: Comparison of Membrane Types. Inlet and outlet gauge pressures, respectively, 172 kPa, 69 kPa; temperature 300 K.

○, PM 50 membrane; fibre length, 0.31 m; membrane area 0.65 m²; fibre diameter, 1.52 mm; initial fraction of total protein soluble, 0.24. ■, XM 50 membrane; fibre length 0.31 m; membrane area, 0.70 m²; fibre diameter, 1.52 mm; initial fraction of protein soluble, 0.18.

region 1 (up to 200 kg/m³ for the longer cartridge) a small reduction in flux rate was observed for increased fibre length. More significantly, the change in fibre length resulted in a difference in the point at which the transition to region 2 occurred. For the longer cartridge this point was reached at 200 kg/m³ while for the shorter cartridge region 1 continued up to 260 kg/m³.

Figure 4.5 shows the effect of changing the fibre diameter for fixed cartridge length and membrane type. The cartridges were examined in parallel to ensure identical processing conditions throughout. The wider diameter fibres (1.52 mm) gave lower flux rates as the precipitate suspension was concentrated up to 210 kg/m³ and reached the transition point to region 2 at 230 kg/m³. The narrower fibres (1.14 mm) reached the transition to region 2 at a lower concentration, 200 kg/m³, and consequently the flux of the narrower fibres declines below that of the wider fibres for concentrations above 210 kg/m³.

4.1.4 Suspension Rheology

Cone and plate measurements of the variation of shear stress with shear rate with total protein concentrations of 206, 281 and 304 kg/m³ (16% soluble protein) and total protein of 199 kg/m³ (30% soluble protein) are shown in Figure 4.6. Non-Newtonian behaviour was observed for all soya protein precipitate suspensions and the viscosity was found to be dependent on the proportion of soluble protein as well as the total protein concentration.

The shear thinning behaviour of the suspensions is illustrated in Figure 4.7 where the apparent viscosity is observed to decrease with shear rate for the 3 samples having 16% soluble protein. The suspension of lowest concentration (206 kg/m³, Fig 4.7) shear thins up to about 2000 s⁻¹ but then displays constant viscosity with further increase in shear rate; the suspensions of higher concentration (281, 304 kg/m³) show decreasing viscosity across the range of shear rates to 3950 s⁻¹. The increase in apparent

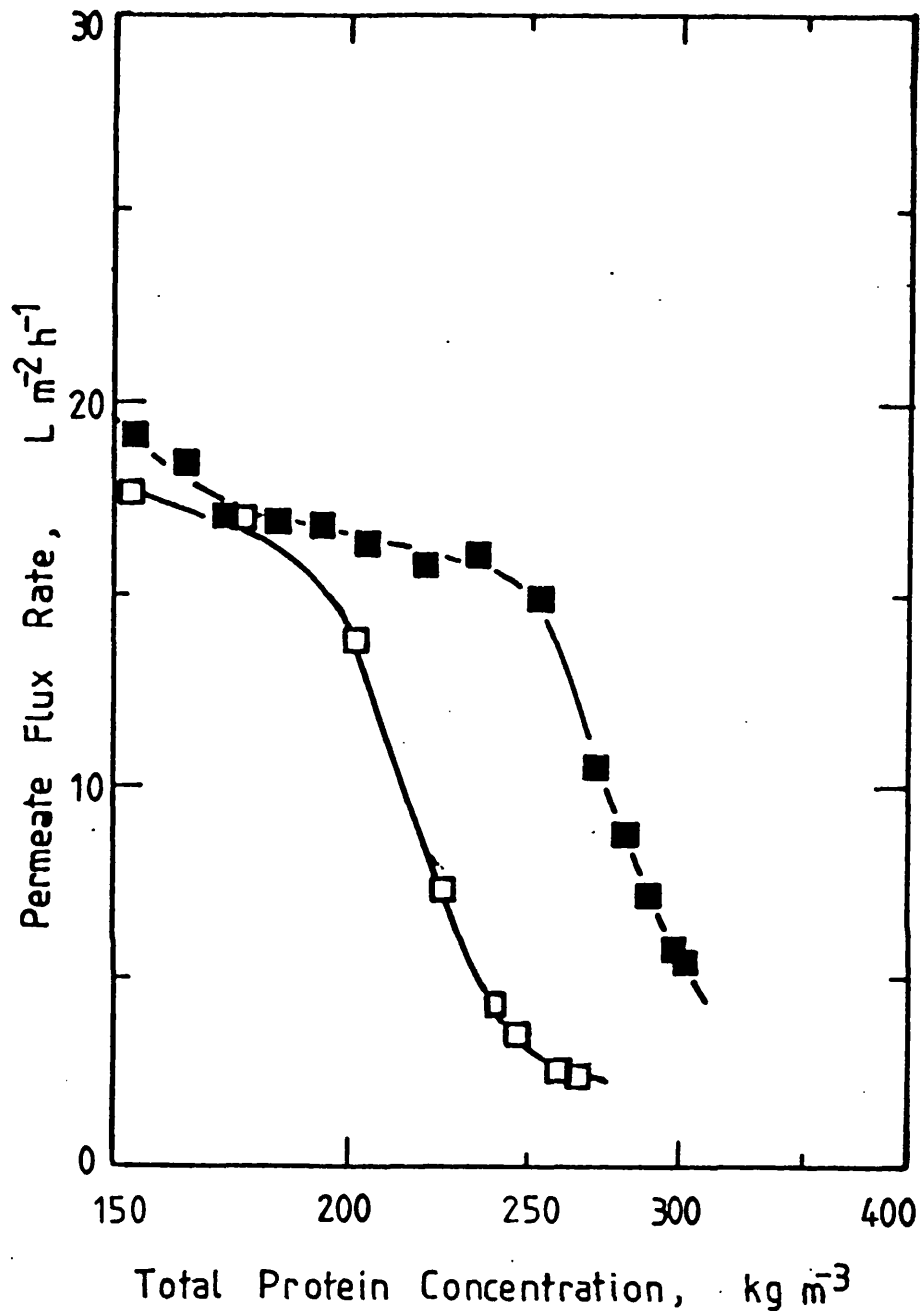


Figure 4.4 The Concentration of Soya Protein Precipitate Suspension: Effect of Changing Fibre Length. Inlet and outlet gauge pressures, respectively, 172 kPa, 69 kPa; XM 50 membrane; fibre diameter 1.52 mm; temperature, 300 K. ■, Fibre length, 0.31 m, membrane area 0.70 m²; initial fraction of protein soluble, 0.18. □, Fibre length 0.635 m, membrane area, 1.39 m²; initial fraction of protein soluble, 0.19.

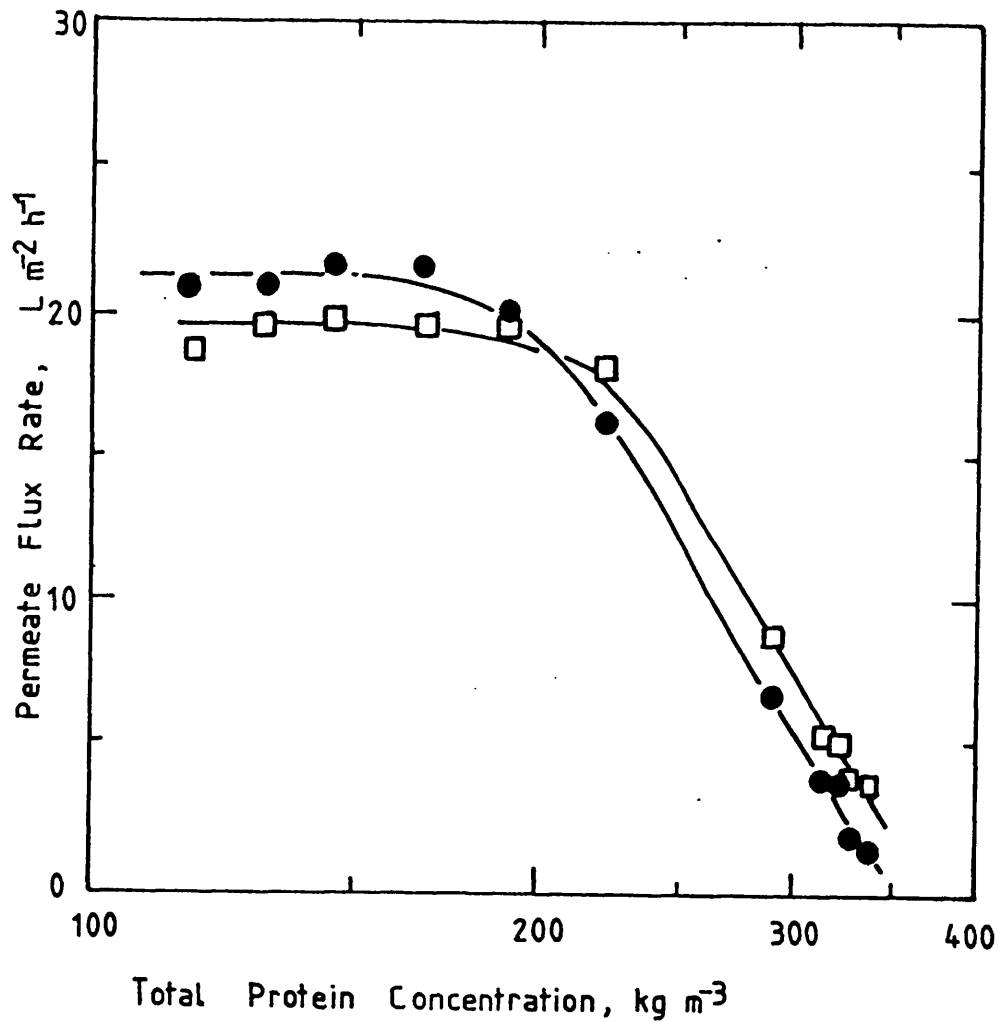


Figure 4.5 The Concentration of Soya Protein Precipitate Suspension: Effect of Changing Fibre Diameter. Inlet and outlet gauge pressures, respectively, 207 kPa, 138 kPa; XM 50 membrane; fibre length, 0.31 m, membrane area 0.70 m²; temperature, 300 K; initial fraction of protein soluble, 0.18. ●, Fibre diameter, 1.14 mm. □, Fibre diameter, 1.52 mm.

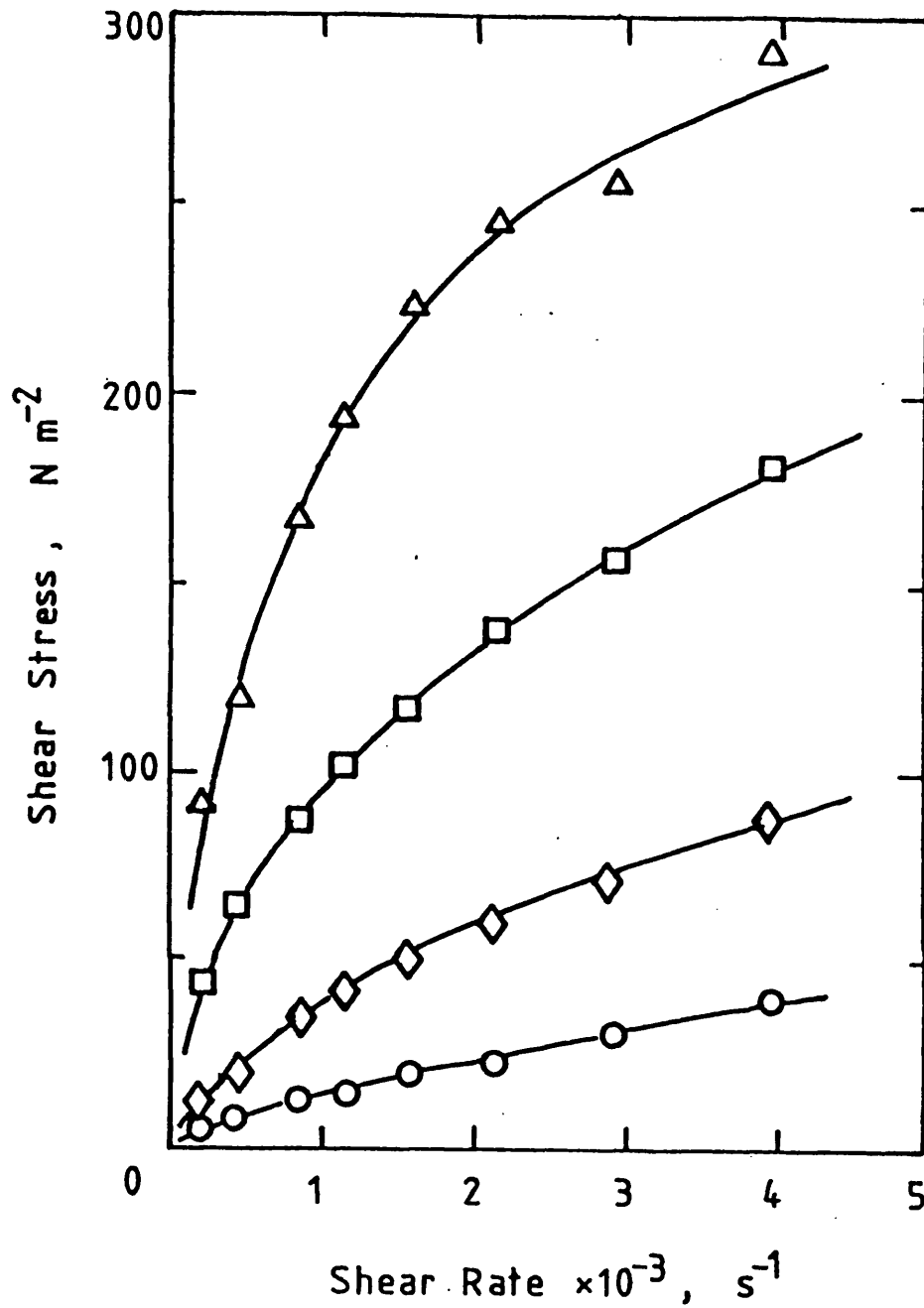


Figure 4.6 Shear Stress versus Shear Rate for Soya Protein Precipitate Suspension. Temperature, 303 K. \diamond , Fraction of protein soluble, 0.30; total protein concentration, 199 kg/m^3 . $\circ, \square, \triangle$, Fraction of protein soluble, 0.16. Total protein concentration: \circ , 206 kg/m^3 ; \square , 281 kg/m^3 ; \triangle , 304 kg/m^3 .

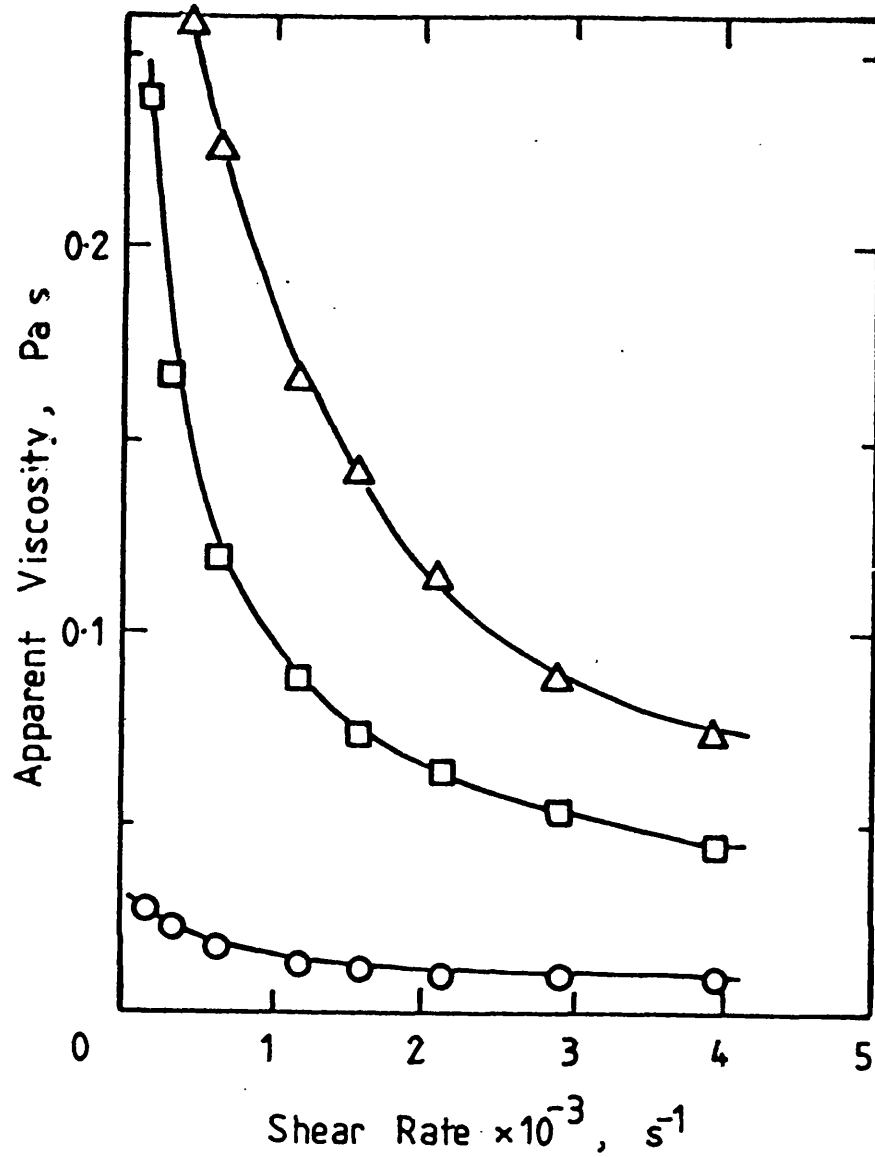


Figure 4.7 Variation of Apparent Viscosity with Shear Rate for Soya Protein Precipitate Suspension. Temperature, 303 K. Fraction of total protein soluble, 0.16. Total protein concentration: ○, 206 kg/m³; □, 281 kg/m³; △, 304 kg/m³.

viscosity with protein concentration is shown by Figure 4.8 where, at fixed soluble protein content (16%), viscosity is plotted at shear rates of 1160 s⁻¹ and 3950 s⁻¹. The increase is particularly marked as the concentration exceeds 270 kg/m³.

Log-log plots of the shear stress versus shear rate (Fig.4.9) were found to be linear over the measured range enabling the determination of n and k in accordance with the power law model for a pseudoplastic fluid:

$$\tau = k\dot{\gamma}^n \quad \text{Equation 4.1}$$

Values of n and k are listed in Table 4.1 for total protein concentrations in the range 206-304 kg/m³ with 16% of the protein soluble along with comparative values for a suspension having a higher proportion (30%) of the total protein soluble.

Since the soluble protein content is dependent on the initial make up of the precipitate and the soluble protein rejection of the membrane, n and k were determined for each experimental run (Table 4.2) in order to estimate the flow conditions in the hollow fibres at the point of transition from region 1 to region 2 on the flux rate profiles (Figs 4.1-4.5). Where data for n and k were not available at the transition point concentration values were estimated from available measurements for soya precipitate suspensions of similar soluble protein content. The rheology data of Table 4.2 was used to calculate the linear mean velocity in the fibres and the values at the fibre wall of the shear stress, shear rate and Reynolds number (Table 4.3) in accordance with the general equations of pipe flow of a power law fluid given in Section 1.5.3. The shear stresses applied to the fluid (56-118 N/m²) resulted in Reynolds numbers of 27 to 84 at the transition concentrations. The wall shear rates at this point were found to be around 4000 s⁻¹ and the mean velocity in the fibres ranged from 0.56 m/s to 0.75 m/s.

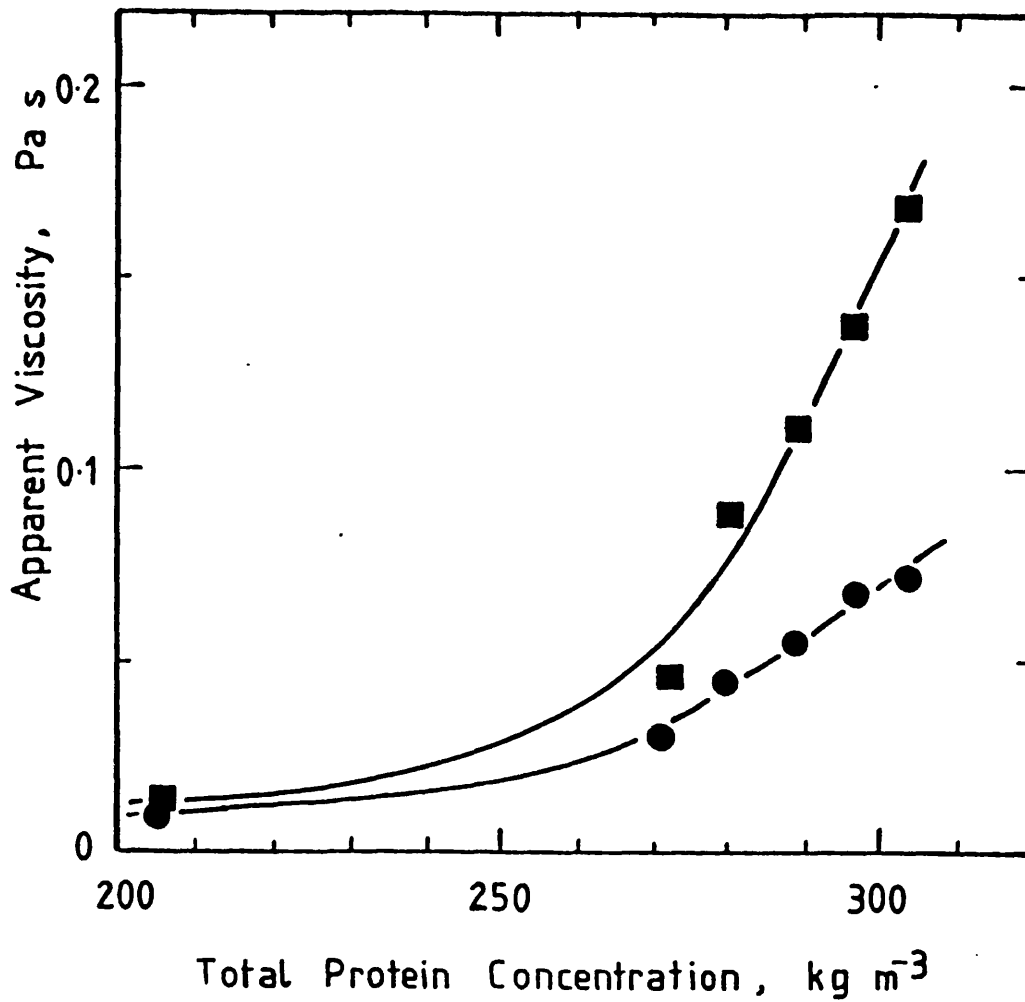


Figure 4.8 Variation of Apparent Viscosity with Total Soya Protein Concentration. Temperature, 303 K; fraction of total protein soluble, 0.16; shear rates: ■, 1160 s⁻¹, ●, 3950 s⁻¹.

Table 4.1 Power Law Index and Consistency for Soya Protein Precipitate Suspension.

C_s/C_t	0.16						0.30
C_t	206	272	281	289	297	304	199
n	0.72	0.64	0.48	0.51	0.49	0.46	0.51
k ($N s^n/m^2$)	0.10	0.61	3.41	3.49	4.86	7.14	0.64

Table 4.2 Power Law Index and Consistency at Transition Point in Soya Protein Ultrafiltration.

Figure	1(O)	2(□)	3(■)	4(□)5(●)	5(□)
C_t	236	249	272	202	239
C_s	44	42	37	29	35
n	0.55	0.54	0.64	0.95	0.73
k ($N s^n/m^2$)	1.14	0.92	0.61	0.021	0.22

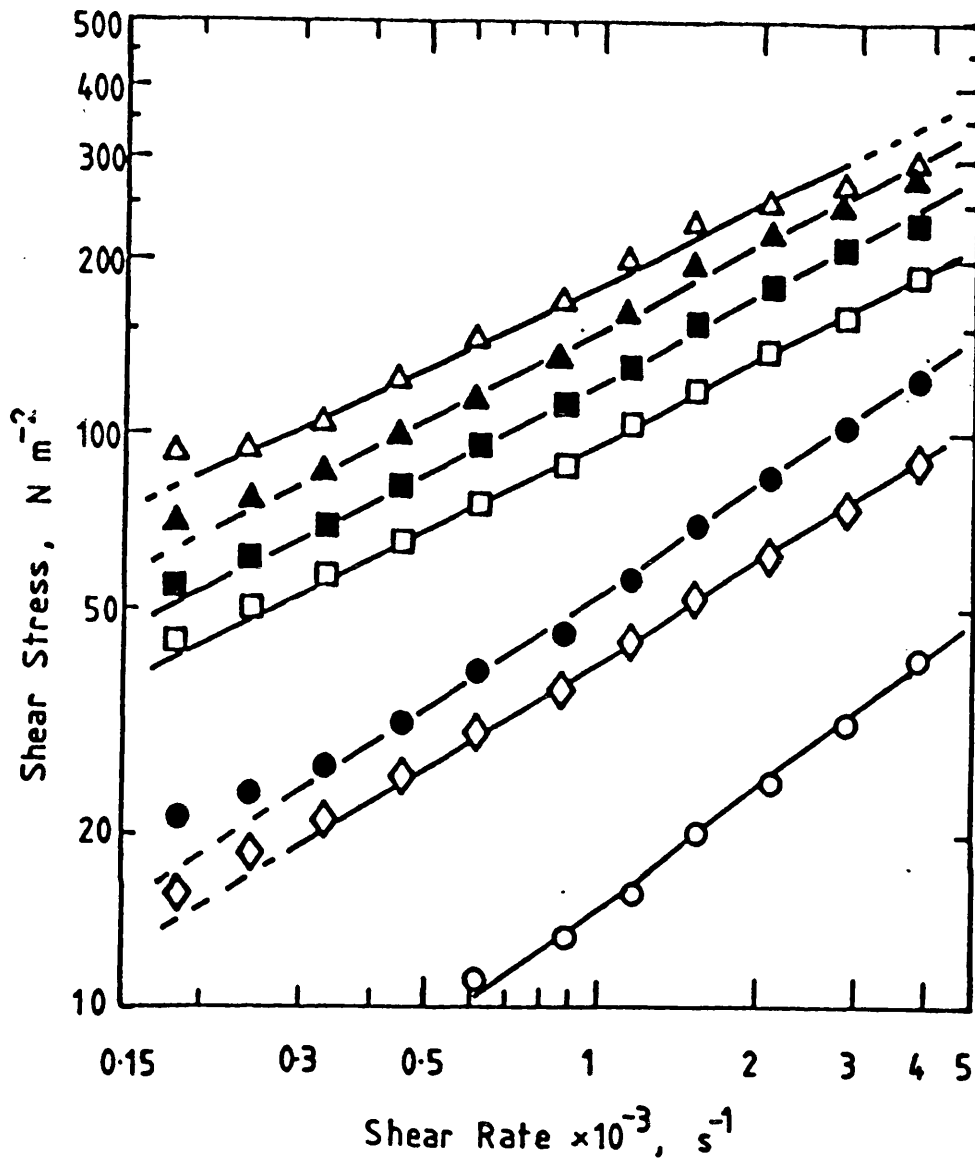


Figure 4.9 Log-log Plot of Shear Stress versus Shear Rate for Soya Protein Precipitate Suspension. Temperature, 303 K. \diamond , Fraction of protein soluble, 0.30; total protein concentration, 199 kg/m^3 . \circ , \bullet , \square , \blacksquare , \triangle , \blacktriangle , Fraction of protein soluble, 0.16; total protein concentration: \circ , 206 kg/m^3 ; \bullet , 272 kg/m^3 ; \square , 281 kg/m^3 ; \blacksquare , 289 kg/m^3 ; \blacktriangle , 297 kg/m^3 ; \triangle , 304 kg/m^3 .

Table 4.3 Flow Conditions at the Transition Point during Hollow-Fibre Ultrafiltration of Soya Protein Precipitate.

Figure	Membrane	Length	Diameter	P	C _t	C _s	τ _w	Re	$\dot{\gamma}_w$	u
		m	mm	kPa	kg/m ³	kg/m ³	Pa		s ⁻¹	m/s
1(O)	PM50	0.31	1.52	96	236	44	118	37	4600	0.72
2(□)	XM50	0.31	1.52	62	249	39	76	34	3600	0.56
3(■)	XM50	0.31	1.52	103	260	37	118	27	3700	0.62
4(□)	XM50	0.64	1.52	93	202	29	56	84	4000	0.75
5(●)	XM50	0.31	1.14	62	210	27	57	49	4100	0.58
5(□)	XM50	0.31	1.52	62	230	30	76	41	5200	0.68

Wall shear rate, $\dot{\gamma}_w$, linear mean velocity, u , and Reynolds Number, Re , calculated using Equations 4.1-4.2 for a power law fluid ($\tau = k\dot{\gamma}^n$) with n and k taken from Table 4.2.

4.2 Discussion

4.2.1 Flux Prediction in the Ultrafiltration of Soya Suspension

For the ultrafiltration of colloids in the presence of soluble macromolecules the mechanism of flux control, in addition to the polarisation of the surface by soluble macromolecules or fine particles, may include the scouring of the membrane surface proposed by Fane et al. (1982), the tubular pinch effect described by Porter (1972), or the radial migration effect of Altena and Belfort (1984). Further uncertainties in the mechanism of flux control are introduced by the problem of estimating the physical properties of the suspension, such as viscosity and diffusivity, which will be a function of the concentration gradient perpendicular to the membrane surface.

For soya protein precipitate suspensions, Devereux et al. (1986) found that the gel polarisation model, based of the concentration of soluble protein, overestimated the actual flux rates as the material was concentrated from total protein concentration of 50 kg/m³ to 325 kg/m³ by hollow fibre ultrafiltration on a laboratory scale.

In scaling this process up to pilot plant they observed a region in which the flux rates were independent of the protein concentration. At the upper end of the concentration range the precipitation of the soya protein increased the flux rates that could be obtained when compared to solutions of soya protein. The investigation was limited by the sharp decline in flux, attributed to the increasing viscosity of the suspension, and it was not possible to reach the the protein concentrations obtained on the laboratory scale.

Goldsmith et al. (1972) found that the dewatering of sludge concentrate was limited by the pumping capabilities of the centrifugal pump and this type of pump is generally not recommended for use with viscous suspensions [Coulson and Richardson (1977)]. A rapid decline in flux was observed in this study when a centrifugal pump was used for the recirculation of

the suspension but the decline was arrested by the replacement of this pump with a positive displacement pump (Fig. 4.2). It was then possible to examine the pilot scale concentration of the suspension at high protein concentrations where the suspension rheology and hollow-fibre geometry are important factors in sustaining high flux rates. These factors are discussed in Sections 4.2.3 and 4.2.4.

4.2.2 Polarisation of the Membrane

The independence of the flux rate with transmembrane pressure observed at the higher concentrations of the process (Fig. 4.1, region 2) indicates that this region corresponds to the 'gel-polarised' condition of ultrafiltration theory [Blatt et al. (1970)]. At the lower concentrations (region 1) the protein concentration is too low, or the shear rate is too high, for the formation of a gel-polarised layer at the membrane to control the flux rate. Consequently the flux rate can be increased by increasing the transmembrane pressure but is not greatly influenced by the flow rate across the membrane or the protein concentration. The flux rates obtained during the ultrafiltration of the suspension are an order of magnitude lower than those obtained with pure water (Section 4.1.1). In the presence of dissolved and suspended solids the flux rates will be controlled by the interaction of the process stream with the membrane. Although the mechanism of increased resistance to permeation is uncertain, flux reduction will occur due to polarisation, osmotic pressure differences across the membrane and fouling.

The water flux rates (Section 4.1.1) indicate a higher membrane permeability for the XM type membrane compared to the PM type. This is reflected in the different flux rates observed for the different membranes in Figure 4.3. However, at higher concentrations, in region 2, the flux rate profiles converge indicating that the flux rate is becoming independent of the membrane permeability - the membrane is gel-polarised and the flux depends only on the gel layer.

The results in Table 4.3 suggest that the transition to gel-polarised conditions during the concentration is determined by the flow velocity or the wall shear rate. Values of the wall shear rate at this transition point, 3600 s^{-1} to 5200 s^{-1} , are close to the upper limit of the measurement range of the cone and plate viscosity measurements although the majority of the fluid in the fibre will be exposed to shear rates within the measured range. In all cases the flow conditions at the transition point can be represented by low Reynolds number ($Re < 100$) indicating laminar flow in the fibres. A more detailed evaluation of the trends is difficult since the point of transition between the two regions is obtained by the interpolation of data in a region of sharply changing flow properties and there will be a number of approximations in the calculations.

4.2.3 Hollow Fibre Geometry

In the polarised region, where the cross-flow controls the flux rate through the membrane, changes in the hollow fibre dimensions can affect the flux rates at fixed transcartridge pressure. Decreasing the fibre length (Fig. 4.4) or increasing the fibre diameter (Fig. 4.5) delayed the onset of the gel-polarised conditions in the membrane. When operated in the gel-polarised region the increased cross-flow velocities or wall shear rates obtained with the wider and shorter fibres result in higher fluxes but do not increase the flux rates when operated before the gel-polarised region is reached. Indeed, the wider fibres have lower fluxes in the pre-gel region due to the lower porosity of these fibres (Section 4.1.1).

4.2.4 Suspension Rheology

The treatment of the flow of the suspension in the hollow fibres assumes that the equations for pipe flow of a power law fluid (Section 1.5.3) can be used for the fibres. Belfort and Nagata (1985) have shown that the permeation of fluid through a porous steel microfiltration tube can have a significant affect on the axial flow and have correlated the friction factors for porous and non-porous tubes using a Reynolds number based on the

permeation velocity of the fluid in addition to the channel Reynolds number. The data of Belfort and Nagata (1985) do not extend to the low Reynolds numbers observed here (channel Reynolds number <100 ; permeation Reynolds number <0.01) but it is possible that the relationship for the friction factor of the porous tube becomes coincident with that of the non-porous tube for the very low permeation rates and Reynolds numbers observed for concentrated precipitate suspensions.

As indicated by the log-log plot of shear stress and shear rate (Fig. 4.9) the suspension behaves as a power law fluid over the range $400-4000 \text{ s}^{-1}$. However, at lower shear rates ($150-400 \text{ s}^{-1}$, Fig. 4.9) the measured shear stress deviates from the straight line obtained for higher shear rates indicating higher viscosities than would be predicted from the power law fit. This increased viscosity may be attributed to structuring of the fluid at very low shear rates. Since the protein precipitate is at its isoelectric point there will be little particle-particle repulsion due to Coulombic forces and particle interaction will be controlled by attractive Van der Waals' forces. With increasing shear rate the break down of floc structures, the disentanglement of particles and soluble macromolecules, and the release of water trapped in the particle structure will lead to shear thinning behaviour for the suspension. This breakdown of structure may be reversible but there will also be irreversible effects such as the break down of precipitate particles leading to the thixotropic behaviour observed by Devereux et al. (1984) for soya precipitate suspension.

The results calculated in Table 4.3 from the cone and plate data are based on the power law fit for the range $400-4000 \text{ s}^{-1}$. Since there is a continuous variation of shear rate in the hollow fibre from 0 on the centre line to a maximum at the wall the fluid in the fibre will exhibit a range of shear rates. There will be a section of fluid near the centre line which will be largely unsheared while, in some cases, the calculated shear rate at the wall exceeds 4000 s^{-1} . It is possible to include a yield stress to allow for structure formation at low shear rates but the exact determination of this parameter is difficult since it requires

extrapolation of cone and plate measurements in a region of rapidly changing viscosity. The development of a yield stress in the suspension will be important if flow through the fibres is stopped with concentrated suspension in the cartridge since blockage of fibres may occur on restarting the pump.

The low shear viscosity of the suspension will also influence the flow in the pipe system leading from the pump to the hollow fibre cartridge since the shear rates here will be much lower than in the hollow fibres. Devereux (1983) found changes in the header design at the entrance to the cartridge could improve the recirculation of the suspension through the hollow fibres.

The increasing viscosity of the soya protein suspension at concentrations beyond 270 kg/m^3 (Fig. 4.8) plays a significant role in the flux rates obtained in the ultrafiltration of the suspension. In the gel-polarised region the flux rate decline may be caused by both the increasing protein concentration and the increasing viscosity of the retentate. Higher flux rates can therefore be obtained by increasing the transcartridge pressure as shown in Figures 4.1 and 4.2.

The influence of the soluble protein content on the rheology of soya protein precipitate suspensions, prepared by ultrafiltration and centrifugation, has been noted by Devereux et al (1984) and is illustrated here by an example of a suspension containing 30 % soluble protein (Table 4.1). The higher proportion of soluble protein leads to higher viscosities and hence will require higher pressure to maintain the same cross-flow velocity.

4.3 Conclusion

The pressure limitations on the operation of hollow-fibre cartridges lead to two regions in which the basis for the optimisation of the operating conditions will differ. In the region before gel polarisation it is desirable to operate at the highest possible transmembrane pressure while maintaining sufficient cross flow to prevent polarisation of the membrane.

In the gel-polarised region flux may be increased by increasing the transcartridge pressure while maintaining a minimum transmembrane pressure. In this second region the control of the suspension rheology can be used to improve the flux rate by, for example, reduction in the soluble protein content of the suspension.

Where the inlet and outlet pressures are fixed, changing the geometry of the hollow fibre system (to shorter or wider fibres) can improve the overall process by prolonging the region in which the membrane is not gel-polarised or by increasing the flux in the gel-polarised region. The use of the alternative membrane configuration of a spiral wound module may lead to severe problems when processing highly viscous suspensions due to the additional contribution to flow resistance by the spacer material. Where very high concentrations are required a tubular configuration (i.e. very wide membrane channels) may be preferred to the hollow-fibre system.

5. SEPARATION OF BORAX-FLOCCULATED YEAST CELL DEBRIS

5.1 Introduction

The results of laboratory experiments [Bonnerjea et al (1988)] indicate that borax is a suitable reagent for the flocculation of yeast cell debris. The activity of the yeast enzymes, e.g. fumarase and alcohol dehydrogenase, can be maintained in solution while the borax-flocculated debris separates in a short time at low centrifugal force.

The scale-up of the laboratory procedure to pilot-scale operation using a scroll decanter centrifuge is reported here. The centrifugal force generated by this centrifuge, ca. 3,000g, is comparable to the force used for laboratory separation of the flocs. Higher centrifugal forces are possible with other types of centrifuge such as the disc-stack or tubular-bowl centrifuges. Indeed, a disc-stack centrifuge has been used by Mosqueira et al (1981) for the separation of mechanically disrupted yeast cells but separation of sediment was hampered by the blockage of discharge ports with viscous solids. Also the low flowrates employed led to a temperature rise which was potentially damaging to biological materials.

In the scroll decanter centrifuge the constant scrolling of solids out of the bowl enables the continuous processing of suspensions with high solids content over a wide range of flowrates. The discharge of the settled material is critical to the success of the continuous separation of the cell debris from the homogenate. Shear modulus measurements were used to compare the structure of flocculated and non-flocculated sediments and to indicate the dewatering conditions under which the sediment could be discharged from the centrifuge.

5.2 Results

5.2.1 Variation of Shear Modulus with Dry Weight

For flocculated and non-flocculated sediments, with samples having dry weights ranging from 18% to 27%, the values of the shear modulus at 10 Hz are compared in Figure 5.1. Higher values for the flocculated sediment were apparent over this range of dry weights, particularly when the dry weight exceeded 22%. The variation of shear modulus with frequency of oscillation, Figure 5.2, revealed significant differences between the behaviour of flocculated and non-flocculated yeast homogenate when settled to approximately the same dry weight. The shear modulus of the homogenate sediment, dry weight 23.5%, remained constant at ca. 1.3 kPa over the range of frequencies examined while for the flocculated sediment, dry weight 23.3%, the modulus rose from 2.9 kPa at 0.01 Hz to 15.3 kPa at 10 Hz.

5.2.2 Variation of Dry Weight with Relative Centrifugal Force

The dry weights of sediments obtained from the centrifugal settling of yeast cell debris for 0.5 h are shown on Figure 5.3. Similar dry weights, ranging from 11% (rcf=35) to 29.5% (rcf=160000), were obtained for flocculated and non-flocculated suspensions. With rcf values comparable to that of the scroll centrifuge (rcf=3000) laboratory centrifugation produced sediment of dry weight 22% after 0.5 h.

5.2.3 Clarification and Dewatering using a Scroll Decanter Centrifuge

Adjusting the height of the liquid discharge allows the fluid level in the centrifuge, the pond depth, to be varied from a minimum value of 13.1 mm to a maximum value of 21.3 mm. The level of the solids discharge at the conical end of the centrifuge corresponds to a pond depth of 20 mm. A maximum value of 19.3 mm was used here as this corresponded to operation of the centrifuge with the beach almost totally flooded while 13.1 mm corresponds to the maximum area of dry beach in the centrifuge.

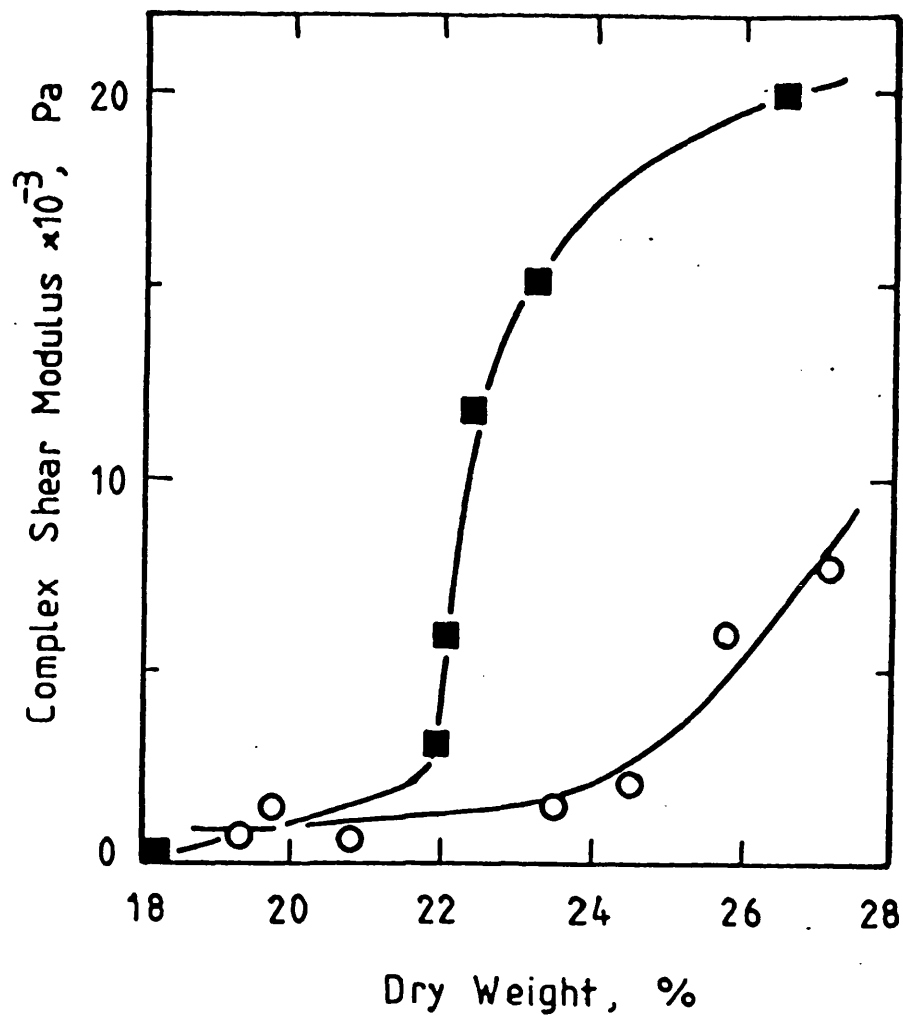


Figure 5.1 Variation of Shear Modulus with Sediment Dry Weight. ■, Flocculated yeast homogenate sediment; ○, non-flocculated yeast homogenate sediment. Oscillation frequency, 10 Hz.

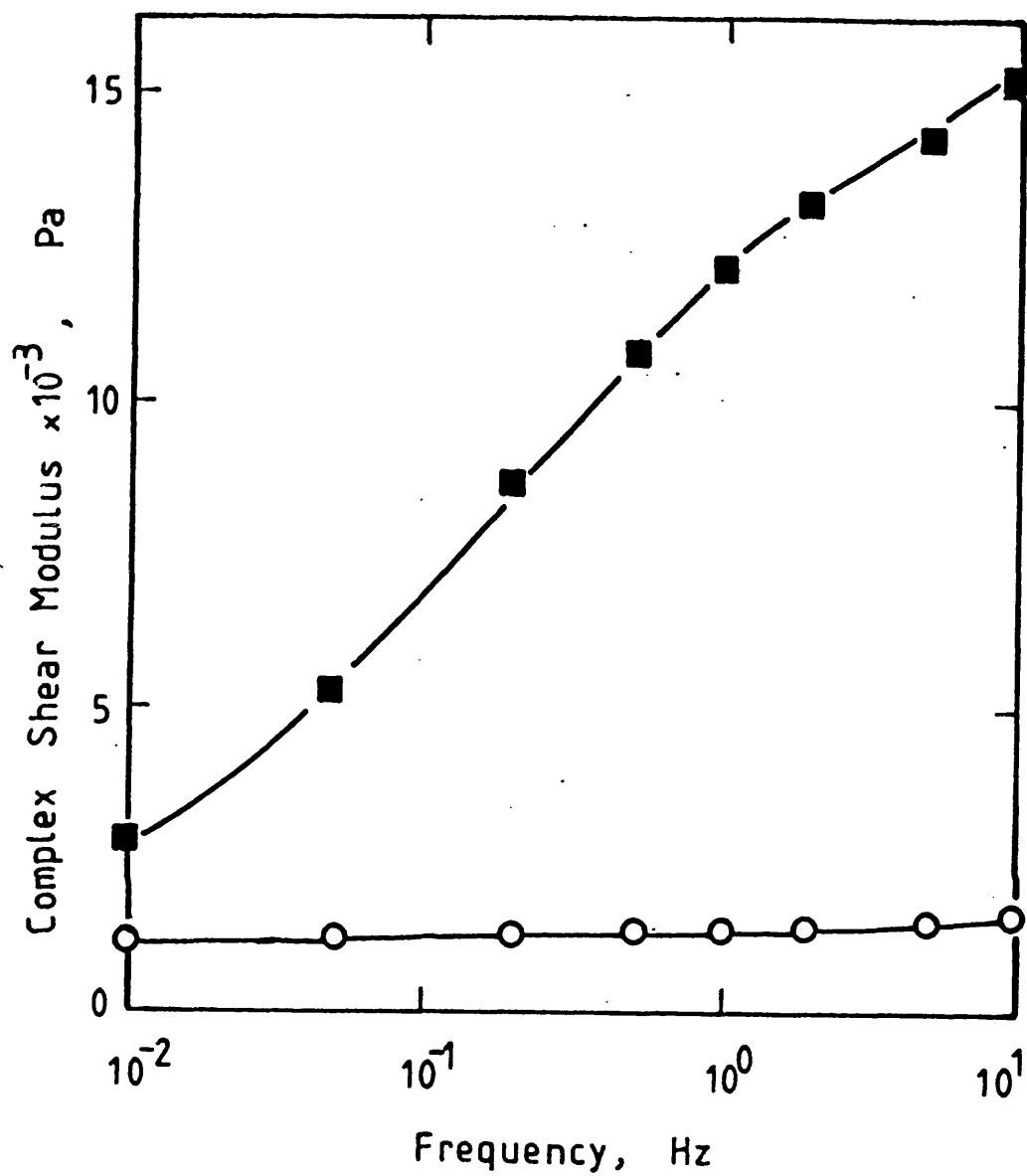


Figure 5.2 Variation of Shear Modulus with Oscillation Frequency. ■, Flocculated yeast homogenate sediment, dry weight, 23.3%; ○, non-flocculated yeast homogenate sediment, dry weight, 23.5%.

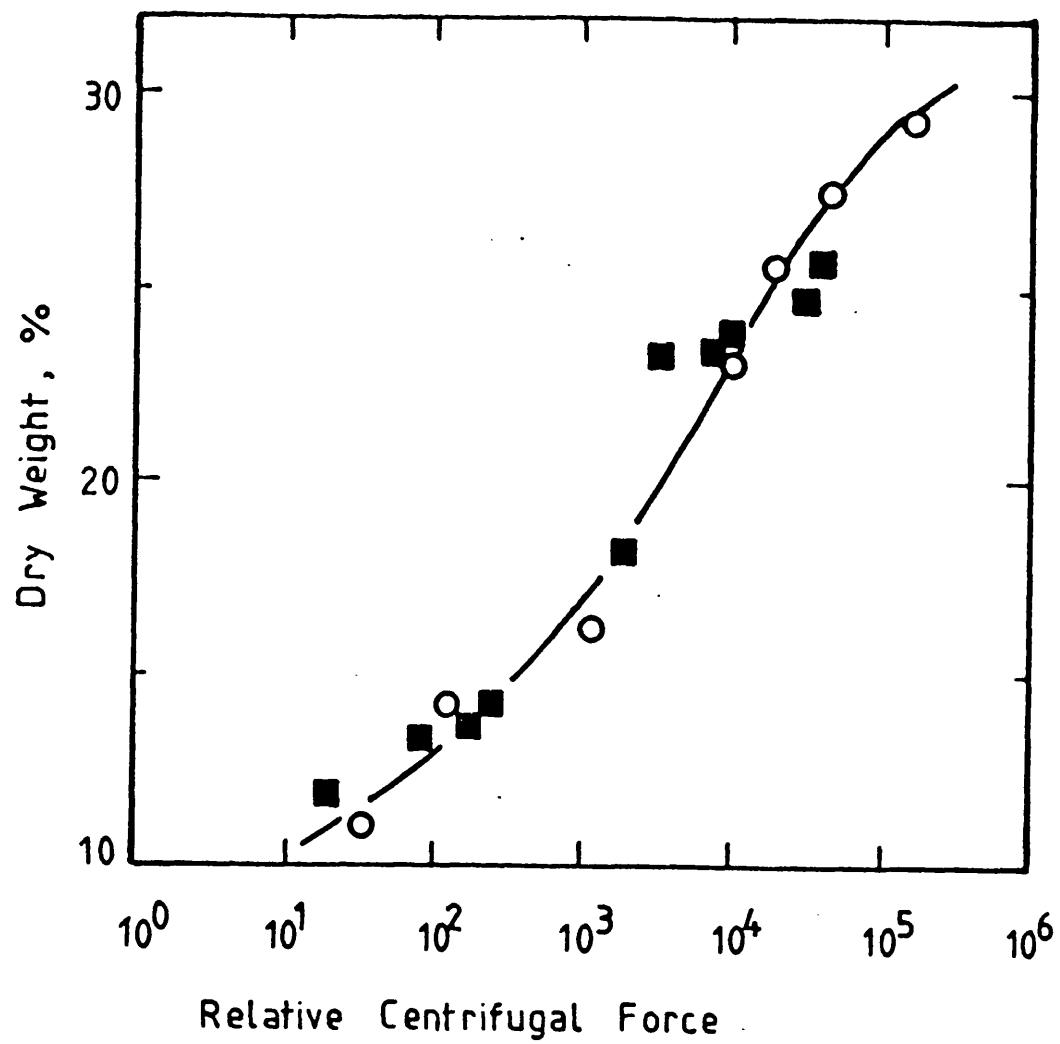


Figure 5.3 Variation of Sediment Dry Weight with Relative Centrifugal Force. Laboratory centrifugation for 0.5h; ■, flocculated yeast homogenate; ○, non-flocculated yeast homogenate.

At an intermediate pond depth of 16.2 mm, as shown in Figure 5.4, changes in the feed flow rate over the range 0.1-0.8 m³/h had no significant effect on the separation performance of the scroll centrifuge. The reduced efficiency remained constant at ca. 85% and the dry weight of the underflow was ca. 24%. A constant value of the overflow dry weight, 8.4%, was observed. The dry weight of the supernatant obtained after removal of the solids by high-speed centrifugation was found to be 7.8%. Hence the dry weight of soluble material in the overflow stream (allowing for the volume of solids removed, 4.0%, Table 5.1) was calculated as 7.5%. The dry weight of the solid material is therefore 0.9% in the overflow stream.

The effect of differential scroll rate was examined for the extreme values of the pond depth, 13.1 mm and 19.3 mm, giving operation of the centrifuge with the maximum and minimum length of dry beach, respectively. In both cases the overflow dry weight, ca. 8.4%, was unaffected by changes of scroll rates (Fig. 5.5). The sediment dry weights also appear to be independent of the scroll rate over the range 10-50 rpm. However, the sediment dry weights are consistently higher (ca. 24%) when separated with the lower pond depth (13.1 mm) than the dry weight (ca. 19%) obtained with the higher pond depth (19.3 mm).

The decrease in sediment dry weight with increasing pond depth is further illustrated by Figure 5.6, although there is some scatter in the results due to the problem of sampling the sediment discharge. Also shown in this figure is the effect of mixing conditions (batch mixing versus continuous mixing - as described in Section 2.2.2) before centrifugation. The solids content of the overflow stream was constant over the range of pond depths employed and was not affected by the method of mixing the borax with the yeast homogenate. Both mixing methods produced similar sediment dry weights although at the lower pond depths of 13.1 mm and 16.2 mm slightly higher dry weights were obtained with the batch-mixed material.

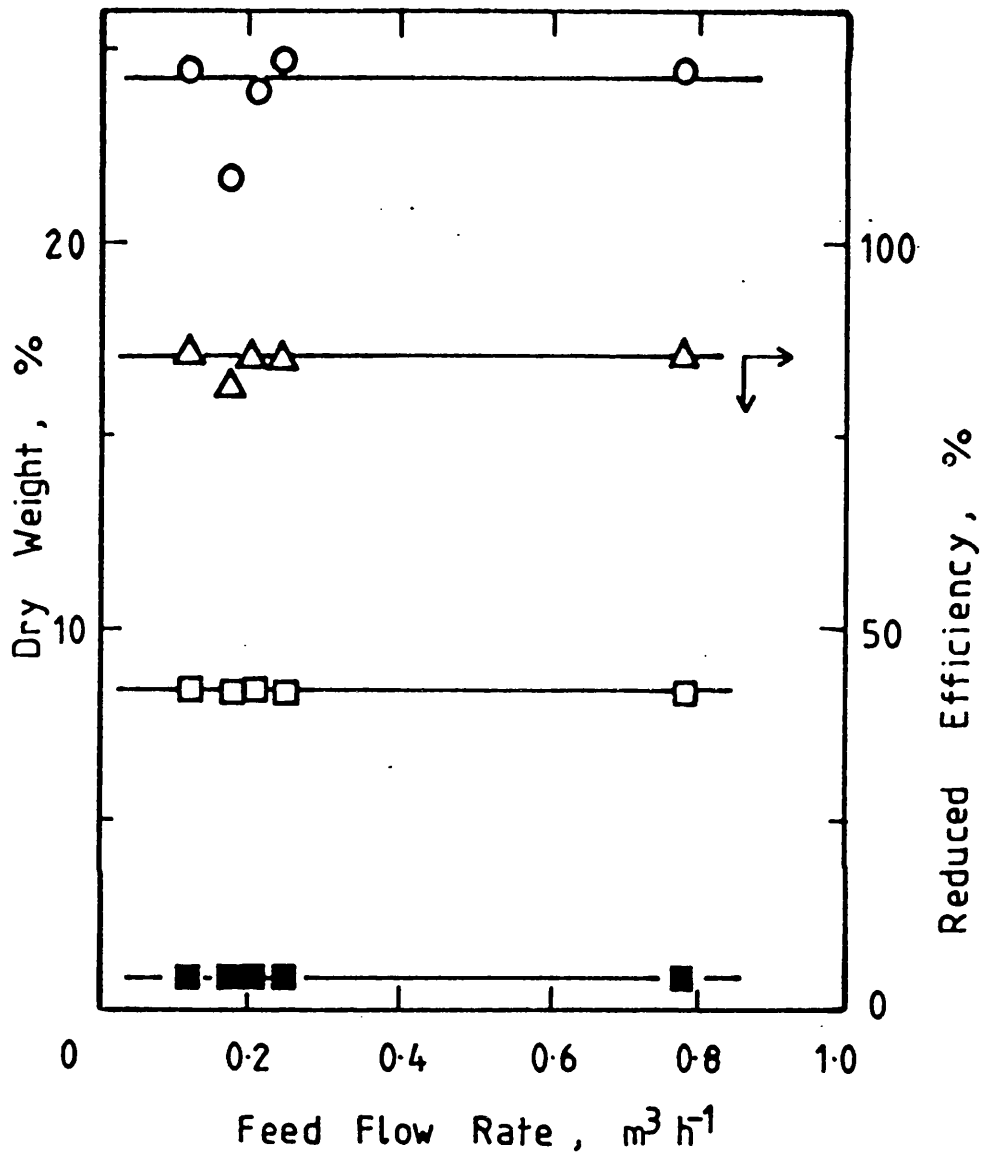


Figure 5.4 Effect of Feed Flow Rate on Separation of Flocculated Yeast Homogenate. \circ , Sediment dry weight; \square , overflow dry weight; \blacksquare , overflow solids dry weight; \triangle , reduced efficiency. Differential scroll rate, 30 rpm; batch mixing. Pond depth, 16.2 mm

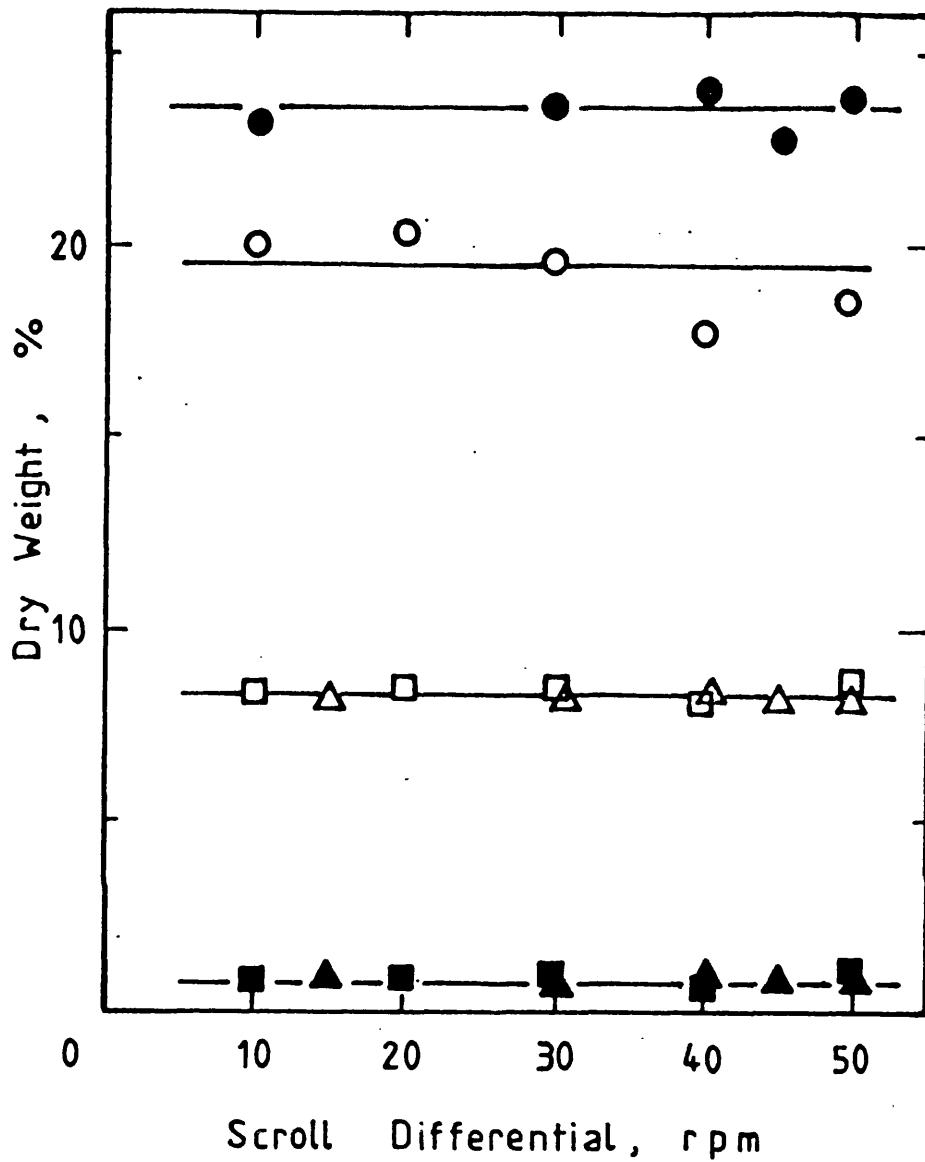


Figure 5.5 Effect of Differential Scroll Rate on Separation of Flocculated Yeast Homogenate. \circ, \bullet , Sediment dry weight; \square, \triangle , overflow dry weight; $\blacksquare, \blacktriangle$, overflow solids dry weight. Pond depths: $\circ, \triangle, \blacktriangle$, 19.3mm; $\bullet, \square, \blacksquare$, 13.1 mm. Feed flow rate, 0.10 m³/h, batch mixing.

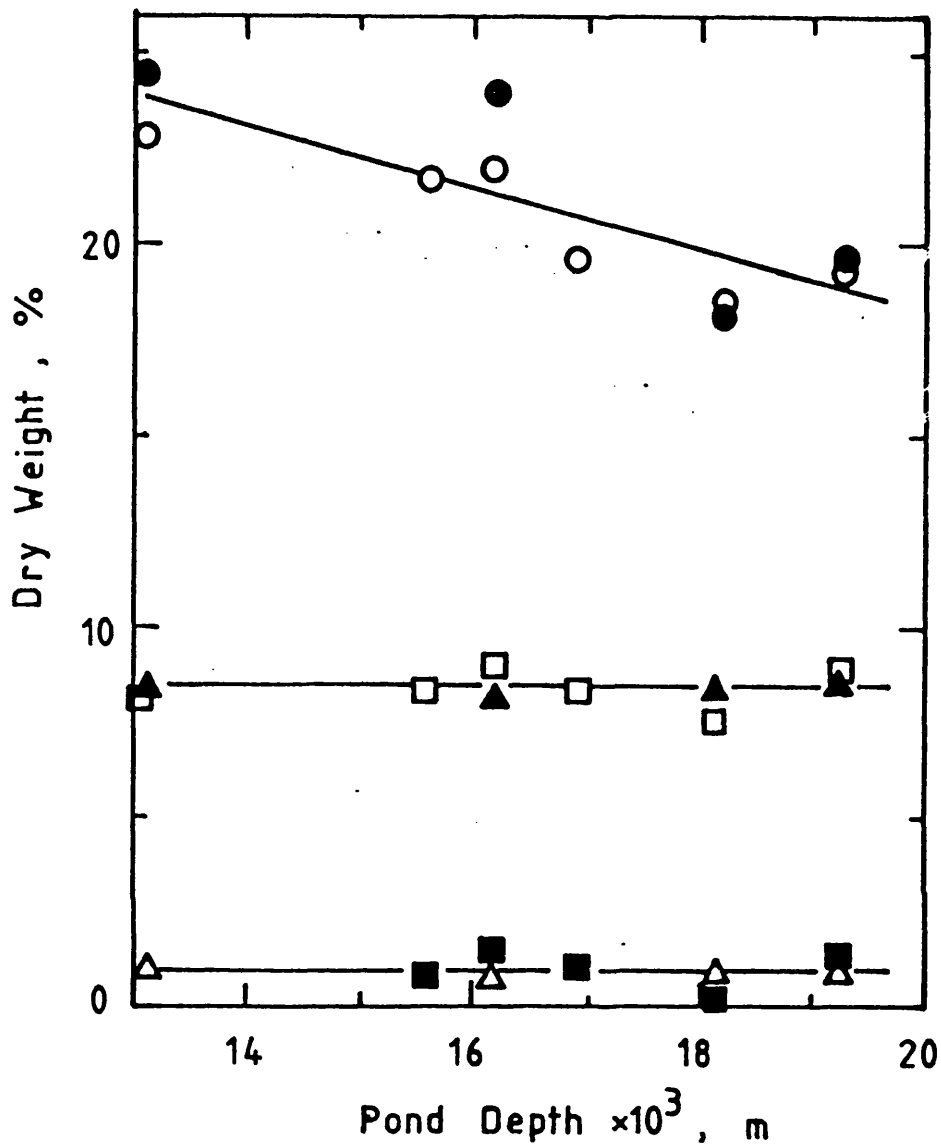


Figure 5.6 Effect of Pond Depth on Clarification and Dewatering of Flocculated Yeast Homogenate. \circ , \bullet , Sediment dry weight; \square , \blacktriangle , overflow dry weight; \blacksquare , \triangle , overflow solids dry weight. Feed flow rate, $0.18 \text{ m}^3/\text{h}$, differential scroll rate, 30 rpm. \circ , \blacktriangle , \triangle , batch mixing; \circ , \square , \blacksquare , continuous mixing.

Table 5.1 Comparison of Dry- and Flooded-beach Operation of the Scroll Decanter Centrifuge.

Pond Depth mm	Feed Rate m ³ /h	Overflow m ³ /h	R	Efficiency		Protein Recovery %
				E %	E' %	
19.3	0.180	0.126	0.3	87	82	82
13.1	0.180	0.144	0.2	86	82	93

Feed: Wet solids, 18%; Protein, 30 kg/m³

Overflow: Wet solids, 4.0%; Protein, 35 kg/m³

5.2.4 Protein Recovery

Protein concentration in the supernatant obtained after removal of the solids by high-speed centrifugation was typically 37 mg/mL. When allowance was made for the volume occupied by the solid material (18%, Table 5.1), the protein concentration in the feed stream was calculated as 30 mg/mL of suspension, and in the overflow stream, 35 mg/mL of suspension. Since the composition of the overflow stream in terms of solids content, dry weight, and protein concentration was unchanged by the centrifuge operating conditions, the protein recovery depends only on the relative flow rates of the feed and overflow streams. Two examples of the values of the flow rates and calculated protein recoveries are recorded in Table 5.1. The protein recovery for operation with a 19.3 mm pond at a feed rate of 0.180 m³/h and a measured overflow rate of 0.126 m³/h was found to be 82%. Higher protein recovery, 93%, was obtained at the lower pond depth setting, 13.1 mm. The improved dewatering of the sediment at the lower pond depth gave a higher overflow rate, 0.144 m³/h, and therefore increased the protein recovery.

5.2.5 Particle Size Analysis

Figure 5.7 compares the particle size distribution of whole yeast and yeast homogenised in accordance with the method described in Section 2.2.1. The whole yeast particle size distribution gave a median diameter of 4.29 μm with 90% of the volume of the particles in the range 3.06 μm to 5.38 μm . For yeast homogenate a median size of 3.27 μm and 90% between 1.26 μm and 4.7 μm was observed. Measurement of the total volume indicates that the volume (or mass, assuming constant density for whole yeast and homogenate) detected by the particle counter after homogenisation is 37% of the volume detected in the original whole yeast suspension. The particle size distribution of the supernatant after flocculation and centrifugation of the homogenate is shown by the smallest curve which has a median particle size of 1.18 μm and 90% of the particles between 0.77 μm and 2.06 μm . The total volume from this curve is ca. 4-5% of the volume for the yeast homogenate curve indicating removal of >95% of the solids

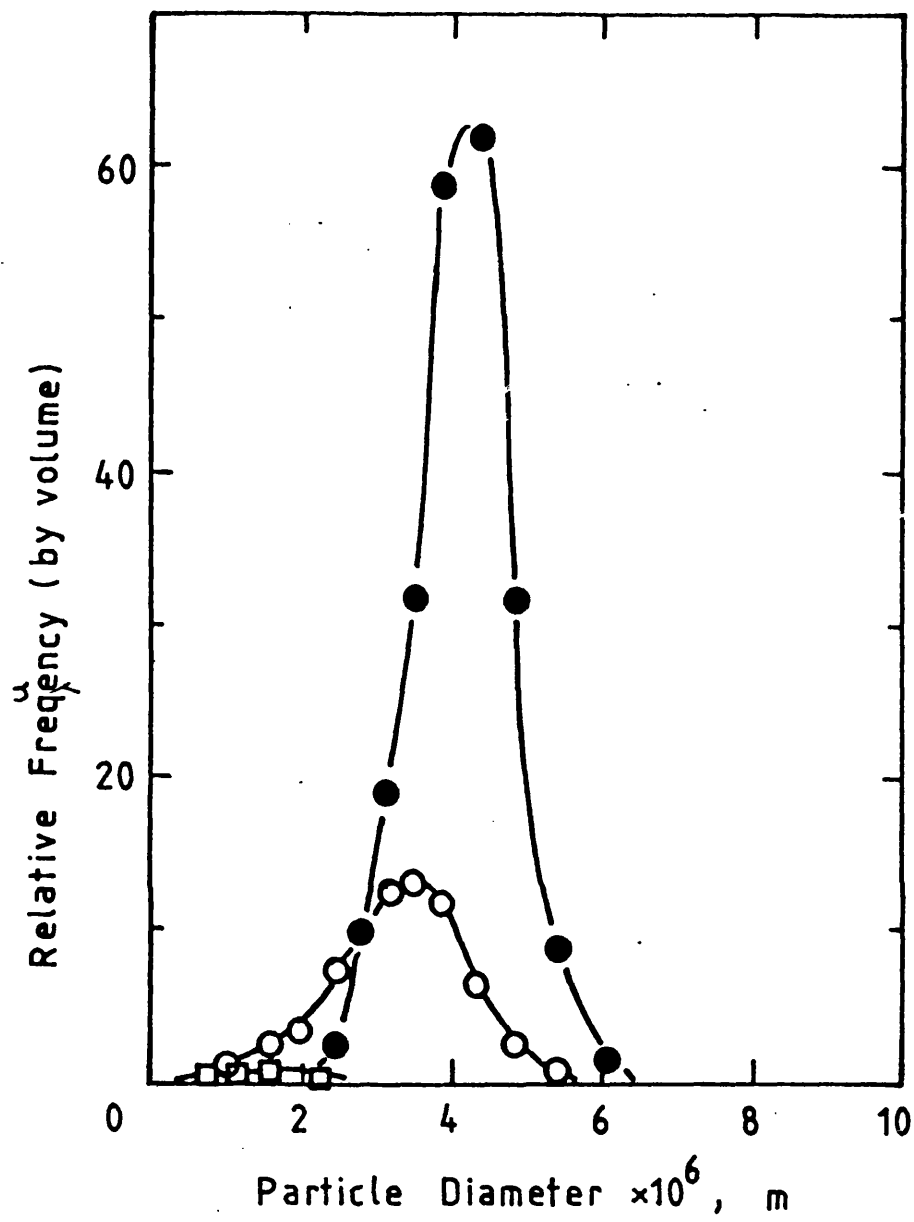


Figure 5.7 Yeast Particle Size Distribution. ●, Whole yeast; ○, yeast homogenate; □, borax-clarified yeast homogenate.

However, this is in excess of the solids removal calculated from dry weight measurements which indicate solids recoveries of ca. 86% (Table 5.1).

5.3 Discussion

Measurements of shear modulus have been used by Buscall et al. (1987) to indicate the formation of structure in a flocculated dispersion and, as shown by Ward (1989), can be used to predict the dewatering behaviour of such dispersions. The increase of shear modulus with yeast homogenate sediment dry weight (Fig. 5.1) indicates that there will be an increasing resistance to dewatering as the dry weight exceeds 22% for the flocculated material. The non-flocculated material exhibits a lower shear modulus at this dry weight and greater extents of dewatering might be expected. However, a typical non-flocculated sediment has less structure than the flocculated sediment over a wide range of frequencies (Fig. 5.2). Hence, more efficient scrolling of solids will be expected for the flocculated material due to the formation of structure in the sediment and consequent resistance to return flow down the beach of the centrifuge.

Operating the scroll decanter with a low pond depth (Fig. 5.6) allows drainage of the solids material prior to discharge and it is possible to achieve sediment dry weights exceeding the values obtained at comparable *ref* in laboratory centrifugation for 0.5 h (Fig. 5.3). Although sediment dry weights were unaffected by changes in the centrifuge scroll rate down to 10 rpm, it is possible that lower scroll rates could give greater dewatering. Investigation of low scroll rates (below 10 rpm) was limited by the tripping of the centrifuge motor as the solids loading on the centrifuge increased.

Slight improvements in sediment dewatering appear to result from batch mixing the borax and homogenate compared to continuous mixing (Fig. 5.6, low pond depths). The results are inconclusive since representative sampling of the solid discharged from the centrifuge is difficult and there are examples of identical

sediment dry weights at higher pond depths (Fig. 5.6) for material prepared by batch and continuous mixing. It may be possible to condition the flocculated material before centrifugation to improve sediment dewatering but further investigation into the effect of mixing conditions on the rheology of the sediment is required for firm conclusions to be drawn.

The use of particle size distributions from electrical sensing measurements for the calculation of solids removal results in an overestimate of solids removed when compared to dry weight measurements derived from high-speed centrifugation. It is possible that fine cell debris is present below about $1\ \mu\text{m}$, the lower limit of detection for the Elzone particle size analyser. Failure to detect this debris in the overflow stream could give an overestimate of the solids recovered by the centrifuge.

Another source of error may arise from the conductivity of the cell debris since, in this method of size analysis, the particle diameter is estimated by assuming that the particles do not conduct electricity as they pass through the detection zone. In a comparison of the mobility of whole cells and isolated cell walls, Neihof and Echols (1973) concluded that differences in the mobility behaviour could result from increases in conductivity of the isolated cell wall. Changes in resistance for the particles in the whole yeast, yeast homogenate and centrifuge overflow streams could therefore make comparison of the solids content by electrical sensing unreliable.

5.4 Conclusion

The results reported here indicate that scale-up to pilot-plant operation is possible. The scroll decanter centrifuge removes the flocculated cell debris from the crude yeast homogenate with continuous solids discharge and can cope with very high solids content.

Protein recovery is dependent on the dewatering of the settled

material which is governed by the pond depth setting of the centrifuge. Increased protein recovery may be obtained by improving the rheology of the sediment to give even greater dewatering or by washing the sediment and repeating the centrifugation.

The observed independence of the separation results as the flowrate and scroll rate are varied can be understood in terms of two distinct solid fractions in the homogenate. The flocculated cell wall material is sufficiently enhanced in size that it is separated under all conditions tested while the non-flocculated solids fraction is not sedimented under the same range of conditions. The small amount of solid remaining in the overflow stream is not flocculated by borax and appears to be intracellular material rather than fragments of the cell wall. Removal of this material has been achieved by flocculating agents that work by different mechanisms to borax (Milburn et al., in preparation) and is discussed in Section 6.

6. POLYETHYLENE IMINE IN THE CLARIFICATION OF YEAST HOMOGENATE

6.1 Mobility and Zeta Potential

The variation in electric potential with distance from the surface of a particle is an important factor in the behaviour of fine particle suspensions. Lowering this potential reduces the electrical repulsion between particles and increases the tendency for the particles to aggregate. The electric potential is represented by the zeta potential, ζ , which can be derived from measurement of the velocity in an electric field, i.e. the particle mobility, U . The general relation between mobility and zeta potential is described by the Henry equation,

$$U = \frac{\zeta \epsilon f(\kappa a)}{6 \pi \mu} \quad \text{Equation 6.1}$$

where ϵ is the permittivity of the medium, μ is the viscosity and $f(\kappa a)$ is a screening function related to the particle radius, a , and the Debye length, $1/\kappa$. For moderate to high electrolyte concentrations, where $\kappa a > 200$, a limiting case for the Henry equation has been identified by Smoluchowski,

$$U = \frac{\zeta \epsilon}{4 \pi \mu} = \frac{\zeta \epsilon_r \epsilon_0}{\mu} \quad \text{Equation 6.2}$$

The assumption that $\kappa a > 200$ implies that the particle radius is much greater than the extent of the double layer given by the Debye length, $1/\kappa$. This assumption will break down for very small particles and low electrolyte concentrations. When $\kappa a < 0.1$ another limiting case is obtained from Equation 6.1 by inserting $f(\kappa a) = 1$ to give the Huckel equation.

The Smoluchowski equation (Equ. 6.2) is valid for microorganisms at ionic concentrations typical of biological suspensions and has been used in this section for the conversion of mobility measurements to zeta potential. For yeast suspensions, the ionic environment, which determines the Debye length, will include contributions from the salts in the yeast suspension before homogenisation, intracellular components released by cell

disruption, borax added for the initial flocculation and polyethylene imine for the final clarification. It is therefore difficult to define the ionic strength in this complex medium in order to estimate the Debye length. The system is further complicated by a distribution of particle sizes ranging from ca. $0.1 \mu\text{m}$ in the homogenate to over $6 \mu\text{m}$ in the whole yeast suspension. The Smoluchowski equation is likely to be valid over most of this range but may not apply for the finest of the particles. The results are therefore discussed in terms of the particle mobility, since it is this property which is actually measured, rather than the zeta potential which is derived from the mobility.

6.2 Results

6.2.1 Effect of Ionic Environment on Mobility of Yeast

Figure 6.1 compares the effect of pH variation in the range pH 2-9 at a fixed sodium chloride concentration, 1.0 kg/m^3 , on the mobilities of whole yeast, yeast homogenate and borax-clarified yeast homogenate. The whole yeast cells exhibited negative mobilities throughout the range examined with the magnitude of the mobility increasing from $-2 \times 10^{-9} \text{ m}^2 \text{ V}^{-1} \text{ s}^{-1}$ at pH 2.4 to ca. $-8 \times 10^{-9} \text{ m}^2 \text{ V}^{-1} \text{ s}^{-1}$ at pH 7.0. As the pH was further increased from 7.0 to 9.1 the mobility remained approximately constant. For yeast homogenate a point of zero charge was observed at pH 4.0. Below pH 4 the mobility increased to $10 \times 10^{-9} \text{ m}^2 \text{ V}^{-1} \text{ s}^{-1}$ at pH 3.1 while between pH 4 and pH 6 the mobility became more negative before levelling out at ca. $-11 \times 10^{-9} \text{ m}^2 \text{ V}^{-1} \text{ s}^{-1}$ above pH 6.

The values of the mobility for borax-clarified homogenate were slightly more positive than the mobility of the homogenate (before clarification) over the range pH 2.5-5.5. The two curves had a similar shape over this range but above pH 5.5 the mobilities determined for the borax-clarified homogenate continue to become more negative without the levelling out observed for the unclarified samples in this pH range.

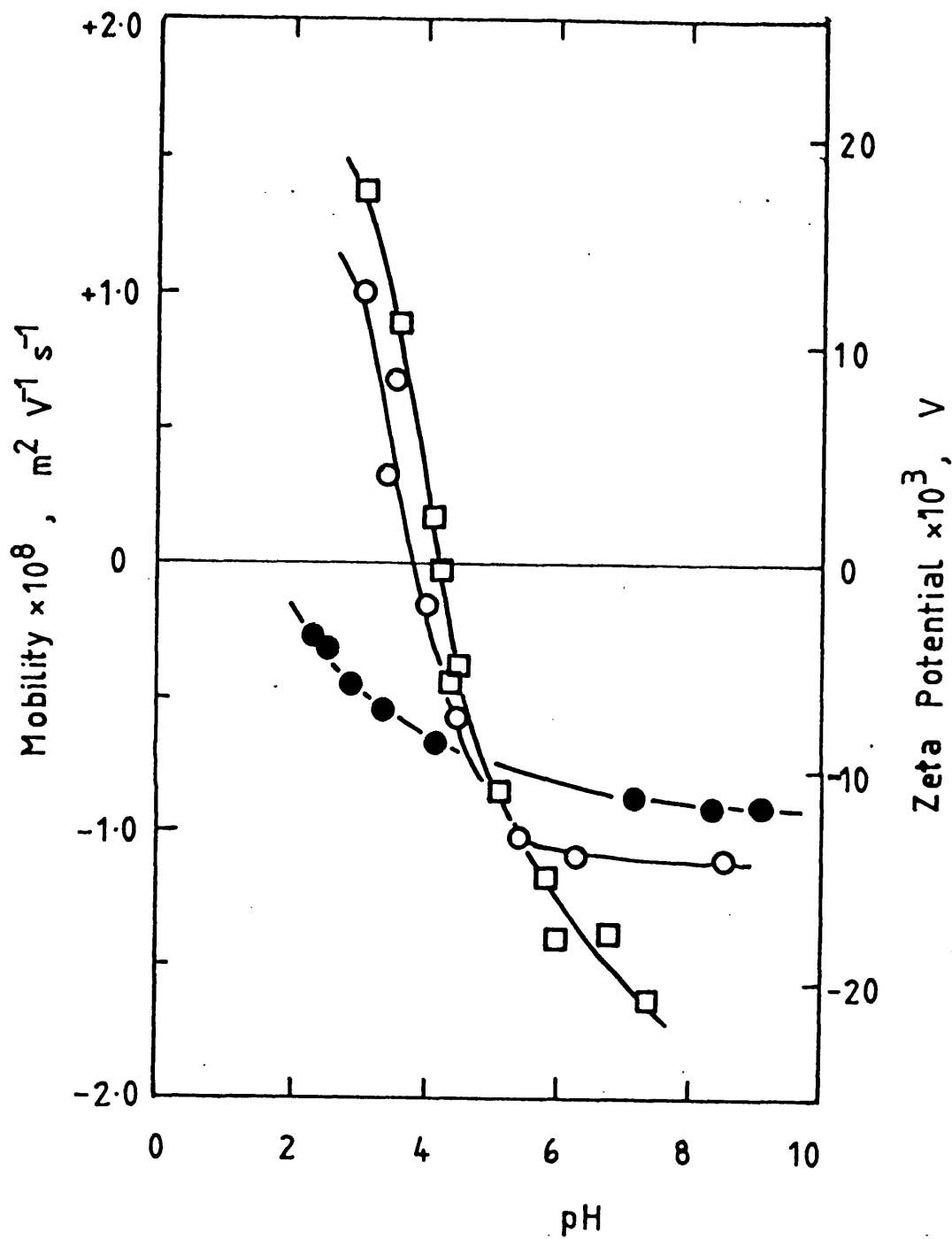


Figure 6.1 Effect of pH on Yeast Mobility. ●, whole yeast; ○, yeast homogenate; □, borax-clarified yeast homogenate. Sodium chloride, 1 kg/m^3 , temperature, 298 K.

Increasing the sodium chloride concentration from 1 to 5 kg/m³ at a fixed pH of 7.8, Figure 6.2, produced a change in the mobilities measured for borax-clarified homogenate from $-17.4 \times 10^{-9} \text{ m}^2 \text{ V}^{-1} \text{ s}^{-1}$ to $-13.3 \times 10^{-9} \text{ m}^2 \text{ V}^{-1} \text{ s}^{-1}$. Figure 6.3 shows more negative mobilities, ranging from $-22.8 \times 10^{-9} \text{ m}^2 \text{ V}^{-1} \text{ s}^{-1}$ at 1 kg/m³ to $-17.9 \times 10^{-9} \text{ m}^2 \text{ V}^{-1} \text{ s}^{-1}$ at 5 kg/m³, were obtained when the clarified homogenate was diluted into dipotassium hydrogen phosphate.

6.2.2 Effect of Polyethylene Imine on Mobility

For measurements involving variation of sodium chloride and dipotassium hydrogen phosphate concentrations the mobilities obtained were found to be independent of the particle concentration at the concentrations suitable for the Zetasizer. However, when borax-clarified homogenate was diluted into polyethylene imine solutions the values of the mobilities were found to be dependent on the degree of dilution. This effect is clearly seen in Figure 6.4 where 3 curves were obtained for the variation of mobility measured for clarified homogenate diluted in solutions of PEI 50,000. Dilution factors of 1/50, 1/100 and 1/200 for homogenate (clarified in accordance with the method described in Section 2.2.2) produced particle concentrations suitable for the Zetasizer. The shape of the curve is the same for each dilution factor: the mobility was found to increase (i.e. become less negative) sharply at low PEI concentrations (of the order of 0.01 kg/m³) but each curve began to flatten out at higher PEI concentrations. The figure shows that the concentration required to change the mobility from the original negative value (ca. $-17 \times 10^{-9} \text{ m}^2 \text{ V}^{-1} \text{ s}^{-1}$ at pH 7.3) to, for example, zero increases as the particle concentration increases. A dilution of 1/50 requires a PEI concentration of ca. 0.04 kg/m³ to produce a mobility of zero while a dilution of 1/200 requires only 0.01 kg/m³ PEI to give the same effect.

When PEI solutions were used to clarify the homogenate (as described in Section 2.2.7) a dilution factor of 1/2 was introduced due to the mixing of the homogenate with the PEI solution in the ratio 1:1. The results of the mobility

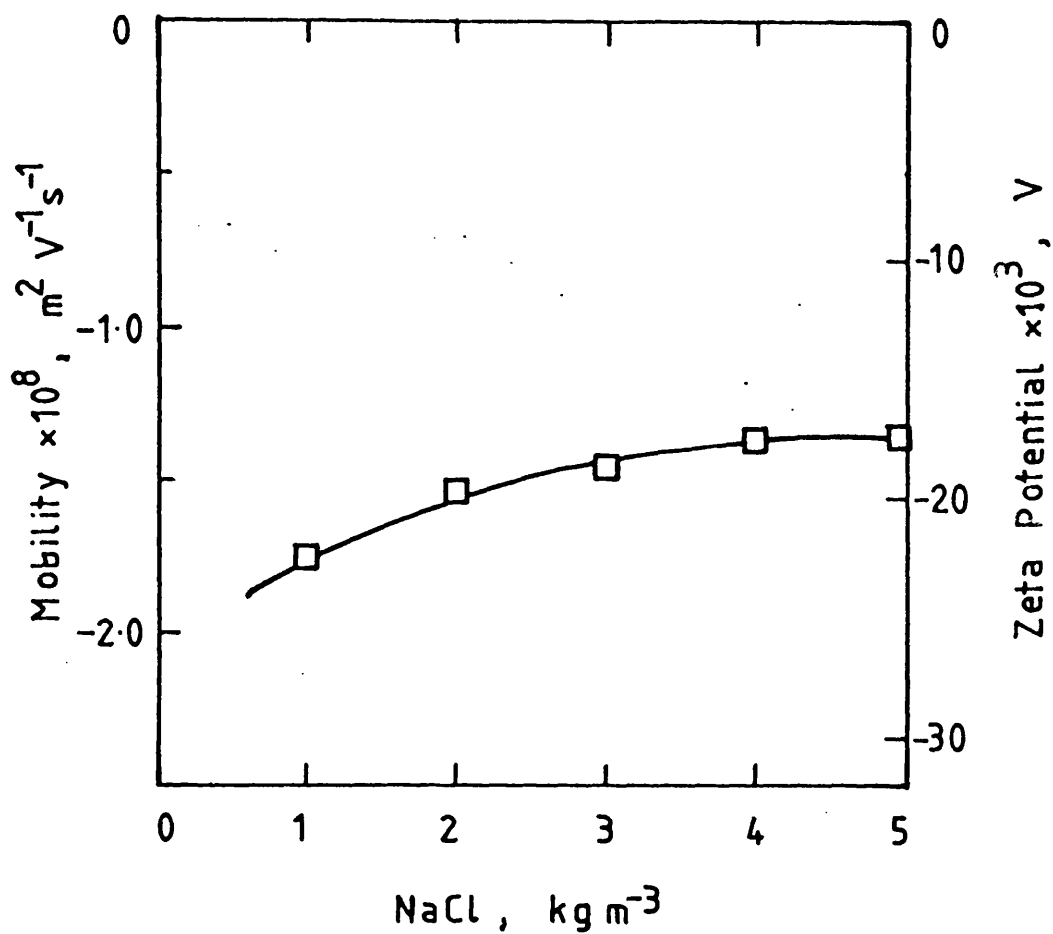


Figure 6.2 Effect of Sodium Chloride Concentration on Mobility.

□, Borax-clarified homogenate, temperature, 298 K, pH 7.8.

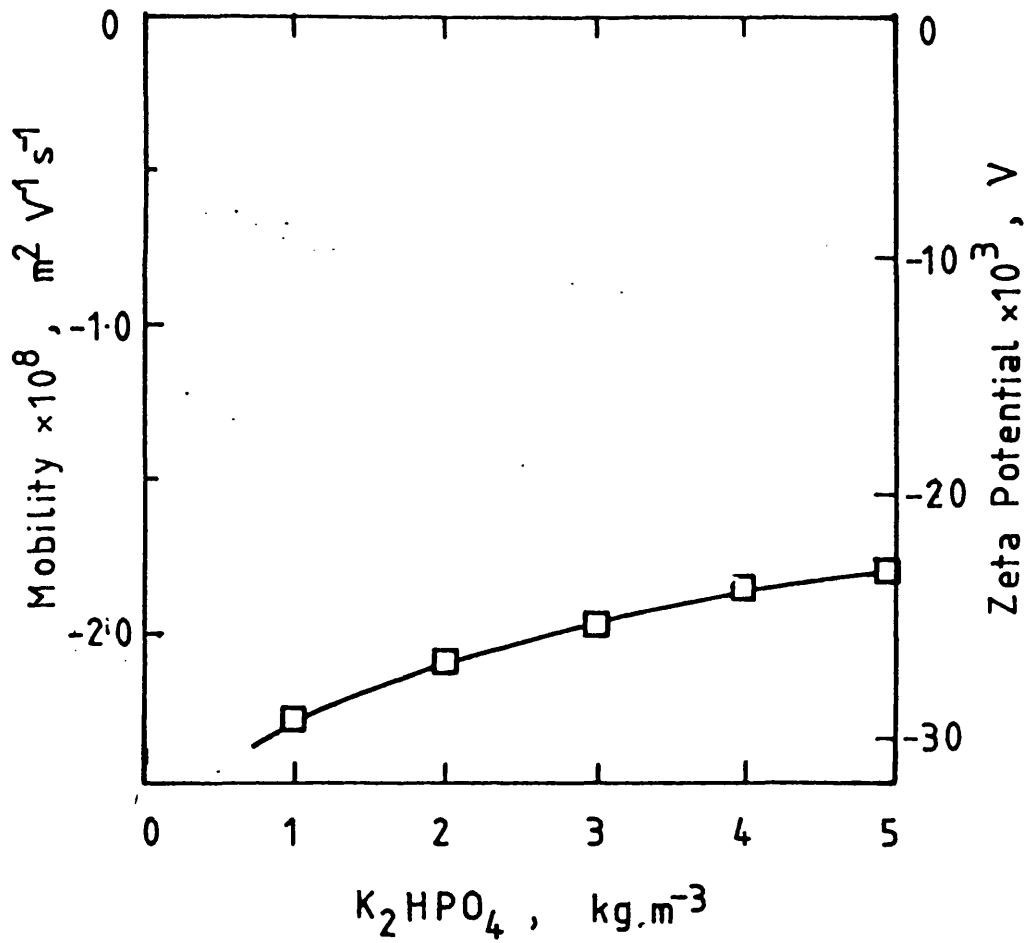


Figure 6.3 Effect of Phosphate Concentration on Mobility.

□, Borax-clarified homogenate, temperature, 298 K, pH 7.9.

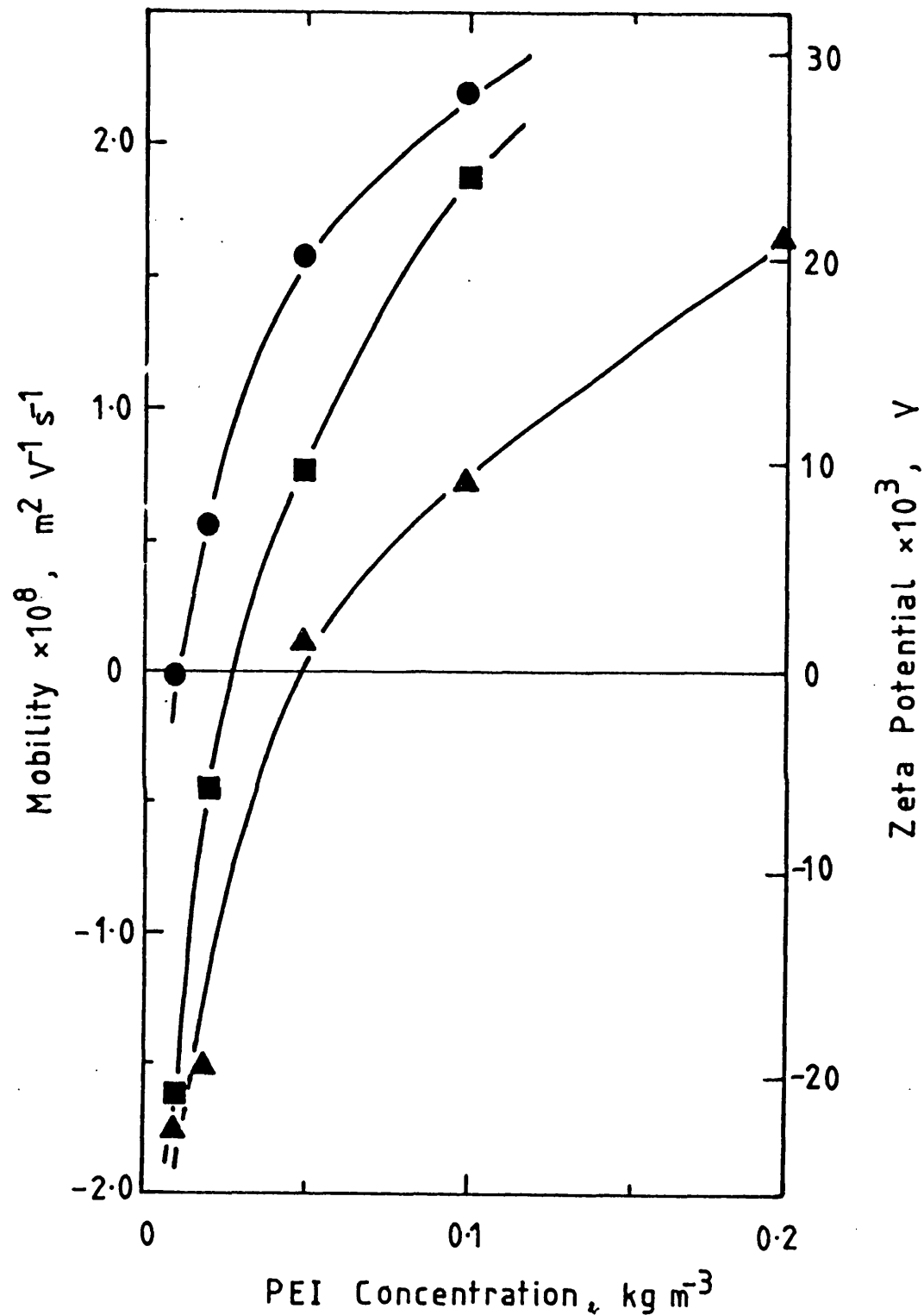


Figure 6.4 Variation of Mobility with PEI Concentration: Effect of Homogenate Dilution. PEI (Sigma) m.wt. 50,000. Borax-clarified homogenate, dilution before mobility measurement: ●, 1/200; ■, 1/100; ▲, 1/50. Temperature, 298 K, pH 7.3.

measurements were adjusted for solids dilution to express the PEI concentration for the mobility results on the same basis as the PEI:solids ratio used in the clarification experiments. Hence the PEI concentrations for the 1/200 mobility measurements are multiplied by 100 to give the appropriate final PEI concentration for 1/2 dilution. Similar adjustments are made for the 1/50 and 1/100 dilutions to give the curve on Figure 6.5. In this figure the data for each dilution (Fig. 6.4) now appear on one curve. Also included on Figure 6.5 are the results obtained in the same manner for a PEI sample obtained from a different source. This second PEI sample had a higher molecular weight of 70,000 compared with the first sample of 50,000 and produced a greater change in mobility at equivalent weight concentrations.

The charge densities of the different PEI samples that were used for the treatment of borax-clarified homogenate were compared by following the change in pH of PEI solutions as hydrochloric acid was added. It was observed that approximately the same amount of acid was required for the samples supplied by Polyscience to change the pH from pH 10 to pH 4, Figure 6.6, indicating similar charge densities for the samples of different molecular weights. The lowest molecular weight sample, PEI 600, required 1.77 mL of hydrochloric acid, 1 M, to change the pH of 25 mL of solution, 5 kg/m³, from pH 10 to pH 4. PEI 10,000 required 1.88 mL and PEI 70,000 required 1.74 mL to give the same pH change under the same conditions. The sample obtained from Sigma (M.wt. 50,000) had a somewhat lower charge density as indicated by the lower amount of acid, 1.37 mL, required for the same change in pH.

The effect of polymer molecular weight on the mobility of clarified yeast homogenate for the PEI samples of the same charge density (molecular weights of 600, 10,000 and 70,000) is shown in Figure 6.7. As in Figure 6.5 the x-axis represents a PEI concentration adjusted to the solids concentration in a 1:1 mixture of PEI solution and borax-clarified homogenate. All three molecular weights of polymer were found to give large changes in mobility at low concentrations. A PEI 600 concentration of ca. 1 kg/m³ was sufficient to change the mobility from $-18 \times 10^{-9} \text{ m}^2 \text{ V}^{-1} \text{ s}^{-1}$ to $-2 \times 10^{-9} \text{ m}^2 \text{ V}^{-1} \text{ s}^{-1}$ but

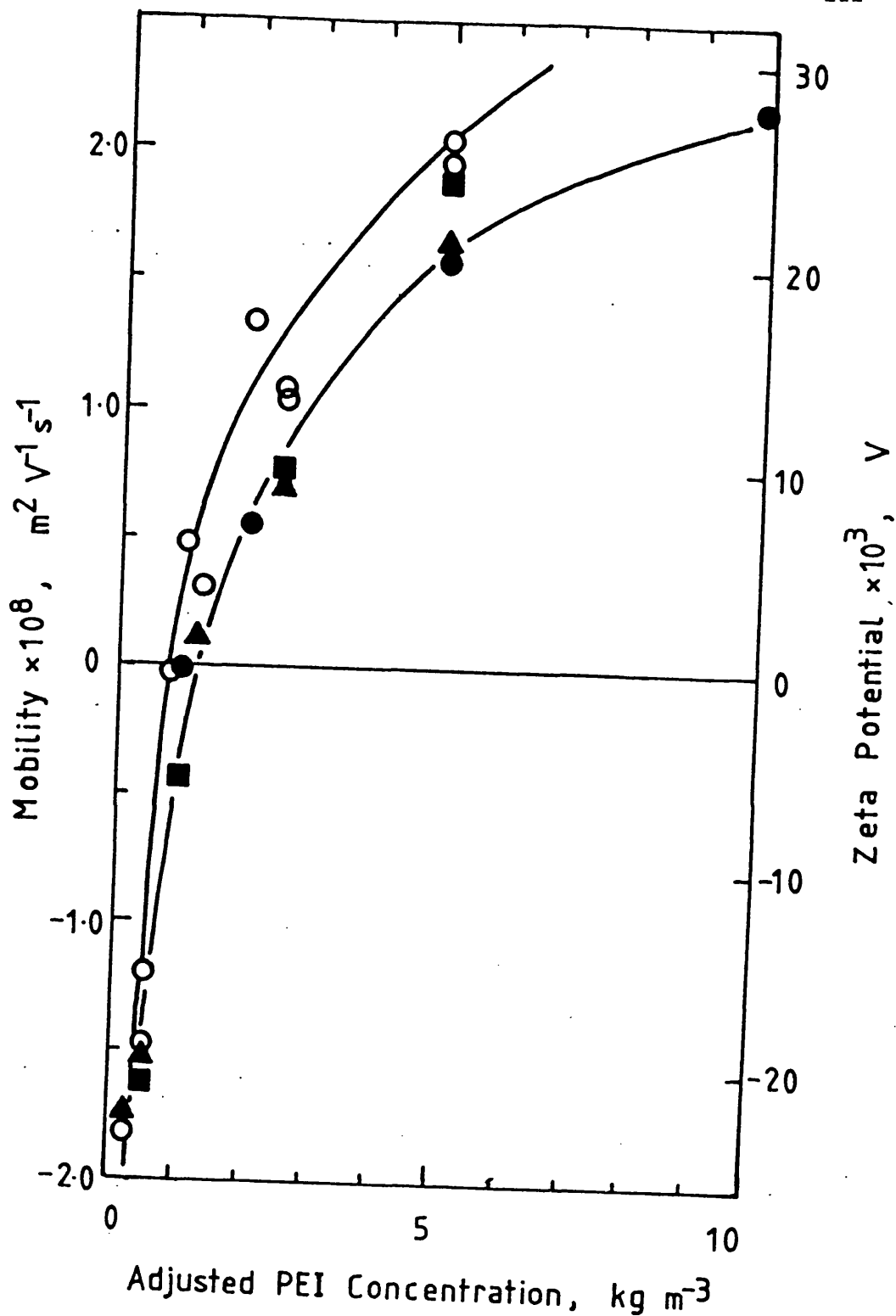


Figure 6.5 Variation of Mobility with PEI Concentration. (x-axis adjusted for solids dilution). Borax clarified homogenate dilution: ●, 1/200; ■, 1/100; ▲, 1/50. ●, ■, ▲, PEI M.wt. 50,000; ○, PEI M.wt. 70,000. Temperature, 298 K, final pH 7.3.

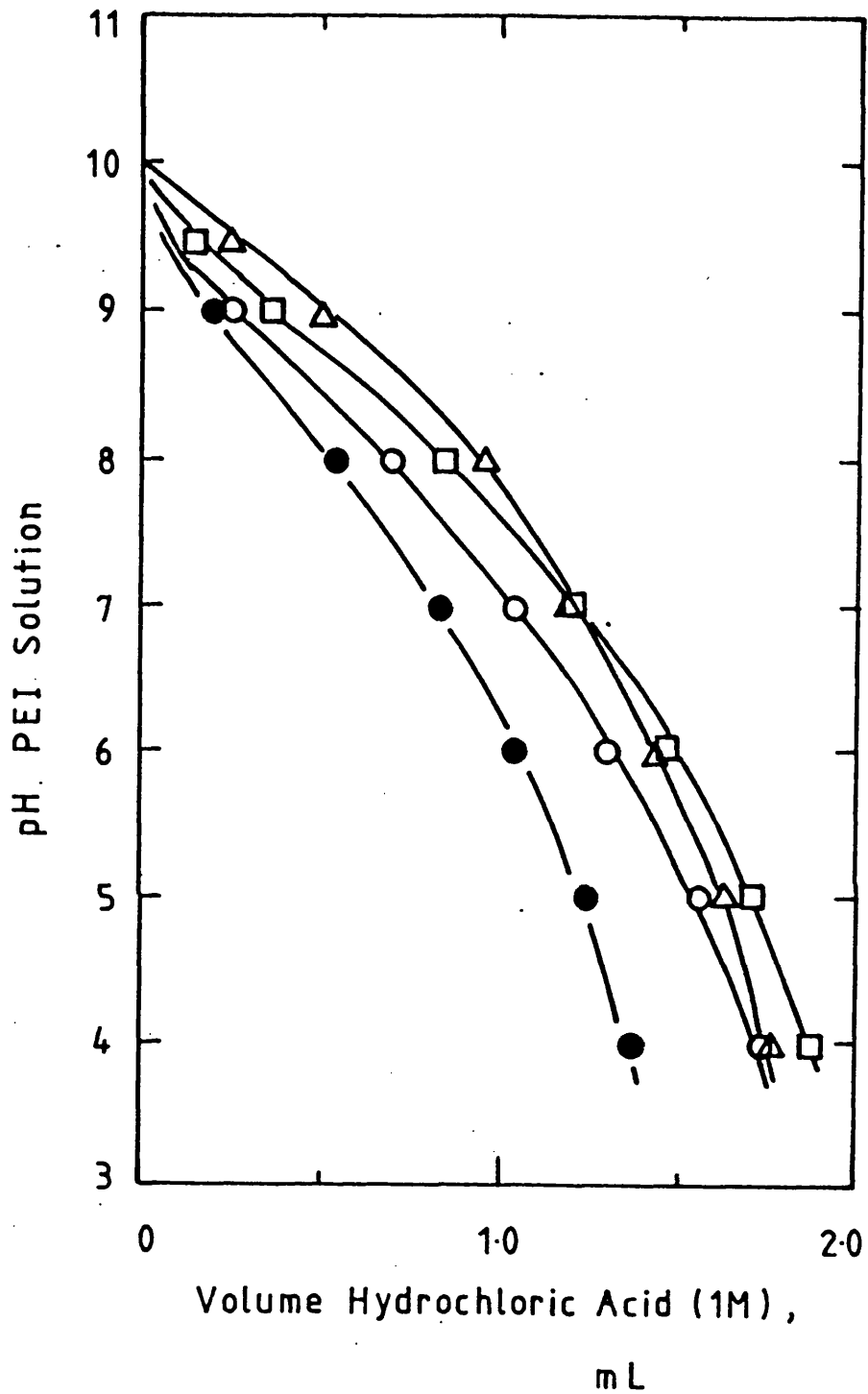


Figure 6.6 Titration of PEI against Hydrochloric Acid.
 PEI solution, 25 mL, initially pH 10, hydrochloric acid, 1 M,
 temperature, 293 K. PEI M.wt.: Δ , 600; \square , 10,000; \circ , 70,000;
 \bullet , 50,000.

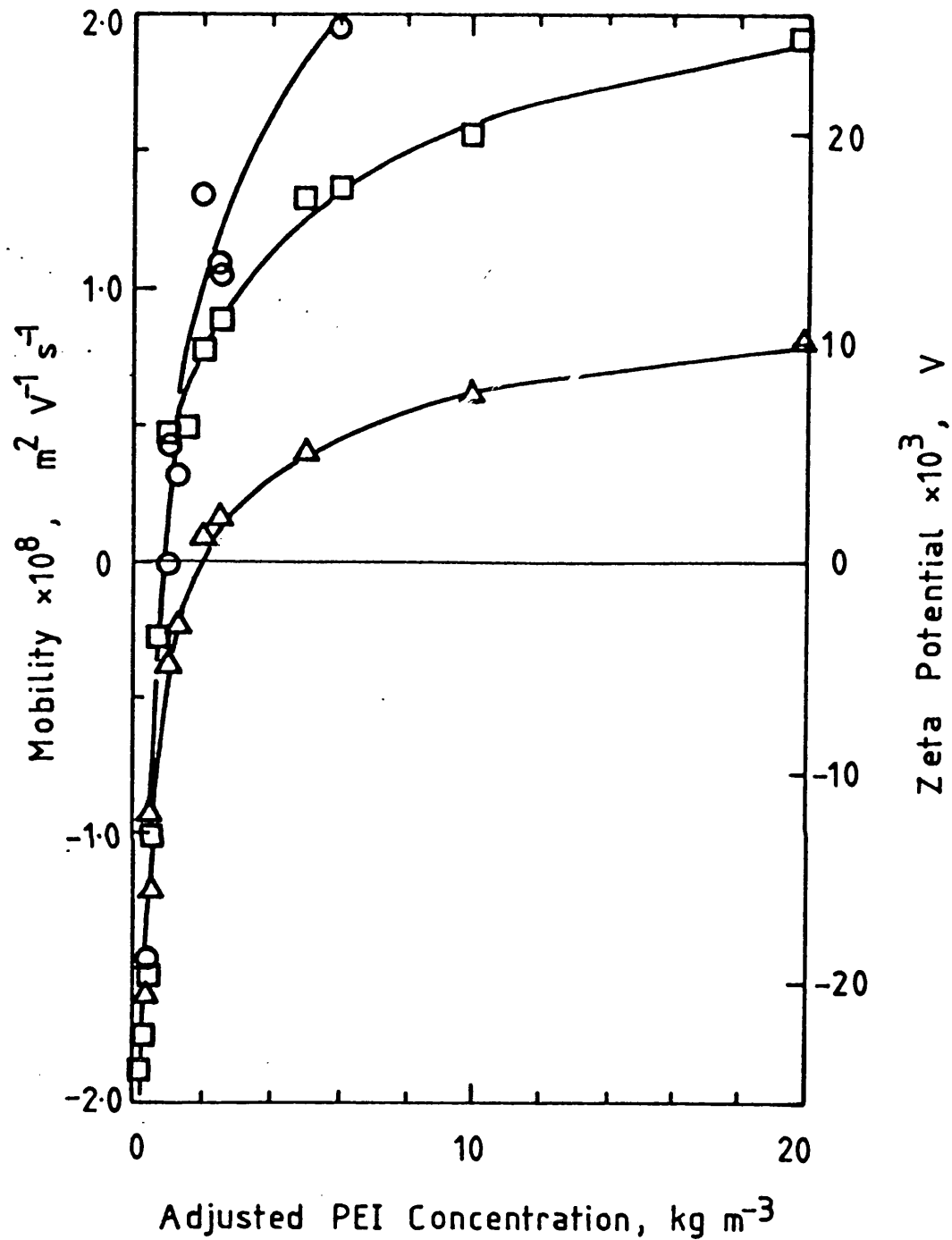


Figure 6.7 Variation of Mobility with PEI Concentration: Effect of Polymer Molecular Weight. PEI M.wt.: \triangle , 600; \square , 10,000; \circ , 70,000. Temperature, 298 K, final pH 7.3.

at higher concentrations the higher molecular weight PEI samples were found to be more effective at modifying the particle mobility. The positive mobility increases gradually with increasing PEI 600 from $4.2 \times 10^{-9} \text{ m}^2 \text{ V}^{-1} \text{ s}^{-1}$ at 5 kg/m^3 to $8.1 \times 10^{-9} \text{ m}^2 \text{ V}^{-1} \text{ s}^{-1}$ at 20 kg/m^3 . Higher positive mobilities were observed with PEI 10,000 and PEI 70,000 with the mobility approaching $20 \times 10^{-9} \text{ m}^2 \text{ V}^{-1} \text{ s}^{-1}$ at 20 kg/m^3 (M.Wt. 10,000) and 6 kg/m^3 (M.Wt 70,000).

In the presence of a fixed concentration of PEI, sodium chloride was observed to give more negative mobilities. Two examples for PEI 600 are given in Figure 6.8a. At 1 kg/m^3 PEI the mobility of borax-clarified homogenate changed from $-1.7 \times 10^{-9} \text{ m}^2 \text{ V}^{-1} \text{ s}^{-1}$ to $-4.1 \times 10^{-9} \text{ m}^2 \text{ V}^{-1} \text{ s}^{-1}$ as the sodium chloride concentration was increased from 0.1 kg/m^3 to 3 kg/m^3 . At 2.5 kg/m^3 PEI the same increase in sodium chloride concentration produced a change from a positive mobility of $2.7 \times 10^{-9} \text{ m}^2 \text{ V}^{-1} \text{ s}^{-1}$ to a negative mobility of $-2.5 \times 10^{-9} \text{ m}^2 \text{ V}^{-1} \text{ s}^{-1}$.

Changes of pH of the PEI solution after the addition of the clarified homogenate also affected the resulting mobility as shown in Figure 6.8b. Over the range of pH 6 to pH 8 a linear decrease of mobility was observed for concentrations of PEI 600 of 1, 2.5 and 5 kg/m^3 . Similar behaviour was also found when PEI 50,000 at 1.25 kg/m^3 was subjected to changes in pH. The pH can therefore modify the effect of PEI on the mobility of the borax-clarified homogenate as illustrated by Figure 6.9 where mobilities are plotted for PEI concentrations (adjusted for dilution as in Figure 6.5) up to 5 kg/m^3 for fixed pH values of 5.9, 7.3 and 7.9. It is evident from this figure that the lower the pH the lower the dose of PEI required to bring the mobility of clarified homogenate to zero.

6.2.3 Settling of PEI Floccs

The mean size of the floccs formed by mixing PEI solutions with borax clarified homogenate to a final PEI concentration of 1 kg/m^3 (method of Section 2.2.8) is plotted on Fig. 6.10. For the different molecular weights of PEI the mean diameter (d_{50}),

Figure 6.8 Variation of Mobility in PEI 600. Temperature, 298 K.
Adjusted PEI concentration: ▲, 1 kg/m³; △, 2.5 kg/m³; ◇, 5.0 kg/m³. ●, PEI 50,000, 1.25 kg/m³. a) Effect of Sodium Chloride Concentration, pH 7.3. b) Effect of pH.

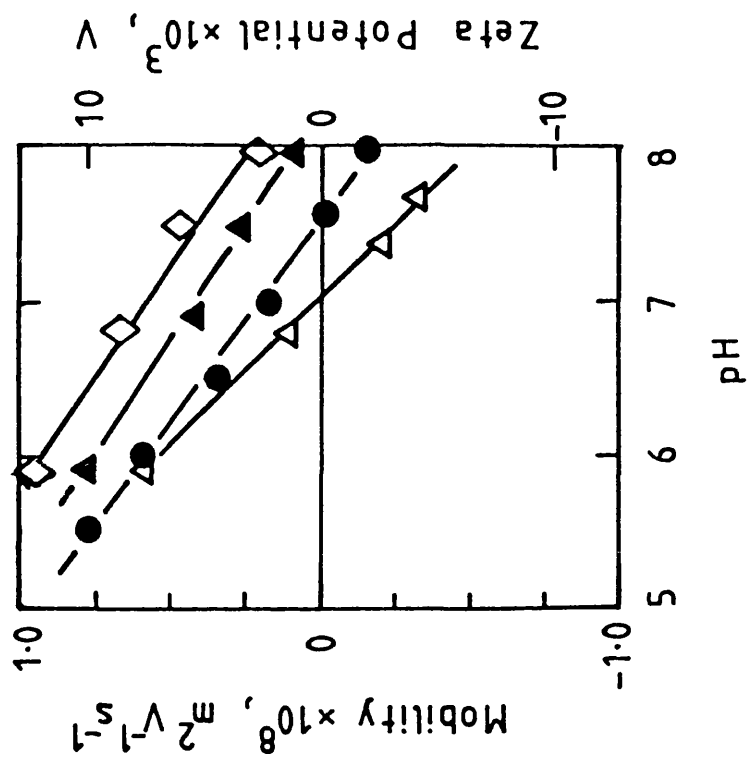


Figure 6.8a

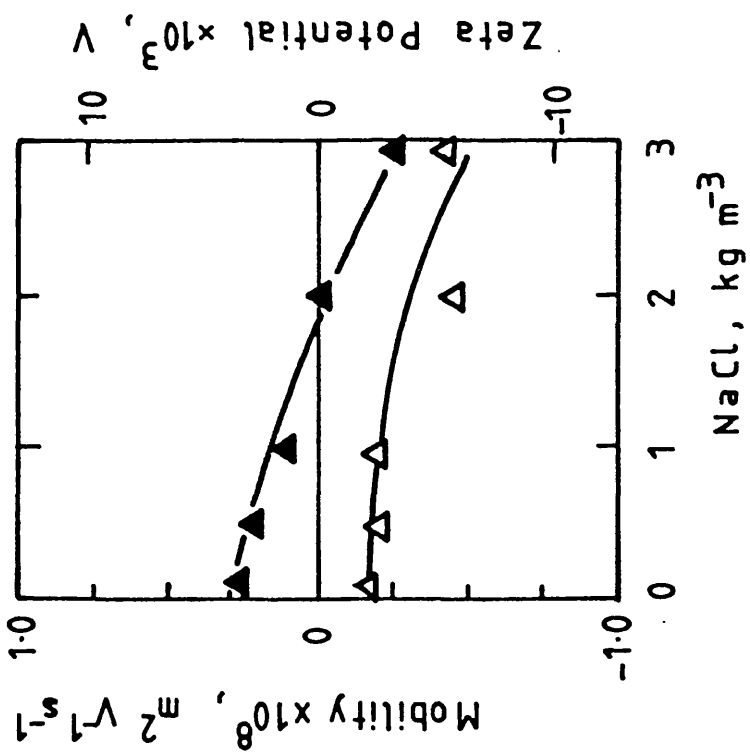


Figure 6.8b

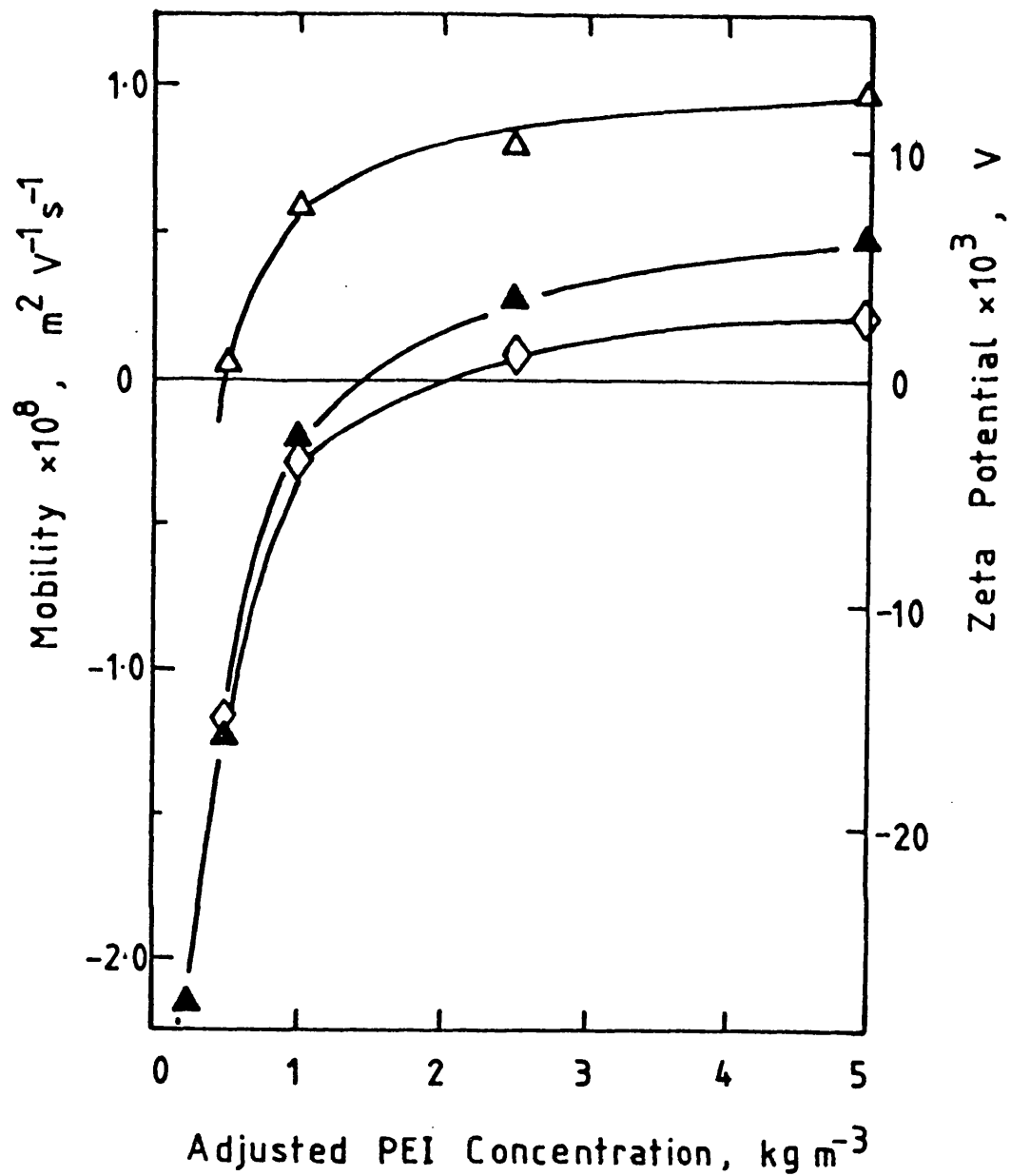


Figure 6.9 Variation of Mobility with PEI 600 Concentration: Effect of pH. \triangle , pH 5.9; \blacktriangle , pH 7.3; \diamond , pH 7.9. Temperature, 298 K.

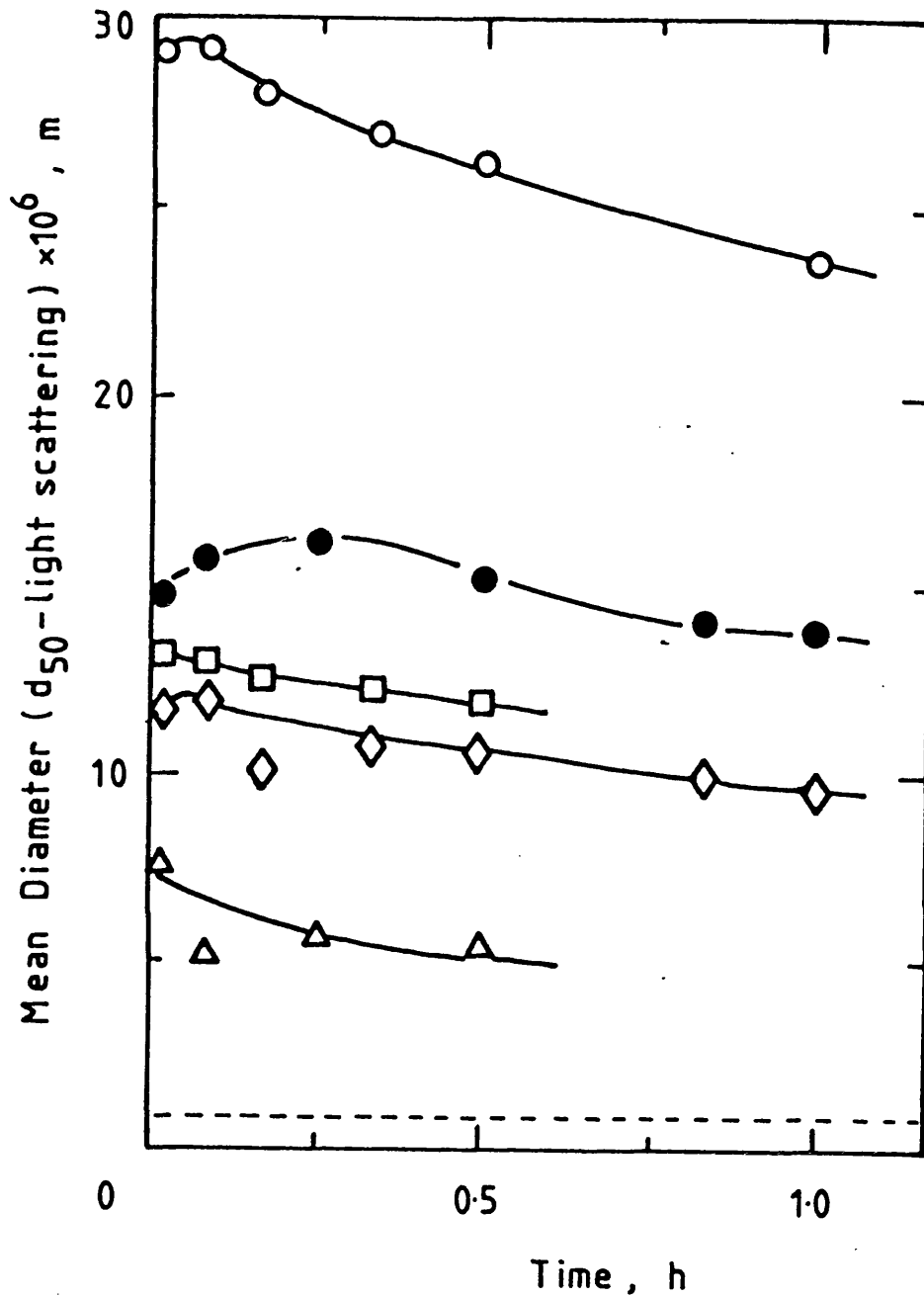


Figure 6.10 Mean Floc Size during Mixing of Borax-clarified Homogenate and PEI. Sized by light scattering (Malvern, model 3600). Δ , \square , \bullet , \circ , Laboratory scale, magnetic stirrer, final PEI concentration, 1 kg/m^3 ; homogenate dilution, $1/2$; final pH 7.4. PEI M.wt.: Δ , 600; \square , 10,000; \bullet , 50,000; \circ , 70,000. \diamond , Pilot scale, stirring, 49 rad/s; tank volume, 0.12 m^3 ; paddle diameter 0.18 m; final PEI concentration, 0.75 kg/m^3 ; homogenate dilution, $1/2$; PEI m.wt.: 50,000. (-----) before PEI addition (Malvern Zetasizer size analysis).

obtained from light scattering, is recorded for samples taken from a stirred beaker at different times. Also included are the floc sizes obtained for samples taken from a pilot plant stirred tank of borax-clarified homogenate mixed with PEI 50,000 to a final concentration of 0.75 kg/m^3 . It can be seen that the flocs break down with time in the stirred beaker and that the higher molecular weight PEI gives larger flocs. The floc sizes ranged from $7.6 \mu\text{m}$ after 60 s mixing with PEI 600 to $29.1 \mu\text{m}$ after 60 s mixing with PEI 70,000. The pilot plant flocculation with PEI 50,000 resulted in a floc size below that of the laboratory stirred beaker results using PEI 10,000 but the pilot plant PEI concentration and shear conditions were different to those employed on the laboratory scale. A slight increase in floc size was noted for the high molecular weight polymers (50,000 and 70,000) in the early stages of the flocculation (0.1-0.25 h) before the floc size began to decline.

Figures 6.11a-d show the effectiveness of the different PEI samples in the clarification of the yeast homogenate (after initial treatment with borax). In these figures the relative turbidities and relative protein concentrations are given as a percentage of the value obtained by mixing the borax-clarified homogenate with deionised water. With identical centrifugation conditions an increase in turbidity was found at very low PEI concentrations (ca. 0.5 kg/m^3) except for the 70,000 molecular weight material which showed a decrease in turbidity. The turbidity decreased at higher concentrations of PEI and exhibited a minimum turbidity in the range $1\text{-}10 \text{ kg/m}^3$ PEI. PEI 600 (Fig.6.11a) produced a relative turbidity of 5.1% at 5 kg/m^3 and then the turbidity increased slightly at higher PEI doses. Similar behaviour was found for PEI 10,000 (Fig.6.11b) with a minimum relative turbidity of 6.8% at 1 kg/m^3 . The high molecular weight samples (Figs.6.11c and 6.11d) of 70,000 and 50,000 gave turbidity minima at 1 kg/m^3 and 5 kg/m^3 respectively but in contrast to the lower molecular weight PEI high turbidities were found when the PEI concentration was further increased. At 25 kg/m^3 the relative turbidity reached 92.9% with PEI 50,000 while 173% was obtained with PEI 70,000.

Figure 6.11 Effect of PEI on Turbidity and Protein Concentration in Borax-clarified Homogenate. Temperature, 298 K, final pH 7.0, absorbance measured at 650 nm.

a) \triangle , \blacktriangle , PEI m.wt. 600. b) \square , \blacksquare , PEI m.wt. 10,000.
c) \diamond , \blacklozenge , PEI m.wt. 70,000. d) \circ , \bullet , PEI m.wt. 50,000.

\triangle , \square , \diamond , \circ , relative turbidity, 650 nm;

\blacktriangle , \blacksquare , \blacklozenge , \bullet , relative protein concentration, Pierce assay.

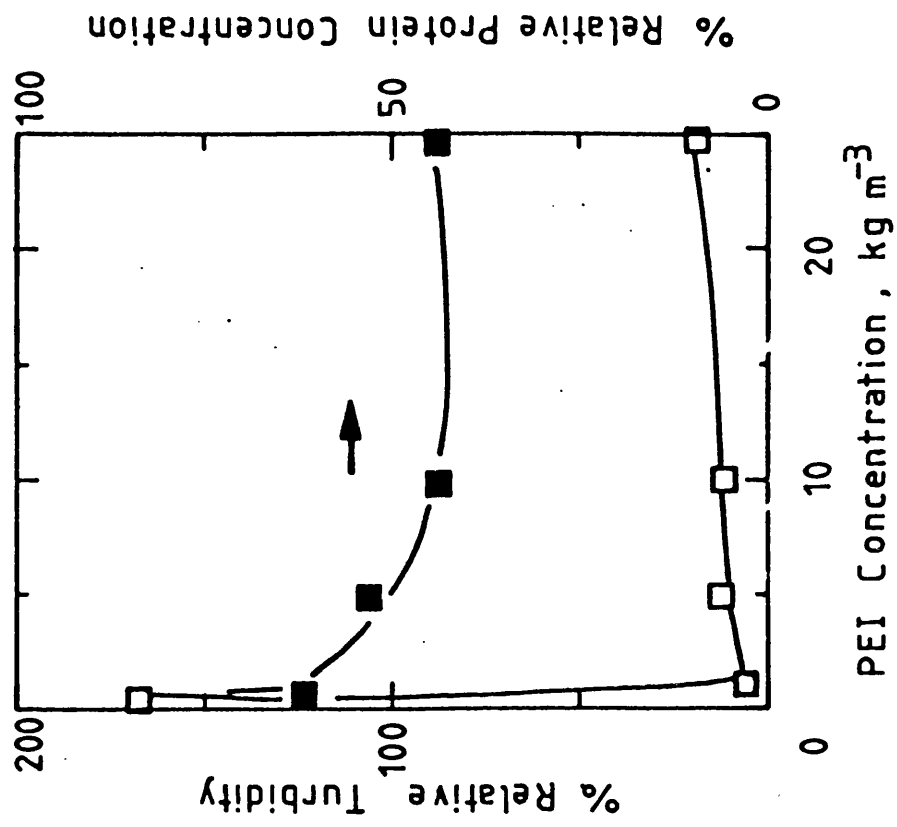


Figure 6.11b

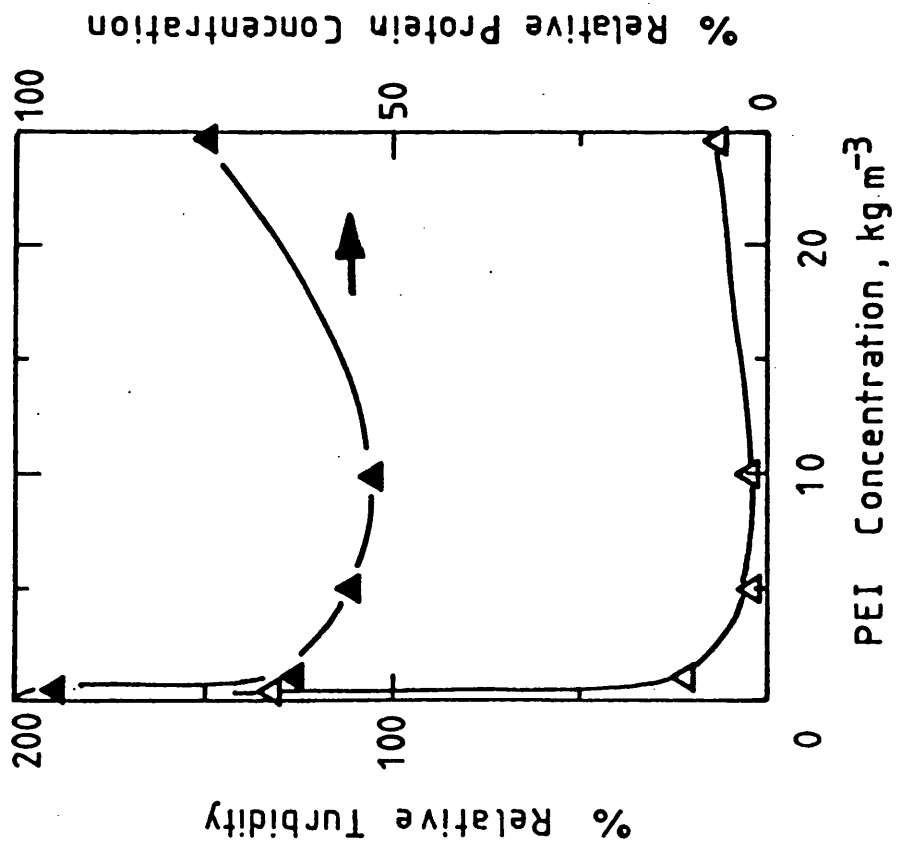


Figure 6.11a

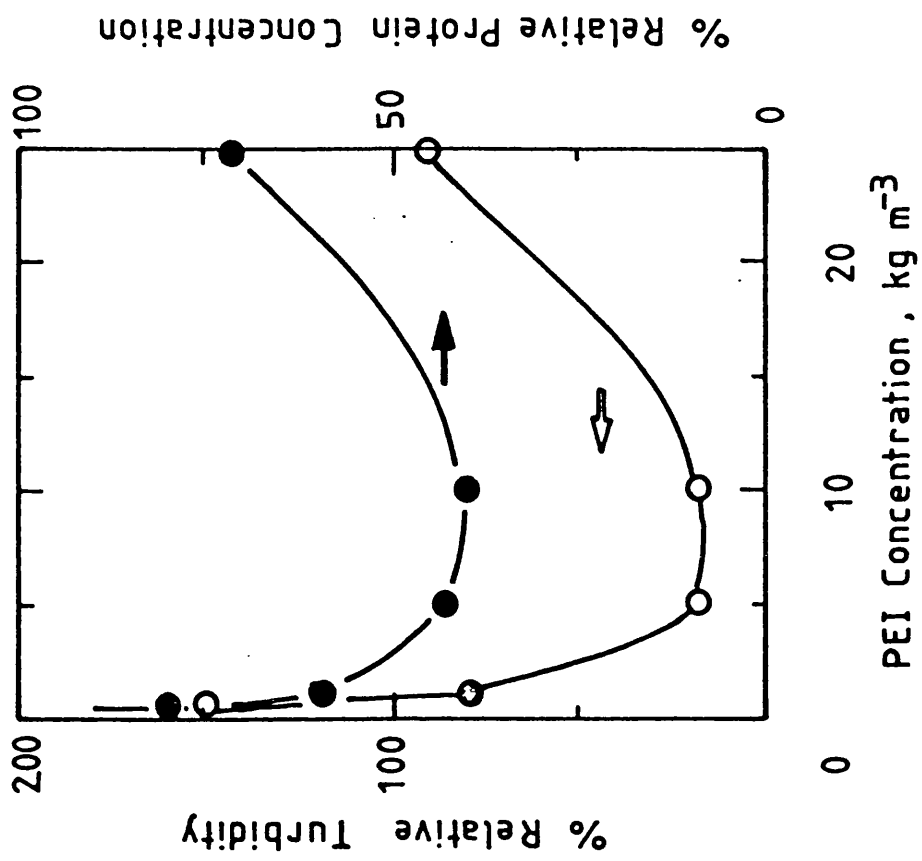


Figure 6.11d

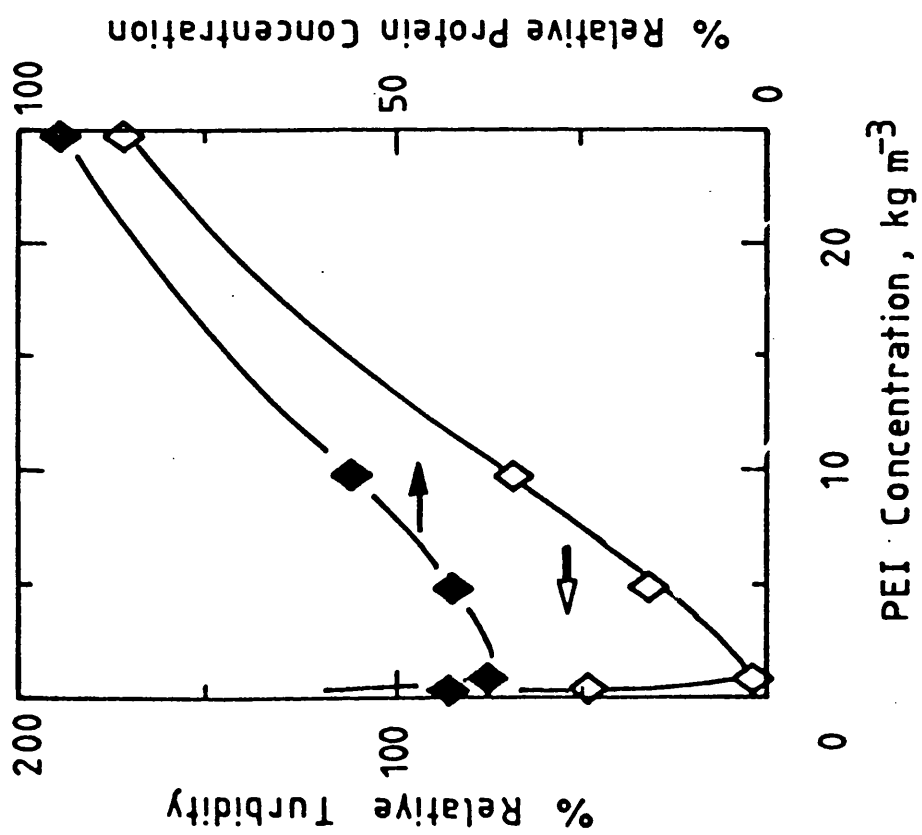


Figure 6.11c

The level of protein in the supernatant after treatment with PEI and centrifugation is also recorded on Figures 6.11a-d. Similar losses of protein of ca. 50% were found for each molecular weight of PEI at PEI concentrations of 1-10 kg/m³. At high doses of PEI more protein appears to remain in the supernatant. This feature was most pronounced in Figure 6.11c where supernatant relative protein concentration increased from 38% at 1 kg/m³ to 95% at 25 kg/m³. Increases in relative protein concentration to 75% and 72% were observed for M.Wts. of 600 and 50,000 respectively (Figs 6.11a and 6.11d) but the concentration obtained for PEI 10,000 remained below 50% at PEI concentrations of 10 kg/m³ and 25 kg/m³ (Fig.6.11b).

6.2.4 Pilot-scale Clarification of Yeast Homogenate using PEI

Pilot-scale removal of PEI-flocculated material was achieved using a disc-stack centrifuge. Two trials were performed with homogenate that had initially been treated with borax and then scroll centrifuged as described in Section 2.2.2. In the first trial the centrifuge (SAOOH 205, Westfalia) had a calculated settling area of 1245 m² and the feed flowrates ranged from 7.2 x 10⁻³ m³/h to 42 x 10⁻³ m³/h. The solids remaining in the overflow from the centrifuge, as a fraction of the wet solids in the feed, varied from 10% at the lowest feed rate to 87% at the highest as shown by the % not settled on Figure 6.12. The results are presented with an x-axis of flow rate divided by settling area to enable comparison with the performance of a larger centrifuge at higher flow rates. The two points obtained for the larger centrifuge (BSP7-47, Westfalia), calculated settling area 9720 m², at feed rates of 0.1 and 0.2 m³/h gave improved separation when compared to the SAOOH centrifuge at equivalent values of flow rate/settling area. At 0.2 m³/h 23% of the solids remained unsettled while at 0.1 m³/h 16% remained.

In a control experiment, borax-clarified homogenate was diluted with phosphate buffer before feeding to the disc-stack (BSP7-47) centrifuge. No clarification was observed and the unsettled solids in the overflow stream remained at 100% at a feed rate of 0.1 m³/h.

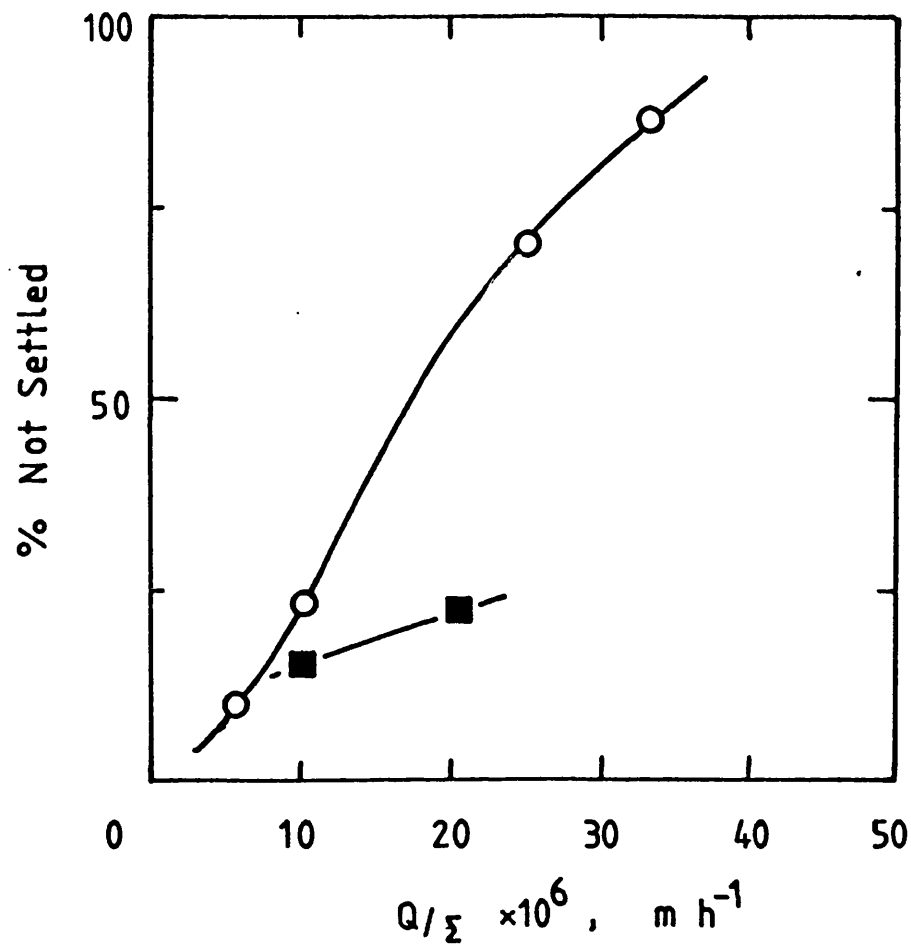


Figure 6.12 Clarification of PEI-flocculated Yeast Homogenate using Disc-stack Centrifuges. Effect of throughput and separation area. PEI m.wt. 50,000, final concentration, 0.75 kg/m^3 . ■, Westfalia BSP7, settling area, 9720 m^2 ; ○, Westfalia SAOOH, settling area, 1245 m^2 .

6.3 Discussion

6.3.1 Cell Surface

For a number of microorganisms, including *S. cerevisiae*, Neihof and Echols (1973) found small differences in mobilities when comparing intact cells and isolated cell walls. They attributed the slightly less negative mobilities of the disrupted cells to the higher surface conductivity expected when the insulating intracellular materials have been removed and concluded that the surfaces of the whole cells and isolated walls were essentially the same. The disruption conditions of Neihof and Echols were milder than those employed here, therefore avoiding fragmentation of the cell wall, and mobility measurements were made after washing to remove the released intracellular material.

In this study, as shown by the variation of mobility with pH (Fig.6.1), the electrokinetic behaviour of the material produced by the high pressure homogenisation of yeast cells differs markedly from the behaviour of intact yeast cells. Below pH 5 the mobility of the whole cells becomes gradually less negative while the mobility of the homogenised yeast and the borax-clarified homogenate changes from negative to positive at pH 4 and rises sharply to over $10 \times 10^{-8} \text{ m}^2 \text{ V}^{-1} \text{ s}^{-1}$ at pH 3. Exposure of the internal surface of the cell wall and adsorption of intracellular material by the cell wall may cause changes in the mobility of the homogenate particles. Amory and Rouxhet (1988) correlated mobility with the presence of surface phosphate groups for different brewery yeast strains at pH 4. Differences in mobility at this pH may indicate changes have occurred to phosphate groups.

Above pH 6, where the surface charge is expected to be controlled by carboxylic acid groups [Amory and Rouxhet (1988)], the curve of mobility against pH flattens out to a constant negative value for both the whole cells and the homogenate. The mobility of the homogenate becomes more negative than that of the whole cells. The mobility for the borax-clarified homogenate did not level out up to pH 7.5 and became even more negative than the unclarified

homogenate above pH 6. Incorporation of borate anions into the cell debris and ionisation of these groups with increasing pH may account for the increased mobility of the particles remaining in the homogenate after borax treatment.

6.3.2 Flocculation with PEI

Low doses of the polyelectrolyte, PEI, have been found to be effective in the removal of the residual turbidity in yeast cell homogenate which has been initially clarified with borax. Variations of particle mobility with electrolyte concentration, pH and PEI concentrations for a range of PEI molecular weights indicate the mechanism of particle aggregation and the conditions under which the clarification can be optimised.

Whereas the effect of ionic species (sodium chloride and dipotassium hydrogen phosphate) on the mobility was found to be small in the range 1-5 kg/m³ (Figs. 6.2, 6.3), low concentrations of the polyelectrolyte, polyethylene imine, produced large changes in observed mobility. In the treatment of borax-clarified homogenate with 3 samples of PEI of similar charge densities, it was found that the concentration producing zero mobility also produced minimum supernatant turbidity after centrifugation (compare Figs. 6.5, 6.7 and 6.11). Critical flocculation concentrations (cfc) of 5 kg/m³ (Fig 6.11a, PEI 600) and 1 kg/m³ (Figs 6.11b and 6.11c, PEI 10,000 and PEI 70,000 respectively) may be deduced from the turbidity data.

Above the cfc values a large increase in turbidity to nearly twice the original turbidity was found for the highest molecular weight polymer (70,000) but the lower molecular weight polymers displayed only a slight turbidity increase with increased polymer dose. Similar turbidity and mobility behaviour was observed with the PEI of molecular weight 50,000, obtained from a different source from the other 3 samples of PEI. A turbidity minimum at PEI 50,000 concentration between 1 and 5 kg/m³ (Fig.6.11d) correlates with a concentration at which zero mobility is observed (1 kg/m³, Fig. 6.5). At higher PEI concentrations (up to 25 kg/m³) an increase in turbidity to a value approaching the

initial turbidity indicates behaviour intermediate between that of the PEI 10,000 and PEI 70,000.

The turbidity results at concentrations beyond the cfc can also be correlated with the mobility measurements (Figs. 6.5, 6.7). The mobilities obtained with the lower molecular weight polymers begin to level out at mobilities around $5 \times 10^{-9} \text{ m}^2 \text{ V}^{-1} \text{ s}^{-1}$ (PEI 600, ca. 6 kg/m^3) and $15 \times 10^{-9} \text{ m}^2 \text{ V}^{-1} \text{ s}^{-1}$ (PEI 10,000, ca. 8 kg/m^3), while higher mobilities, reaching $20 \times 10^{-9} \text{ m}^2 \text{ V}^{-1} \text{ s}^{-1}$ at 6 kg/m^3 and still increasing, were observed with PEI 70,000. Evidently, as the dose of PEI 70,000 is increased in the treatment of borax-clarified homogenate the particulate material is becoming restabilised by the high positive charge produced by the adsorbed polymer. The adsorption of the lower molecular weight PEI appears to reach a plateau value before the positive charge becomes high enough to restabilise the particles. PEI 50,000, producing higher positive mobilities than the lower molecular weight samples (Figs. 6.5 and 6.7), is also capable of restabilising the particles with adsorbed positive charge.

A comparison of the turbidity readings at 1 kg/m^3 for molecular weights 10,000 and 50,000 (Figs 6.11b and 6.11d) illustrates conditions where the effect of charge density may outweigh molecular weight. At this concentration the lower molecular weight PEI produces a turbidity minimum while for the higher molecular weight, but lower charge density, the turbidity is still decreasing with a minimum lying between 1 and 5 kg/m^3 .

Maibre et al. (1984) explained the importance of molecular weight for polymer adsorption in terms of the requirement of the number of anchoring points for complete adsorption of polymer. In the adsorption of cationic polymers on silica they observed that an equilibrium between free and adsorbed polymer was set up when the polymer molecular weight was below 20,000 - above this value the adsorption was essentially complete. Differences in the amount adsorbed account for the different plateau mobility values observed for each molecular weight PEI and the consequent ability to restabilise the yeast homogenate particles.

The clarification behaviour at low PEI doses can be explained using the observation of Linquist and Stratton (1976) that, at the dose required to initiate flocculation of silica with PEI, complete adsorption occurred irrespective of molecular weight with narrow molecular weight fractions of PEI in the range 1,760 to 18,400. In the clarification of yeast homogenate similar doses (1 kg/m^3) of PEI 10,000 and 70,000 gave the same turbidity reduction indicating adsorption of the same amount of polymer. The slightly higher dose required with PEI 50,000 results from the lower polymer charge density which reduces the amount of positive charge acquired for the adsorption of equivalent mass of polymer.

Changes in the ionic environment may affect the clarification by modifying the interaction of PEI with the particles. In the range 0-3 kg/m^3 of sodium chloride (Fig. 6.8a, PEI 600, 1 kg/m^3) increased negative mobilities are produced with increasing sodium chloride concentration. At a final PEI 600 dose of 2.5 kg/m^3 the positive mobilities at sodium chloride concentration of 1 kg/m^3 become negative at sodium chloride of 3 kg/m^3 . Double layer theory would require that the negative mobility of the particles reduce towards zero as the electrolyte concentration increased, as observed in the absence of PEI (Fig. 6.2). However, in the presence of PEI, modification of the mobility may result from changes in the amount of PEI adsorbed and changes in the polyelectrolyte configuration, in addition to compression of the double layer. The effect of electrolyte on higher molecular weight polymers may produce a different effect on mobility but this was not investigated.

Figure 6.8b illustrates that more positive mobilities can be obtained by reducing the pH from 8 to 6 at different concentrations of PEI 600. This result may be attributed to a shift in mobility of the homogenate particles to less negative values (as observed in Fig. 6.1 in the absence of PEI) together with increased positive charge on the PEI molecule due to protonation of the amine groups. The increased polymer charge may reduce adsorption of PEI due to electrostatic repulsion but at low PEI doses adsorption has been found to be independent of

pH [Lindquist and Stratton (1976)]. PEI 50,000 produces similar variation in mobility with pH to that of PEI 600.

In addition to adsorption on solid material, PEI is known to interact with other components of the cell such as nucleic acids and proteins. Atkinson and Jack (1973) and Milburn et al. (1989) have reported on the removal of nucleic acids with PEI and Jendrisak (1987) describes the fractionation of proteins from a number of microorganisms. In Figures 6.11a-d all molecular weights of the polymer led to losses of ca. 50% of the protein when the PEI concentration was adjusted to the cfc. Where restabilisation of the particles occurred and turbidity increased with polymer dose (Figs. 6.11c, 6.11d), a corresponding increase in measured protein in the supernatant was also observed. In the flocculation of *E. coli* debris with PEI Persson and Lindman (1987) found protein losses approaching 50%. Milburn et al. (1989) found protein losses of ca. 30% after PEI treatment of borax-clarified homogenate but did not observe loss of enzyme activity for a number of the yeast enzymes.

Differences in electrolyte conditions may be responsible for the variations in protein losses reported in the literature. The work of Jendrisak (1987) demonstrates how PEI can become a selective precipitating agent by exploiting variation in PEI/protein interactions at different salt concentrations. The amount of protein precipitated from wheat germ extracts was reduced from ca. 50% with no sodium chloride to less than 10% at 0.5 M sodium chloride. While protein precipitation can be reversed by increasing the salt concentration, nucleic acids cannot be resolubilised by this method indicating stronger interactions in the formation of the PEI/nucleic acid complex.

The pilot-scale separation of PEI flocs employed PEI 50,000 at a final concentration of 0.75 kg/m³. This is below the value indicated to give settling of the flocs in a laboratory centrifuge (ca. 4000g) but the separation of up to 90% of the solid material could be achieved at the lowest throughputs with a disc-stack centrifuge operating at ca. 12,000g (Fig. 6.12). The reduced dose of PEI in the pilot-scale flocculation produces

smaller mean floc size (Fig. 6.10) in comparison with the laboratory flocculation at 1 kg/m³ PEI, although differences in shear conditions during the addition of the polymer may also be important. The flocs are also likely to break up under the high shear forces on entry into the centrifuge but this break-up, if it is occurring, is not extensive enough to prevent settling in the centrifuge. The effect of mixing conditions and shear in the centrifuge feed zone play an important part in the precipitation and separation of protein precipitates as described by Bell et al. (1983).

6.3.3 Flocculation Mechanism

It is generally believed that flocculation with cationic polyelectrolytes does not involve polymer bridging since ionic interactions cause the polymer to adopt a flat configuration on the particle surface [Gregory (1976)]. A mechanism of adsorption-coagulation, i.e. a reduction of the particle surface charge by adsorption of oppositely charged polymer, appears to be the dominant mechanism for cationic polyelectrolytes. Support for this mechanism has been provided by the observations of Treweek and Morgan (1977) that optimum flocculation can be achieved at polymer concentrations below the value required for coverage of half the particle [the value calculated for optimum bridging flocculation by La Mer and Healy (1963)], that the optimum polyelectrolyte dose is independent of molecular weight [Gregory (1973)], and that optimum flocculant doses produce particle mobilities close to zero.

Complete neutralisation is not required to promote aggregation - reduction of particle charge to the point where Van der Waals' attraction predominates over electrostatic repulsion is sufficient. Treweek and Morgan (1977) found optimum flocculation of E. coli cells at PEI doses at which the cells were still negatively charged. The presence of patches of negative charge after the adsorption of positively charged electrolyte has been used by Gregory (1976) to explain the enhancement of flocculation rates observed with polyelectrolytes of medium molecular weight through a mechanism of the attraction of 'electrostatic patches'

of opposite charge on the particles. This charge patch mechanism was used by Maibre et al. (1984) in the interpretation of the behaviour of silica particle flocculation.

The correspondence of PEI dose and particle mobility in the results for the treatment of borax-clarified homogenate support a mechanism of adsorption-coagulation. Bridging does not seem to be important under the conditions used since PEI of molecular weight 10,000 was shown to produce the same clarification as molecular weight 70,000 at the same concentration. However the presence of some particle bridging cannot be entirely ruled out. Lindquist and Stratton (1976) found, in accordance with the La Mer (1963) theory of polymer bridging, a strong dependence of critical flocculation concentration on molecular weight when PEI was used to flocculate silica at pH 11 - the pH at which the PEI molecule becomes uncharged.

6.4 Conclusion

There are a number of parameters, such as floc size, settling rate or supernatant turbidity, that may be used to assess the efficiency of a particular flocculating agent. There is therefore a degree of uncertainty in the measurement of a critical flocculation concentration since the value obtained will depend on the method of measurement. In the determination of an optimum flocculation concentration the method of separating the flocs should be considered. In this study the turbidity of the supernatant after centrifugal settling has been used to evaluate the flocculation efficiency in order that the performance of pilot scale centrifuges could be assessed.

Each PEI sample has a distribution of molecular weight about the mean value quoted and the particle mobilities measured represent a mean value of a distribution of mobilities of the cell wall material and precipitated intracellular material. Furthermore, the mobility results were obtained with much lower solids concentrations than in the settling experiments. Despite these uncertainties, the data for mean particle mobility correlates

well with the settling behaviour in the laboratory and allows a suitable concentration of PEI to be chosen for the pilot-scale centrifugation.

All the samples of PEI used were found to be effective in the clarification of borax-clarified homogenate. The dose required to give optimum flocculation for centrifugal settling is determined by the adsorption of sufficient charge to neutralise the negatively charged material in the homogenate. While, at similar charge densities, any molecular weight in the range used (600-70,000) will result in clarification, in practice a medium molecular weight polymer may be preferred. At the lower end of the molecular weight range polymer adsorption may be limited by the equilibrium between free and adsorbed polymer [Maibre et al. (1984)]. With PEI 600 a higher dose is required for charge neutralisation than with PEI 10,000 or PEI 70,000. With molecular weights below 600 even higher doses will be required and it is possible that a low molecular weight polymer may not produce sufficient adsorption for charge neutralisation and no clarification will be obtained.

Increasing the molecular weight of the positively charged polyelectrolyte increases the probability of the formation of patches of positive charge on the negatively charged surface [Gregory (1976)]. The interaction of patches of positive and negative charge may therefore produce stronger flocs, resistant to shear breakdown. On the other hand the use high molecular weight PEI can produce charge reversal with low doses of polymer. It is then difficult to identify the optimum polymer concentration and there is a risk of overdosing and stabilising the homogenate particles at high positive mobilities. Other limitations in the use of higher molecular weight polymers include cost of polymer and ease of mixing since higher molecular weight polymers become more difficult to manufacture and their viscosity increases.

The effect of PEI on the soluble components in the homogenate may determine the choice of molecular weight and concentration in the optimisation of the PEI-flocculation of debris. The work of

Milburn et al. (1989) and Jendrisak (1987) suggests that suitable conditions can be found where the removal of unwanted proteins, nucleic acids and lipids can be achieved while maintaining the activity of a selected enzyme in solution.

7. CONCLUSION

In this study, solutions to the problems in the separation of fine biological materials have been sought by adjustment of the properties of the suspension/solution to facilitate solid-liquid separation. The settling of the solids, flow properties of the suspension, dewatering of the solid and interaction with membranes can be changed by inducing aggregation of the material.

The isoelectric precipitation of soya improves ultrafiltration flux rates when compared to ultrafiltration of the solution due to the reduction in soluble protein content which polarises the membrane. The reduction in soluble protein content also lowers the viscosity of the suspension - thus aiding the management of flow conditions which become critical at high concentrations. Control of the fluid viscosity and adjustment of the hollow-fibre geometry and pumping system have enabled the soya protein concentration in ultrafiltration to reach the levels obtained in the scroll centrifugation [ca. 400 kg/m³, Devereux et al. (1984)] of this material. In a similar manner, the use of precipitation has now been applied to the improvement in flux rates for cheese whey ultrafiltration [Kaiser and Glatz (1988)].

There are potential improvements in flux to be gained by increasing the membrane pore size to allow passage of the soluble components in the suspension. Efforts with microfiltration membranes have suffered from the depth fouling of the membrane, due to entrapped particles, and protein adsorption within the pores. Ultrafiltration membranes do not seem to be as severely affected by depth fouling since the particles cannot enter the pores. There is some room for flux improvement in ultrafiltration by using higher molecular weight cut-off membrane, such as 100,000 or 500,000, instead of the 50,000 cut-off used here. It is likely that such membranes will give higher flux rates, due to reduced membrane resistance, without high transmission of soluble protein. The formation of a secondary layer on the membrane will lower the flux but may be advantageous if total protein retention is required.

In the aggregation of debris in cell homogenates there is the additional difficulty of ensuring the separation and activity of the soluble fraction of enzymes and proteins. Borax has been found to be a suitable reagent for the aggregation of yeast homogenate since it does not interfere with the soluble components and produces a sediment which can be discharged readily from a continuous centrifuge. The structure of the sediment has been characterised in terms of the shear modulus and the centrifuge conditions can be manipulated to change the extent of solids dewatering. There is scope for improved dewatering by the adjustment of flocculation conditions (borax concentration, mixing conditions, etc.) and tuning of the centrifuge to accommodate even higher torque loading (giving higher solids).

Since borax acts on yeast by cross-linking cis-1,2 diols in the mannan of the cell wall, it cannot be generally applied for the aggregation of other microorganisms, such as bacteria, since they do not contain the required diol groups. Another flocculating agent, polyethylene imine, also used for yeast aggregation, appears to be less specific in its interaction and may be of general use for other microorganisms. However, because it is less specific it is critical that the interaction with the components of the cell homogenate, in terms of aggregate size and protein precipitation, are well understood.

Particle size analysis is a valuable tool in the assessment of aggregation and the effectiveness of separation equipment but the techniques are difficult to apply to sizing low density fines such as those present in cell homogenates. Advances in light-scattering instrumentation are facilitating such measurements, could be usefully applied to the calculation of centrifuge efficiency and the evaluation of flocculating agents (such as, in this study, polyethylene imine), and could also be used for on-line control of these operations.

The use of light scattering to detect the movement of particles in an electric field is also useful in the measurement of particle surface charge (mobility) and has been successfully employed here to elucidate the mechanism of yeast debris

flocculation with polyethylene imine (PEI). The polyelectrolyte was found to promote aggregation of fine debris by neutralising the particle charge but protein loss of up to 50% was also observed. The control of the flocculation conditions was found to be critical since overdosing with PEI can restabilise the debris in suspension and changes in pH or salt concentration can change the interaction of PEI with the solids and the soluble protein. It has been reported that PEI can remove debris, nucleic acids and lipids [Milburn et al. (1989), Jendrisak (1987)], while the loss of soluble protein can be limited by using high salt concentration. Such work could be extended to determining the specific interaction of flocculating agents with the components of the homogenate in order to maximise the yield of a selected product during the clarification.

The mobility results are reported here as mean values from a distribution of mobilities in a complex mixture. It may be possible to refine this analysis further to identify the mobilities of individual components in the homogenate. This data may prove valuable in selectively flocculating the components of the mixture to remove specific fractions. Particle charge measurements could also be usefully applied to membrane separation of precipitates since membranes can be designed with charge characteristics which minimise interaction of membrane with the suspension.

8. SUGGESTIONS FOR FURTHER WORK

8.1 Microfiltration of Protein Precipitate

Since microporous membranes are susceptible to fouling by protein adsorption and blockage by fine particles, leading to flux reduction and rejection of soluble protein, it would be useful to study specific interactions of the membrane with soluble and precipitated protein. The extent of protein adsorption as a function of concentration, pH and salt concentration should be determined. The effect of protein adsorption could be investigated by measuring the flux of pure, particle-free water through membranes with a known amount of adsorbed protein. By examining the adsorption of a number of different proteins to membranes made from a variety of polymer or ceramic materials it may be possible to find a low fouling system in which change in membrane resistance with time has a negligible effect on the water flux. The microfiltration of precipitated protein could then be examined in terms of precipitate particle size, membrane pore size and the effect of cross flow. An alternative approach would be to observe the microfiltration of non-adsorbing particles with well-defined particle sizes to determine the effects of pore blockage and particle cake resistance under a variety of cross flow conditions.

8.2 Ultrafiltration of Protein Precipitate

While it has been shown that the cross flow conditions can be critical in maintaining high flux rates during hollow fibre ultrafiltration of protein precipitate, it has not been possible to determine whether cross flow velocity or shear rate at the membrane surface is the most important factor in determining flux through the membrane. The cross flow parameters have been calculated from viscosity measurements but could be accurately determined from direct measurement of the flow through the fibre using a magnetic flow meter. Measured cross flow velocities should be compared with values calculated from the viscosity of the precipitate suspension and a wider range of flow conditions should be used to distinguish the relative importance of cross flow velocity and wall shear rate in determining the flux rate.

Pilot scale ultrafiltration experiments for the dewatering of protein precipitate are limited by the available sizes and safe working pressures of manufactured ultrafiltration modules. More information could be obtained concerning the effect of flow conditions on the ultrafiltration flux rate from laboratory experiments using variable precipitation and cross flow conditions. Protein precipitate suspension could be prepared with a wider range of soluble protein content and precipitate particle size to establish the influence of particle properties and protein gel layer formation on flux rate. The results reported in this work could be extended to a wider variation in fibre diameter, fibre length and inlet/outlet pressure in order to define the flow conditions required to maintain high flux rates.

8.3 Scroll Centrifugation of Flocculated Yeast Homogenate

The use of a microprocessor control system, now available from the centrifuge manufacturer, permits accurate monitoring and control of operating parameters of the scroll decanter centrifuge and it would be valuable to examine a wider range of centrifuge operating conditions. Improvements in the dewatering of borax-flocculated yeast cell debris could be achieved by examining very low scroll rates which would give greater residence time of the solids within the centrifuge. It would also be interesting to determine the limit of centrifuge throughput at which the separation efficiency begins to decrease, i.e. the solids content of the centrifuge overflow increases, and the effect of higher throughput rates on the settling and dewatering of the solid underflow stream.

The effect of sediment rheology on dewatering in the centrifuge could be studied by adjusting the flocculation conditions or using alternative microorganisms with differing sediment properties. Changes in the rotational speed of the centrifuge to give higher and lower g-forces in the bowl would provide further information relating the rheology of the settled sediment to the dewatering of the sediment in the centrifuge.

8.4 Clarification of Yeast Homogenate using Polyelectrolytes

The loss of soluble protein is a disadvantage when using PEI to aggregate unwanted material in a cell homogenate. Since it is possible, in some cases, to reduce the loss of soluble protein by increasing the salt concentration, the effect of pH and salt concentration on the interactions of PEI with the individual components of yeast homogenate should be studied in more detail to determine the appropriate conditions for selectively removing the unwanted material. Methods of accurately measuring solids concentration should be developed, since this is an important factor in specifying the appropriate dose of flocculant, and assay procedures for measurement of soluble components should be checked for interference by polyelectrolytes such as PEI. The use of PEI of higher molecular weight or other polymeric flocculants, e.g. polyacrylamides, may alter the selectivity of the flocculation and provide additional information on the mechanism of particle aggregation. An alternative method of flocculation would be to produce positively charged particles with high doses of cationic polymer (PEI) and then aggregate with long chains of neutral or negatively charged polymers.

Further pilot scale trials, with optimisation of the flocculation conditions based on the laboratory scale experiments, should be carried out to improve the clarification that can be obtained using a disc-stack centrifuge. Information on the effect of mixing conditions during flocculation, the kinetics of floc formation and the strength of the resulting flocs could be used to optimise the separation of the solids.

SYMBOLS

A	membrane area	m^2
A_0	constant, Equ. 1.6.3	-
A_1	constant, Equ. 1.6.6	$m^{0.67} s^{-0.67}$
A_2	constant, Equ. 1.6.6	$s m^{-1}$
a	constant, Equ. 1.6.3	-
a	particle radius	m
B	observed gradient of volume permeated versus (time) ^{0.5}	$m^3 s^{-0.5}$
B_m	calculated gradient of volume permeated versus (time) ^{0.5} , macromolecular solutions, Equ. 3.2	$m^3 s^{-0.5}$
B_m'	calculated gradient of volume permeated versus (time) ^{0.5} , macromolecular solutions, Equ. 3.5	$m^3 s^{-0.5}$
B_p	calculated gradient of volume permeated versus (time) ^{0.5} , particle suspensions, Equ. 3.7	$m^3 s^{-0.5}$
b	constant, Equ. 1.6.3	-
C_b	bulk protein concentration	$kg m^{-3}$
C_p	permeate protein concentration	$kg m^{-3}$
C_w	wall protein concentration	$kg m^{-3}$
C_g	gel protein concentration	$kg m^{-3}$
C_s	solution or supernatant protein concentration	$kg m^{-3}$
C_t	total protein concentration	$kg m^{-3}$
D	diffusion coefficient	$m^2 s^{-2}$
d	particle diameter	m
d	pipe diameter, Equ. 1.5.7	m
d_h	hydraulic diameter	m
d_m	mean particle diameter	m
d_p	particle diameter	m
E	efficiency, Equ. 2.1	-
E'	reduced efficiency, Equ. 2.1	-
e	unit of electric charge	C
G	shear modulus	$N m^{-2}$
G'	storage modulus	$N m^{-2}$
G''	loss modulus	$N m^{-2}$
G^*	complex shear modulus	$N m^{-2}$
g	gravitational acceleration	$m s^{-2}$
I	intensity	candela

J	flux rate	m s^{-1}
J	creep compliance	$\text{m}^2 \text{N}^{-1}$
k	Boltzmann constant	J K^{-1}
k	consistency, power law fluid	$\text{N s}^{-n} \text{m}^{-2}$
k_m	mass transfer coefficient	m s^{-1}
L	pipe length	m
M_L	mass of liquid	kg
M_s	mass of solid	kg
n	refractive index relative to surrounding medium	-
n	power law index	-
n	particle number	-
n_o	bulk number concentration	m^{-3}
P	pressure	N m^{-2}
Q	flowrate	$\text{m}^3 \text{s}^{-1}$
R	ratio underflow:feedrate, Equ. 2.1	-
R_f	fouling layer resistance	m^{-1}
R_m	membrane resistance	m^{-1}
R_p	polarisation layer resistance	m^{-1}
r	distance	m
r	membrane pore radius	m
r'	effective radius, Equ. 1.7.4	m
Re	Reynolds number	-
s	settling distance	m
s'	effective settling distance, Equ. 1.7.4	m
Sc	Schmidt number	-
Sh	Sherwood number	-
T	temperature	K
t	time	s
t'	time	s
U	mobility	$\text{m}^2 \text{V}^{-1} \text{s}^{-1}$
u	mean velocity	m s^{-1}
u_t	terminal velocity	m s^{-1}
V	volume of liquid in centrifuge	m^3
x	distance	m
y	distance	m
z	valency	-

Greek Symbols

α	polarisability	$C m^2 V^{-1}$
γ	substituted variable, Equ. 1.3.3	-
γ	shear strain	-
γ_0	amplitude of shear strain	-
$\dot{\gamma}$	rate of shear strain (shear rate)	s^{-1}
$\dot{\gamma}_w$	wall shear rate	s^{-1}
δ	boundary layer thickness	m
δ	phase lag, Equ. 1.5.21	rad
ΔP	pressure drop, transmembrane pressure	$N m^{-2}$
ΔV	permeate volume	m^3
$\Delta \rho$	solid liquid density difference	$kg m^{-3}$
ϵ	permittivity	$C V^{-1} m^{-1}$
ϵ_0	permittivity of vacuum	$C V^{-1} m^{-1}$
ϵ_r	relative permittivity	-
ϵ	porosity	-
ζ	zeta potential	V
θ	angle	rad
κ	Debye-Huckel parameter	m^{-1}
λ	wavelength	m
μ	viscosity	$N s m^{-2}$
μ_a	apparent viscosity	$N s m^{-2}$
$[\mu]$	intrinsic viscosity	-
μ_0	viscosity of suspending liquid	$N s m^{-2}$
π	pore blocking parameter, Equ. 3.8	-
π_0	osmotic pressure	$N m^{-2}$
ρ	charge density, Equ. 1.3.1	$C m^{-3}$
ρ	density	$kg m^{-3}$
ρ_l	liquid density	$kg m^{-3}$
ρ_s	solid density	$kg m^{-3}$
Σ	centrifuge size, Equ. 1.7.3	m^2
τ	shear stress	$N m^{-2}$
τ_0	yield value of shear stress	$N m^{-2}$
τ_0	amplitude of shear stress, Equ. 1.5.21	$N m^{-2}$
τ_w	wall shear stress	$N m^{-2}$
$\dot{\tau}$	rate of change of shear stress	$N m^{-2} s^{-1}$
ϕ	volume fraction	-

Ψ	potential	V
Ψ_d	Stern potential	V
Ψ_0	particle surface potential	V
ω	angular velocity	rad s ⁻¹
ω	frequency	s ⁻¹

Abbreviations

ASU	acidic sub-unit, glycinin
BSA	bovin serum albumin
BSU	basic sub-unit, glycinin
cfc	critical flocculation concentration
OSU	membrane open side up
PEI	polyethylene imine
rcf	relative centrifugal force
SDS	sodium dodecyl sulphate
TSU	membrane tight side up
TWE	total water extract, soya

REFERENCES

- Akers, R.J., Filtration pretreatment, in *The Scientific Basis of Filtration*, Ed., Ives, K.J., Noordhoff, The Netherlands, pp 91-127, 1975.
- Allen, T., *Particle Size Measurement*, Chapman and Hall, London, 1981.
- Altena, F.W., and Belfort, G., Lateral migration of spherical particles in porous flow channels: Application to membrane filtration, *Chem. Engng. Sci.*, 39, 2, pp 343-355, 1984.
- Ambler, C.M., The theory of scaling up laboratory data for the sedimentation type centrifuge, *J. Biochem and Microbiol. Technol. Eng.*, 1, 2, pp 185-205, 1959.
- Amory, D.E., and Rouxhet, P.G., Surface properties of *Saccharomyces cerevisiae*, and *Saccharomyces carlsbergensis*: chemical composition, electrostatic charge and hydrophobicity, *Biochim. et Biophys. Acta*, 938, pp 61-70, 1988.
- Atkinson, A., and Jack, G.W., Precipitation of nucleic acids with polyethyleneimine and the chromatography of nucleic acids and proteins on immobilised polyethyleneimine, *Biochim. Biophys. Acta*, 308, pp 41-52, 1973.
- Axelsson, H.A.C., Centrifugation, in *Comprehensive Biotechnology Vol 2*, Ed., Cooney, C.L., and Humphrey, A.E., Pergamon, pp 325-346, 1985.
- Bauser, H., Chmiel, H., Stroh, N., and Walitza, E., Control of concentration polarization and fouling of membranes in medical, food and biotechnical applications, *J. Membrane Sci.*, 27, pp 195-202, 1986.
- Belfort, G., and Nagata, N., Fluid mechanics and cross flow filtration: some thoughts, *Desalination*, 53, pp 57-79, 1985.

- Belfort, G., and Altena, F.W., Toward an inductive understanding of membrane fouling, *Desalination*, 47, pp 105-127, 1983.
- Belfort, G., Chin, P., and Dziejulski, D.M., New gel polarization model incorporating lateral migration for membrane fouling, *World Filtration Congress*, Vol. 2, pp 548-555, 1982.
- Bell, D.J., and Dunnill, P., Shear disruption of soya protein precipitate particles and the effect of aging in a stirred tank, *Biotechnol. Bioeng.*, 24, pp 1271-1285, 1982.
- Bell D.J., Hoare, M., and Dunnill, P., The formation of protein precipitates and their centrifugal recovery, in *Advances in Biochemical Engineering/Biotechnology* Vol. 26, Ed., Fiechter, A., Springer-Verlag, pp 1-72, 1983.
- Bell, D.J., Heywood-Waddington, D., Hoare, M., and Dunnill, P., *Biotechnol. Bioeng.*, 24, pp 127-141, 1982.
- Bell, D.J., and Dunnill, P., The influence of precipitation reactor configuration on the centrifugal recovery of isoelectric soya protein precipitate, *Biotechnol. Bioeng.*, 24, pp 2319-2336, 1982a.
- Belter, P.A., Filtration of fermentation broths, *Comprehensive Biotechnology* Vol 2, Ed., Cooney, C.L., and Humphrey, A.E., Pergamon, pp 347-350, 1985.
- Bertera, R., Steven, H., and Metcalfe, M., Development studies of crossflow microfiltration, *The Chemical Engineer*, Jun, pp 10-14, 1984.
- Blatt, W.F., Dravid, A., Michaels, A.S., and Nelsen, L., Solute polarization and cake formation in membrane ultrafiltration: causes, consequences and control techniques, pp 47-93, in *Membrane Science and Technology*, Ed., Flinn, J.E., Plenum, New York, 1970.

Bonnerjea, J., Jackson, J., Hoare, M., and Dunnill, P., *Enzyme and Microbiol. Tech.*, 10, pp 357-360, 1988.

Breslau, B.R., Testa, A.J., Milnes, B.A., and Medjanis, G., *Advances in hollow fibre technology*, pp 109-127, in *Ultrafiltration Membranes and Applications*, Ed., Cooper, A.R., Plenum, New York, 1980.

Buscall, R., McGowan, I.J., Mills, P.D.A., Stewart, R.F., Sutton, D., White, L.R., and Yates, G.E., *J. Non-Newtonian Fluid Mech.*, 24, 183, 1987.

Cheryan, M., *Ultrafiltration Handbook*, Technomic, Lancaster, Pennsylvania, U.S.A., 1986.

Chudacek, M.W., and Fane, A.G., *The dynamics of polarisation in unstirred and stirred ultrafiltration*, *J. Membrane Sci.*, 21, pp 145-160, 1984.

Coulson, J.M., and Richardson, J.F., *Chemical Engineering*, Vol 1, Pergamon, Oxford, Third Edition, 1977.

Datar, R., *Studies in the separation of intracellular soluble enzymes from bacterial cell debris by tangential flow membrane filtration*, *Biotechnol. Letters*, 7, 7, pp 471-476, 1985.

Deindoerfer, F.H., and West, J.M., *Rheological properties of fermentation broths*, *Adv. Appl. Microbiol.*, 2, pp 265-273, 1960.

Derjaguin, B.V., and Landau, L.D., *Theory of the stability of strongly charged lyophobic sols and of the adhesion of strongly charged particles in solutions of electrolytes*, *Acta Physicochim. USSR*, 14, p 633, 1941.

Devereux, N., *Membrane Concentration of Precipitated Protein*, PhD Thesis, London University, London, 1983.

Devereux, N., Hoare, M., and Dunnill, P., *Membrane separation of protein precipitates: Unstirred batch studies*, *Biotechnol.*

Bioeng., 28, pp 88-96, 1986.

Devereux, N., Hoare, M., and Dunnill, P., The effect of protein precipitation on the concentration of proteins by ultrafiltration, Chem. Eng. Commun., 45, pp 255-276, 1986a.

Devereux, N., Hoare, M., Dunnill, P., and Bell, D.J., The development of improved methods for the industrial recovery of protein precipitates, pp 143-160, in Solid-liquid Separation, Ed., Gregory, J., Ellis Horwood, Chichester, 1984.

Devereux, N., and Hoare, M., Membrane separation of protein precipitates: Studies with cross flow in hollow fibres, Biotechnol. Bioeng., 28, pp 422-431, 1986.

Dimitrieva, T.F., and Pakshver, A.N., Khim. Prom., p 20, 11, 1951.

Doshi, M.R., and Trettin, D.R., Ultrafiltration of colloidal suspensions and macromolecular solutions in an unstirred batch cell, Ind. Eng. Chem. Fundam., 20, pp 221-229, 1981.

Dunnill, P., and Lilly, M.D., in Single Cell Protein II, Ed., Tannenbaum, S.R., and Wang, D.I.C., MIT Press, Cambridge, Mass., USA and London, UK, pp 179-207, 1975.

Esser, K., Hinrichs, J., and Kues, U., Genetic control of flocculation of yeast with respect to application in biotechnology, pp 383-398, in Flocculation in Biotechnology and Separation Systems, Ed., Attia, Y.A., Elsevier, Amsterdam, 1987.

Fane, A.G., Fell, C.J.D., and Nor, M.T., Ultrafiltration in the presence of suspended solids, I.Chem.E. Symp. Ser., 73, pp C1-C12, 1982.

Fane, A.G., Fell, C.J.D., and Waters, A.G., Ultrafiltration of protein solutions through partially permeable membranes - the effect of adsorption and solution environment, J. Membrane Sci., 16, pp 211-224, 1983.

Fane, A.G., Ultrafiltration: factors affecting flux and rejection, pp 101-179, in Progress in Filtration and Separation, Ed., Wakeman, R.J., Elsevier, Amsterdam, 1986.

Fane, A.G., Ultrafiltration of suspensions, J. Membrane Sci., 20, pp 249-359, 1984.

Faust, T., and Gosele, W., Investigation of the clarification process in decanter centrifuges, Ger. Chem. Eng., 9, pp 136-142, 1986.

Fischer, E., and Raasch, J., Cross-flow filtration, Ger. Chem. Eng., 8 pp 211-216, 1985.

Fish, N.M., and Lilly, M.D., The interactions between fermentation and protein recovery, Biotechnology, 2, pp 623-627, 1984.

Follows, M., Hetherington, P.J., Dunnill, P., and Lilly, M.D., Release of enzymes from Bakers' yeast by disruption in an industrial homogenizer, Biotechnol. Bioeng., 13, pp 549-560, 1971.

Forster, C.F., Knight, N.J.B., and Wase, D.A.J., Flocculating agents of microbial origin, Adv. Biotechnol. Prog., 4, pp 241-274, 1985.

Gabler, F.R., Cell processing using tangential flow filtration, in Comprehensive Biotechnology, Vol 2, Ed., Cooney, C.L., and Humphrey, A.E., Pergamon, pp 351-366, 1985.

Goldsmith, R.J., deFilippi, R.P., and Hossain, S., New membrane process applications, AIChE Symp. Series, 68, 120, pp 7-14, 1972.

Gornall, A.G., Bardawill, C.J., and David, M.M., Determination of serum proteins by means of the Biuret reaction, J. Biol. Chem., 177, pp 751-766, 1949.

Gosele, W., Scale-up of helical conveyer type decanter centrifuges, *Ger. Chem. Eng.*, 3, pp 353-359, 1980.

Gravatt, D.P., and Molnar, T.E., Recovery of an extracellular antibiotic by ultrafiltration, in *Membrane Separations in Biotechnology*, Ed., McGregor, W.C., Marcel Dekker, New York, U.S.A., pp 89-97, 1986.

Gray, P.P., Dunnill, P., and Lilly, M.D., The clarification of mechanically disrupted yeast suspensions by rotary vacuum precoat filtration, *Biotechnol. Bioeng.*, 15, pp 309-320, 1973.

Green, G., and Belfort, G., Fouling of ultrafiltration membranes: Lateral migration and the particle migration model, *Desalination*, 35, pp 129-147, 1980.

Gregory, J., The effect of cationic polymers on the colloidal stability of latex particles, *J. Coll. Int. Sci.*, 55, pp 35-44, 1976.

Gregory, J., Rates of flocculation of latex particles by cationic polymers, *J. Coll. Int. Sci.*, 42, pp 448-456, 1973.

Gregory, J., Interfacial phenomena, in *The Scientific Basis of Filtration*, Ed., Ives, K.J., Noordhoff, The Netherlands, pp 53-90, 1975.

Hacking, A.J., *Economic Aspects of Biotechnology*, pp 127-145, Cambridge university press, Cambridge, 1986.

Hames, B.D., in *Gel Electrophoresis of Proteins*, Ed., Hames, B.D., and Rickwood, D., IRL, London, pp 1-91, 1981.

Hanisch, W., Cell harvesting, in *Membrane Separations in Biotechnology*, Ed., McGregor, W.C., Marcel Dekker, New York, U.S.A., pp 61-88, 1986.

Hardy, W.B., *Proc. Royal Soc.*, 66, p 110, 1900.

Herbert, A., PhD Thesis, London University, London, England, 1985.

Hetherington, P.J., Follows, M., Dunnill, P., and Lilly, M.D., Trans. Inst. Chem. Engrs., 49, pp 142-148, 1971.

Hoare, M., Narandranathan, T.J., Flint, J.R., Heywood-Waddington, D., Bell, D.J., and Dunnill, P., Ind. Eng. Chem. Fundam., 21, pp 402-404, 1982.

Hoare, M., Dunnill, P., and Bell, D.J., Reactor design for protein precipitation and its effect on centrifugal separation, Annals of the New York academy of sciences, 413, pp 254-269, 1983.

Hopwood, D.A., The genetic programming of industrial microorganisms, Scien. American, 224, 3, pp 66-78, 1981.

Howell, J.A., and Velicangil, O., Protein ultrafiltration: Theory of membrane fouling and its treatment with immobilized proteases, pp 217-229, in Ultrafiltration membranes and applications, Ed., Cooper, A.R., Plenum, New York, 1980.

Howell, J.A., and Velicangil, O., J. Appl. Polymer Sci., 27, pp 21, 1982.

Hsu, H.W., Separations by Centrifugal Phenomena, Wiley, New York, 1981.

Huddleston, J.G., Sansome-Smith, A., Deng-Xi, W., and Lyddiat, A., Membrane separations in biochemical recovery: physical and biochemical considerations for general purpose application, pp 253-266, Proceedings of the international conference on membrane separation processes, BHRA, The Fluid Engineering Centre, Cranfield, Bedford, U.K., 1989.

Hunter, R.J., Foundations of Colloid Science, Vol. 1, Clarendon, Oxford, 1987.

Ingham, K.C., Busby, T.F., Sahlestrom, Y., and Castino, F., Separation of macromolecules by ultrafiltration: influence of protein adsorption, protein-protein interactions and concentration polarization, pp 141-158, in Ultrafiltration Membranes and Applications, Ed., Cooper, A.R., Plenum, New York, 1980.

Jelinek, Z.K., Particle Size Analysis, Ellis Horwood, Chichester, 1974.

Jendrisak, J., The use of polyethyleneimine in protein purification, in Protein purification, Ed., Burgess, R., Alan R. Liss Inc., New York, pp 75-97, 1987.

Kaiser, J.M., and Glatz, C.E., Use of precipitation to alter flux and fouling performance in cheese whey ultrafiltration, Biotechnol. Progress, 4, 4, pp 242-247, 1988.

Kinsella, J.E., J. Am. Oil Chem. Soc., 56, p 242, 1979.

Koglin, B., Influence of agglomeration on filterability of suspensions, Ger. Chem. Eng. 8, pp 217-223, 1985.

Kroner, K.H., Schutte, H., Hustedt, H., and Kula, M.R., Cross-flow filtration in the downstream processing of enzymes, Process Biochem., 19, pp 67-74, 1984.

Kroner, K.H., and Schutte, H., Dynamic filtration of microbial suspensions, pp 279-290, Proceedings of the international conference on membrane separation processes, BHRA, The Fluid Engineering Centre, Cranfield, Bedford, U.K., 1989.

Kroner, K.H., Nissinen, V., and Ziegler, H., Bio/Technology, 5, pp 921-926, 1987.

La Mer, V.K., and Healy, T.W., Adsorption-flocculation reactions of macromolecules at the solid-liquid interface, Rev. Pure Appl. Chem., 13, pp 112-133, 1963.

Le, M.S., Spark, L.B., and Ward, P.S., The separation of aryl acylamidase by cross flow microfiltration and the significance of enzyme/cell debris interaction, *J. Membrane Sci.*, 21 pp 219-232, 1984.

Le, M.S., Spark, L.B., Ward, P.S., and Ladwa, N., Microbial asparaginase recovery by membrane processes, *J. Membrane Sci.*, 21, pp 307-319, 1984a.

Lindquist, G.M., and Stratton, R.A., The role of polyelectrolyte charge density and molecular weight on the adsorption and flocculation of colloidal silica with polyethylenimine, *J. Coll. Int. Sci.*, 55, 1, pp 45-59, 1976.

Mackay, D.J., Norton, M.G., Newdick, P.C., Wittington, P.N., and George, N., Developments in solid-liquid separation for biotechnology, pp 227-261, *Solid liquid separation practice 3*, The Institution of Chemical Engineers Symposium Series 113, Rugby, U.K., 1989.

Maibre, F., Audebert, R., and Quivoron, C., Flocculation properties of some water-soluble cationic copolymers toward silica suspensions: A semiquantitative interpretation of the role of molecular weight and cationicity through a patchwork model, *J. Coll. Int. Sci.*, 97, 1, pp 120-136, 1984.

Markwell, M.A.K., Haas, S.M., Bieber, L.L., and Tolbert, N.E., A modification of the Lowry procedure to simplify protein determination in membrane and lipoprotein samples, *Anal. Biochem.*, 87, pp 206-210, 1978.

Matthiasson, E., The role of macromolecular adsorption in fouling of ultrafiltration membranes, *J. Membrane Sci.*, 16, pp 23-36, 1983.

Michaels, A.S., A new separation technique for the CPI, *Chem. Eng. Progress*, 64, 12, pp 31-43, 1968.

Milburn, P., Hoare, M., and Dunnill, P., in preparation, 1989.

Morris, B.G., Application and selection of centrifuges, Part 1, Brit. Chem Eng., 11, pp 347-351, 1966.

Mosqueira, F.G., Higgins, J.J., Dunnill, P., and Lilly, M.D., Characteristics of mechanically disrupted Bakers' yeast in relation to its separation in industrial centrifuges, Biotechnol. Bioeng., 23, pp 335-343, 1981.

Moudil, B.M., and Shah, B.D., Selection of flocculants for solid-liquid separation processes, in Advances in solid liquid separation, Ed., Muralidhara, H.S., Battelle Press, Ohio, U.S.A., pp 191-204, 1986.

Nakao, S., Nomura, T., and Kimura, S., Characteristics of macromolecular gel layer formed on ultrafiltration tubular membrane, A.I.Ch.E.J., 25, pp 615-622, 1979.

Narendranathan, T.J., Ph.D. Thesis, University of London, London, 1981.

Neihof, R.A., and Echols, W.H., Physicochemical studies of microbial cell walls. Comparative behaviour of intact cells and isolated cell walls, Biochim. Biophys. Acta, 318, pp 23-32, 1973.

Orchard, A.C.J., Recent developments in membranes for critical filtration applications, pp 79-92, Proceedings of the international conference on membrane separation processes, BHRA, The Fluid Engineering Centre, Cranfield, Bedford, U.K., 1989.

Patel, P.N., Mehaia, M.A., and Cheyan, M., Cross-flow membrane filtration of yeast suspensions, J. Biotechnol., 5, pp 1-16, 1987.

Pearson, D., and Quirk, A., Recovery of recombinant human serum albumin from yeast fermentation cultures using cross-flow microporous filtration, pp 267-278, Proceedings of the international conference on membrane separation processes, BHRA, The Fluid Engineering Centre, Cranfield, Bedford, U.K., 1989.

Persson, I., and Lindman, B., Flocculation of cell debris for improved separation by centrifugation, pp 457-466, in Flocculation in Biotechnology and Separation Systems, Ed., Attia, Y.A., Elsevier, Amsterdam, 1987.

Phaff, H.J., Structure and biosynthesis of the yeast cell envelope, in The Yeasts, Vol 2, Ed., Rose, A.H., Academic Press, London and New York, pp 135-203, 1971.

Porter, M.C., Concentration polarisation with membrane ultrafiltration, Ind. Eng. Chem. Prod. Res. Dev., 11, 3, pp 234-248, 1972.

Records, F.A., The continuous scroll discharge decanting centrifuge, The Chem. Engineer, 281, pp 41-49, 1974.

Reihanian, H., Robertson, C.R., and Michaels, A.S., Mechanisms of polarization and fouling of ultrafiltration membranes by proteins, J. Membrane Sci., 16, pp 237-258, 1983.

Richardson, P., PhD thesis, University of London, London, 1988.

Rosen, C.G., Biotechnol. News, 3, p 10, 1983.

Rushton, A., and Zhang, G.S., Rotary microporous filtration of organic and inorganic particulates, pp 167-177, Solid liquid separation practice 3, The Institution of Chemical Engineers Symposium Series 113, Rugby, U.K., 1989.

Salt D.J., Leslie R.B., Lillford P.J., and Dunnill, P., Factors influencing protein structure during acid precipitation: a study of soya proteins, European J. Appl. Microbiol. Biotechnol., 14, pp 144-148, 1982.

Schulze, H., Z. Prakt. Chem., 25, p 451, 1882.

Segre, G., and Silderberg, A., Radial particle displacements in Poiseuille flow of suspensions, Nature, 189, pp 209-210, 1961.

Sontheimer, H., Flocculation in water treatment, in The Scientific Basis of Flocculation, Ed. Ives, K.J., Sijthoff and Noordhoff, Alphen aan den Rijn, The Netherlands, pp 193-217, 1978.

Suki, A., Fane, A.G., and Fell C.J.D., Flux decline in protein ultrafiltration, J. Membrane Sci., 21, pp 268-283, 1984.

Sutherland I.W., The bacterial wall and surface, Process Biochem. Apr, pp4-8, 1975.

Svarovsky, L., Solid-Liquid Separation, Butterworths, London, 1977.

Trettin, D.R., and Doshi, M.R., Ultrafiltration in an unstirred batch cell, Ind. Eng. Chem. Fundam., 19, 189, 1980.

Treweek, G.P., and Morgan, J.J., Polymer flocculation of bacteria: The mechanism of E.coli aggregation by polyethyleneimine, J. Coll. Int. Sci., 60, 2, pp 258-273, 1977.

Tutunjian, R.S., Cell separations with hollow fiber membranes, pp 376-381, in Comprehensive Biotechnology 2, Ed., Cooney, C.L. and Humphrey, A.E., Pergamon, 1985.

Van Ebbenhorst, H.J., and Rietema, K., in Cyclones in Industry, Eds., Rietema, K. and Verver, C.G., Elsevier, Amsterdam, 1961.

Verwey, E.J.W., and Overbeek, J.Th.C., Theory of the Stability of Lyophobic Colloids, Elsevier, Amsterdam, The Netherlands, 1948.

Vilker, V.L., Colton, C.K., Smith, K.A., and Green, D.L., The osmotic pressure of concentrated protein and lipoprotein solutions and its significance to ultrafiltration, J. Membrane Sci., 20, pp 63-77, 1984.

Virkar, P.D., Chan, M.Y.Y., Hoare, M., and Dunnill, P., Biotechnol. Bioeng., 24, pp 871-887, 1982.

Wagman, H., Bailey, V., and Weistein, M., Binding of antibiotics to filtration materials, *Antimicrob. Agents Chemother.*, 7, pp 316-319, 1975.

Wagner, J., Membrane filtration and downstream processing - an indispensable combination, pp 93-104, Proceedings of the international conference on membrane separation processes, BHRA, The Fluid Engineering Centre, Cranfield, Bedford, U.K., 1989.

Ward, P.N., PhD thesis, University of London, London, 1989.

Wiesmann, U., and Binder, H., Biomass separation from liquids by sedimentation and centrifugation, *Adv. Biochem Eng.*, 24, pp 119-171, 1982.

Wijmans, J.G., Nakao, S., and Smolders, C.A., Flux limitation in ultrafiltration: osmotic pressure model and gel layer model, *J. Membrane Sci.*, 20, pp 115-124, 1984.

Zeeman, L.J., Adsorption effects in rejection of macromolecules by ultrafiltration membranes, *J. Membrane Sci.*, 15, pp 213-230, 1983.

Zydney, A.L., and Colton, C.K., A concentration polarization model for the filtrate flux in cross-flow microfiltration of particulate suspensions, *Chem. Eng. Commun.*, 47, pp 1-21, 1986.